

ARYNE REACTIONS IN THE SYNTHESIS OF HETEROCYCLIC MOLECULES

Thesis by

Christopher Keating Haley

In Partial Fulfillment of the Requirements

for the Degree of

Doctor of Philosophy

CALIFORNIA INSTITUTE OF TECHNOLOGY

Pasadena, California

2016

(Defended December 2, 2015)

© 2015

Christopher Keating Haley

All Rights Reserved

To my parents.

ACKNOWLEDGEMENTS

I first and foremost have to thank my advisor, Brian Stoltz. Brian has been beyond supportive of me throughout my graduate career both inside and outside of the lab. He's always been a great person to talk to about high concepts in chemistry, the nitty gritty of running a column or just about a movie or his latest trip to Legoland. I could have not asked for a better advisor.

I next need to thank the rest of my committee, Dennis Dougherty, Theo Agapie and Sarah Reisman for being a great resource over the last five years. In particular, Sarah has been provided great insights, especially during our joint group meetings.

My labmates have been truly unparalleled. I've had the opportunity to work with some exceptional people, particularly within the "Benzyne Brigade." I owe a great deal of debt to Drs. Pam Tadross and Chris Gilmore. They put up with me as a procosious first year and really showed me the ropes. I have valued their help early on and have come to really value them as friends. Guillaume Lapointe was a font of chemical knowledge. He never came away from a conversation with him without learning something new. Kenji Negoro and Max Klatte were integral to scaling up the synthesis of jorumycin. I look forward to seeing Austin Wright continue to grow as a graduate student and continue on the tradition of aryne research in the Stoltz Lab.

Beyond being an incredible group of chemists, the Stoltz lab has been a great source of friendship. I've probably spent more time with Kelly Kim than any other person in the lab, and I wouldn't have wanted it any other way. As both hoodmate and office-mate she's been a great person to be around, whose optimism is infectious. Beau Prichett, whose lab coat-wearing habits have been a great source of consternation, has

become one of my closest friends at Caltech. I can honestly say that one of the biggest things I will miss about the Stoltz Lab is being O'Cornered by Nick O'Connor. Our debates and our endless conversations about useless information on wikipedia (and sometimes chemistry) have been integral to my experience during grad school. Kelvin Bates has been a great person to go line dancing with every Friday. Sam Shockley, Katerina Korch, Jeff Holder and Jared Moore have made the last five years memorable and so much fun both in and outside the lab.

I would be remiss not to thank the numerous chemists who I've had the opportunity to learn from, be challenged by and who have helped me grow as a scientist. The other members of my class, Doug Duquette, Rob Craig, Chung Whan Lee and Corey Reeves were great classmates to have. I learned so much from the other members of the lab: Chris Henry, Boger Liu, Kathrin Höferl-Prantz, Jimin Kim, Flo Vogt, Phil Wu, Alex Goldberg, Doug Behenna and Allen Hong.

Beyond the lab, Caltech has been such a supportive and wonderful place to work and be a part of. The other labs, such as the Reisman and Grubbs labs, have made the Chemistry Division a great place to be. Scott and Silva Virgil both are huge assets to the department and have been great companions to see an opera or two with. I appreciate everything Agnes Tong has done to help me succeed at Caltech. She has been so incredibly supportive and encouraging.

I've been fortunate enough to make some close friends beyond Caltech whose friendship and perspective have been of such importance to me over the last five years. I'm so lucky to be able to count Diane Seol as one of my closest friends. We've been friends for over a decade, and I look forward to being friends for the decades to come. I

need to acknowledge Emery Chang, who has truly done so much to help me experience Los Angeles and the rest California to the fullest and is really just an overall amazing guy. Bryan Chamberlain has always been there for me when I need someone. Matthew Schoenherr has become my go-to hiking/camping buddy, but beyond that, he's become a great friend. The guys at Oil Can Harry's have helped me look forward to Friday night line dancing, in particular Jason Schorr and Ben Stagg.

Lastly, and certainly not least, I need to thank my family. My parents and brother have been so amazingly supportive throughout this whole grad school adventure. They weren't thrilled when they found out I was moving 3000 miles away, but we've made it work and, in many ways, have become closer for it. I love you guys so much.

Thank you to all the people who have made the last five years some of the most memorable and exciting of my life.

ABSTRACT

Reactive intermediates play an important role within the realm of chemical synthesis. Their high energy and transient nature make them difficult to observe and characterize, but it is these same properties that empower them to form bonds traditionally seen as difficult to prepare and unusual architectures quickly and efficiently. Herein, two reactive intermediates, arynes and transient (2azaaryl)-cuprates, are exploited for their abilities to prepare important chemical motifs. Both serve as an avenue into the functionalization of arenes to provide products which hold value in a variety of fields including natural product total synthesis, pharmaceuticals and ligand design.

TABLE OF CONTENTS

Dedication	iii
Acknowledgements.....	iv
Abstract	vii
Table of Contents.....	vii
List of Figures	xi
List of Schemes	xii
List of Tables	xiv
List of Abbreviations	xvii

CHAPTER 1 1

The Acyl-Amidation of Arynes

1.1	Introduction	1
1.2	Acyl-Amidation of Arynes	5
1.3	Conclusion	8
1.4	Experimental Procedures.....	9
1.4.1	Materials and Methods.....	7
1.4.2	Representative Procedure for Acyl-Amidation	7
1.4.3	Spectroscopic Data	10
1.5	References	15

APPENDIX 1 17

Spectra Relevant to Chapter 1

CHAPTER 2 38

Progress Toward the Total Synthesis of Jorumycin

2.1	Introduction	39
2.2	Retrosynthetic Analysis of Jorumycin	40
2.3	Synthesis of Jorumycin	41
2.5	Experimental Section	47
2.5.1	Materials and Methods.....	47
2.5.2	Preparative Procedures and Spectroscopic Data.....	48

2.6	References and Notes	69
APPENDIX 2		72
Spectra Relevant to Chapter 2		
APPENDIX 3		91
A Tin-Free Route to a Complex Aryne Precursor		
A3.1	Introduction and Synthesis	91
A3.2	Experimental Section	93
A3.2.1	Materials and Methods.....	93
A3.2.2	Experimental Procedures.....	94
A3.3	References	97
APPENDIX 4		100
Synthetic Summary of the Total Synthesis of Jorumycin		
CHAPTER 3		105
Decarboxylative Cross-Coupling of (2-azaaryl) carboxylates with Aryl Halides		
3.1	Introduction	105
3.2	Optimization of the Decarboxylative Cross-Coupling of Picolinic Acid with Bromobenzene	110
3.3	The Cross Coupling of (2-Azaaryl) Carboxylates with Aryl Halides.....	117
3.4	Conclusion	118
3.5	Experimental Section	119
3.6	References	120
APPENDIX 5		123
The Ring-Expansive Acyl-Alkylation of Arynes		
A5.1	Introduction	123
A5.2	The Development of the Ring Expansive Acyl-Alkylation of Arynes with Heterocyclic β -keto esters.....	125
A5.3	Future Directions	129

APPENDIX 6**130**

Prepartion of Benzotriazoles via an Aryne-Based Three-Component Cross-Coupling

Comprehensive Bibliography	135
About the Author	144

LIST OF FIGURES

APPENDIX 1

Figure A1.1.1	^1H NMR (500 MHz, CDCl_3) of compound 18-2	18
Figure A1.1.2	Infrared spectrum (thin film/NaCl) of compound 18-2	19
Figure A1.1.3	^{13}C NMR (125 MHz, CDCl_3) of compound 18-2	19
Figure A1.2.1	^1H NMR (500 MHz, CDCl_3) of compound 18-3	20
Figure A1.2.2	Infrared spectrum (thin film/NaCl) of compound 18-3	21
Figure A1.2.3	^{13}C NMR (125 MHz, CDCl_3) of compound 18-3	21
Figure A1.3.1	^1H NMR (500 MHz, CDCl_3) of compound 18-6	22
Figure A1.3.2	Infrared spectrum (thin film/NaCl) of compound 18-6	23
Figure A1.3.3	^{13}C NMR (125 MHz, CDCl_3) of compound 18-6	23
Figure A1.4.1	^1H NMR (500 MHz, CDCl_3) of compound 18-9	24
Figure A1.4.2	Infrared spectrum (thin film/NaCl) of compound 18-9	25
Figure A1.4.3	^{13}C NMR (125 MHz, CDCl_3) of compound 18-9	25
Figure A1.5.1	^1H NMR (500 MHz, CDCl_3) of compound 19-5	26
Figure A1.5.2	Infrared spectrum (thin film/NaCl) of compound 19-5	27
Figure A1.5.3	^{13}C NMR (125 MHz, CDCl_3) of compound 19-5	27
Figure A1.6.1	^1H NMR (500 MHz, CDCl_3) of compound 19-6	28
Figure A1.6.2	Infrared spectrum (thin film/NaCl) of compound 19-6	29
Figure A1.6.3	^{13}C NMR (125 MHz, CDCl_3) of compound 19-6	29
Figure A1.7.1	^1H NMR (500 MHz, CDCl_3) of compound 22	30
Figure A1.7.2	Infrared spectrum (thin film/NaCl) of compound 22	31
Figure A1.7.3	^{13}C NMR (125 MHz, CDCl_3) of compound 22	31
Figure A1.8.1	^1H NMR (500 MHz, CDCl_3) of compound 24	32
Figure A1.8.2	Infrared spectrum (thin film/NaCl) of compound 24	33
Figure A1.8.3	^{13}C NMR (125 MHz, CDCl_3) of compound 24	33
Figure A1.9.1	^1H NMR (500 MHz, CDCl_3) of compound 26	34
Figure A1.9.2	Infrared spectrum (thin film/NaCl) of compound 26	35
Figure A1.9.3	^{13}C NMR (125 MHz, CDCl_3) of compound 26	35
Figure A1.10.1	^1H NMR (500 MHz, CDCl_3) of compound 3g	36
Figure A1.10.2	Infrared spectrum (thin film/NaCl) of compound 3g	37
Figure A1.10.3	^{13}C NMR (500 MHz, CDCl_3) of compound 3g	37

CHAPTER 2

Figure 2.1	<i>Tetrahydroisoquinoline natural products</i>	39
------------	--	----

APPENDIX 2

Figure A2.1.1	^1H NMR (500 MHz, CDCl_3) of compound 61	73
Figure A2.1.2	Infrared spectrum (thin film/NaCl) of compound 61	74
Figure A2.1.3	^{13}C NMR (125 MHz, CDCl_3) of compound 61	74
Figure A2.2.1	^1H NMR (500 MHz, CDCl_3) of compound 57	75
Figure A2.2.2	Infrared spectrum (thin film/NaCl) of compound 57	76
Figure A2.2.3	^{13}C NMR (125 MHz, CDCl_3) of compound 57	76
Figure A2.3.1	^1H NMR (500 MHz, CDCl_3) of compound 63	77
Figure A2.3.2	Infrared spectrum (thin film/NaCl) of compound 63	78
Figure A2.3.3	^{13}C NMR (125 MHz, CDCl_3) of compound 63	78
Figure A2.4.1	^1H NMR (500 MHz, CDCl_3) of compound 58	79
Figure A2.4.2	Infrared spectrum (thin film/NaCl) of compound 58	80
Figure A2.4.3	^{13}C NMR (125 MHz, CDCl_3) of compound 58	80
Figure A2.5.1	^1H NMR (500 MHz, CDCl_3) of compound 64	81
Figure A2.5.2	Infrared spectrum (thin film/NaCl) of compound 64	82
Figure A2.5.3	^{13}C NMR (125 MHz, CDCl_3) of compound 64	83
Figure A2.6.1	^1H NMR (500 MHz, CDCl_3) of compound 67	83
Figure A2.6.2	Infrared spectrum (thin film/NaCl) of compound 67	84
Figure A2.6.3	^{13}C NMR (125 MHz, CDCl_3) of compound 67	84
Figure A2.7.1	^1H NMR (500 MHz, CDCl_3) of compound 68	85
Figure A2.7.2	Infrared spectrum (thin film/NaCl) of compound 68	86
Figure A2.7.3	^{13}C NMR (125 MHz, CDCl_3) of compound 68	86
Figure A2.8.1	^1H NMR (500 MHz, CDCl_3) of compound 56	87
Figure A2.8.2	Infrared spectrum (thin film/NaCl) of compound 56	88
Figure A2.8.3	^{13}C NMR (125 MHz, CDCl_3) of compound 56	88
Figure A2.9.1	^1H NMR (500 MHz, CDCl_3) of compound 73	89
Figure A2.9.2	Infrared spectrum (thin film/NaCl) of compound 73	90
Figure A2.9.3	^{13}C NMR (125 MHz, CDCl_3) of compound 73	90

APPENDIX 3

Figure A3.1.1	^1H NMR (500 MHz, CDCl_3) of compound A3-4	98
Figure A3.1.2	Infrared spectrum (thin film/NaCl) of compound A3-4	99
Figure A3.1.3	^{13}C NMR (125 MHz, CDCl_3) of compound A3-4	99

CHAPTER 3

Figure 3.1	The importance of 2-substituted pyridine.....	106
------------	---	-----

APPENDIX 5

Figure A5.2	Benzannulated Heterocycles in Biologically Active Compounds	125
-------------	---	-----

LIST OF SCHEMES

CHAPTER 1

Scheme 1.1	In situ generation of benzyne.....	2
Scheme 1.2	Representative reactions of benzyne (1).....	2
Scheme 1.3	The direct acyl alkylation of arynes.....	3
Scheme 1.4	Insertion of arynes into C–C σ bonds.	3
Scheme 1.5	Greaney's Acyl-Amination and Derivatives.....	4
Scheme 1.6	Acyl-Amidation of Arynes.....	4
Scheme 1.7	Derivatization of ortho-acyl anilides.....	7

CHAPTER 2

Scheme 2.1	Retrosynthetic Analysis of Jorumycin.	41
Scheme 2.2	Preparation of isoquinolines 57 and 58	42
Scheme 2.3	Cross-coupling of isoquinolines 57 and 58	43
Scheme 2.4	Alternative approach to bis-isoquinoline 64	44
Scheme 2.5	The Diastereoselective Reduction of Bis-Isoquinoline 56	45
Scheme 2.6	Completion of the Synthesis of Jorumycin.....	46

APPENDIX 3

Scheme A3.1	First generation synthesis of benzaldehyde A2-4	91
Scheme A3.2	Preparation of Benzaldehyde A2-4	92

APPENDIX 3

Scheme A4.1	Preparation of aryne precursor 59	101
Scheme A4.2	Aryne annulations.....	101
Scheme A4.3	Cross-coupling of isoquinolines 57 and 58	102
Scheme A4.4	Alternative approach to bis-isoquinoline 64	102
Scheme A4.5	Origins of Diastereoselectivity for the Reduction of Bis-Isoquinoline 56	103
Scheme A4.6	Completion of the Synthesis of Jorumycin.....	104

CHAPTER 3

Scheme 3.1	Decarboxylative cross-coupling of aryl carboxylic acids with aryl halides. ..	106
Scheme 3.2	Myers's decarboxylative olefination and Goossen's decarboxylative coupling of benzoic acids and aryl bromides.	108
Scheme 3.3	The decarboxylative cross-coupling of two isoquinolines for the total synthesis of jorumycin.	109
Scheme 3.4	Preparation of isoquinoline triflate 98 and carboxylic acid 99	109
Scheme 3.5	Proposed mechanism of the decarboxylative cross-coupling of picolinic acid with aryl halides	113

APPENDIX 5

Scheme A5.1	Total Synthesis of (+)-amurensinine (A5-5).....	124
Scheme A5.2	Total Synthesis of (−)-curvularin (A5-10)	124
Scheme A5.3	Proposed Products of the Ring Expansive Acyl-Alkylation of Arynes	126
Scheme A5.4	The Acyl-Alkylation of Benzyne with β -ketoester A5-23	126
Scheme A5.5	Potential Unproductive Side Reactions of the Ring-Expansive Acyl-Alkylation of Benzyne	128

APPENDIX 6

Scheme A6.1	Previous Preparations of Benzotriazoles from Benzyne	131
Scheme A6.2	Preparation of Benzotriazoles from Aryne.....	132

LIST OF TABLES

CHAPTER 1

Table 1.1	Scope of the Imide.....	5
Table 1.2	Substituted Aryne Precursors.....	6
Table 1.3	Camps Cyclization of Ketoamide Insertion Products.	7

CHAPTER 3

Table 3.1	Decarboxylative cross-coupling of picolinic acid with aryl halides	111
Table 3.2	Investigation of P- and N- ligands for the decarboxylative cross-coupling of picolinic acid with aryl halides	112
Table 3.3	Investigation of P-ligands and copper sources for the decarboxylative cross-coupling of picolinic acid with aryl halides	114
Table 3.4	Examination of the equivalents of bromobenzene in the decarboxylative cross-coupling of picolinic acid with aryl halides.	115
Table 3.5	Examination of reaction time in the decarboxylative cross-coupling of picolinic acid with aryl halides.....	115
Table 3.6	Control experiments for the decarboxylative cross-coupling of picolinic acid with aryl halides	116
Table 3.7	The decarboxylative cross-coupling of picolinic acid with aryl halides	117

APPENDIX 5

Table A5.1	Optimization of the Ring-Expansive Acyl-Alkylation of Arynes	127
Table A5.2	Solvent Effects on the Ring-Expansive Acyl-Alkylation of Arynes.....	128

LIST OF ABBREVIATIONS

A	adenine
$[\alpha]_D$	angle of optical rotation of plane-polarized light
Å	angstrom(s)
<i>p</i> -ABSA	<i>para</i> -acetamidobenzenesulfonyl azide
Ac	acetyl
AIBN	azobisisobutyronitrile
APCI	atmospheric pressure chemical ionization
app	apparent
aq	aqueous
Ar	aryl group
At	benztriazolyl
atm	atmosphere(s)
BHT	2,6-di- <i>tert</i> -butyl-4-methylphenol (“butylated hydroxytoluene”)
BINAP	(2,2'-bis(diphenylphosphino)-1,1'-binaphthyl)
Bn	benzyl
Boc	<i>tert</i> -butoxycarbonyl
bp	boiling point
br	broad
Bu	butyl
<i>i</i> -Bu	<i>iso</i> -butyl
<i>n</i> -Bu	butyl or <i>norm</i> -butyl
<i>t</i> -Bu	<i>tert</i> -butyl

Bz	benzoyl
C	cytosine
<i>c</i>	concentration of sample for measurement of optical rotation
¹³ C	carbon-13 isotope
¹⁴ C	carbon-14 isotope
/C	supported on activated carbon charcoal
°C	degrees Celcius
calc'd	calculated
CAN	ceric ammonium nitrate
Cbz	benzyloxycarbonyl
CCDC	Cambridge Crystallographic Data Centre
CDI	1,1'-carbonyldiimidazole
cf.	consult or compare to (Latin: <i>confer</i>)
cm ⁻¹	wavenumber(s)
cod	1,5-cyclooctadiene
comp	complex
conc.	concentrated
Cy	cyclohexyl
CSA	camphor sulfonic acid
d	doublet
<i>d</i>	dextrorotatory
D	deuterium
DABCO	1,4-diazabicyclo[2.2.2]octane

dba	dibenzylideneacetone
DBDMH	<i>N,N'</i> -dibromo-5,5-dimethylhydantoin
DBU	1,8-diazabicyclo[5.4.0]undec-7-ene
DCC	dicyclohexyl carbodiimide
DCE	1,2-dichloroethane
DDQ	2,3-dichloro-5,6-dicyanobenzoquinone
<i>de</i>	diastereomeric excess
DIAD	diisopropyl azodicarboxylate
DIBAL	diisobutyl aluminum hydride
DMA	dimethylacetamide
DMAD	dimethyl acetylenedicarboxylate
DMAP	4-dimethylaminopyridine
DME	1,2-dimethoxyethane
DMF	<i>N,N</i> -dimethylformamide
DMSO	dimethylsulfoxide
DMTS	dimethylhexylsilyl
DNA	deoxyribonucleic acid
DPPA	diphenylphosphorylazide
dppp	1,3-bis(diphenylphosphino)propane
dr	diastereomeric ratio
DTT	dithiothreitol
<i>ee</i>	enantiomeric excess
E	methyl carboxylate (CO_2CH_3)

E^+	electrophile
E	trans (entgegen) olefin geometry
EC_{50}	median effective concentration (50%)
EDCI	1-Ethyl-3-(3-dimethylaminopropyl)carbodiimide
e.g.	for example (Latin: <i>exempli gratia</i>)
EI	electron impact
eq	equation
ESI	electrospray ionization
Et	ethyl
<i>et al.</i>	and others (Latin: <i>et alii</i>)
FAB	fast atom bombardment
Fmoc	fluorenylmethyloxycarbonyl
g	gram(s)
G	guanine
h	hour(s)
1H	proton
2H	deuterium
3H	tritium
[H]	reduction
HATU	2-(7-aza-1 <i>H</i> -benzotriazol-1-yl)-1,1,3,3-tetramethyluronium hexafluorophosphate
HMDS	hexamethyldisilamide or hexamethyldisilazide
HMPT	hexamethylphosphoramide
$h\nu$	light

HPLC	high performance liquid chromatography
HRMS	high resolution mass spectrometry
Hz	hertz
IBX	2-iodoxybenzoic acid
IC_{50}	half maximal inhibitory concentration (50%)
i.e.	that is (Latin: <i>id est</i>)
iNOS	human-inducible nitric oxide synthase
IR	infrared spectroscopy
J	coupling constant
k	rate constant
kcal	kilocalorie(s)
kg	kilogram(s)
KHMDS	potassium bis(trimethylsilyl)amide
L	liter or neutral ligand
l	levorotatory
LA	Lewis acid
LD_{50}	median lethal dose (50%)
LDA	lithium diisopropylamide
LHMDS	lithium bis(trimethylsilyl)amide
LICA	lithium isopropylcyclohexylamide
LTMP	lithium 2,2,6,6-tetramethylpiperidide
m	multiplet or meter(s)
M	molar or molecular ion

<i>m</i>	meta
μ	micro
<i>m</i> -CPBA	<i>meta</i> -chloroperbenzoic acid
Me	methyl
mg	milligram(s)
MHz	megahertz
MIC	minimum inhibitory concentration
min	minute(s)
mL	milliliter(s)
MM	mixed method
mol	mole(s)
MOM	methoxymethyl
mp	melting point
Ms	methanesulfonyl (mesyl)
MS	molecular seives
<i>m/z</i>	mass-to-charge ratio
N	normal or molar
NBS	<i>N</i> -bromosuccinimide
nm	nanometer(s)
NMR	nuclear magnetic resonance
NOE	nuclear Overhauser effect
NOESY	nuclear Overhauser enhancement spectroscopy
Nu^-	nucleophile

<i>o</i>	ortho
[O]	oxidation
<i>t</i> -Oct	<i>tert</i> -octyl (1,1,3,3-tetramethylbutyl)
<i>p</i>	para
PCC	pyridinium chlorochromate
PDC	pyridinium dichromate
Ph	phenyl
pH	hydrogen ion concentration in aqueous solution
Piv	pivalate
p <i>K_a</i>	acid dissociation constant
PKS	polyketide synthase
PMB	<i>para</i> -methoxybenzyl
ppm	parts per million
PPTS	pyridinium <i>para</i> -toluenesulfonate
Pr	propyl
<i>i</i> -Pr	isopropyl
<i>n</i> -Pr	propyl or <i>norm</i> -propyl
psi	pounds per square inch
py	pyridine
q	quartet
R	alkyl group
<i>R</i>	rectus
RCM	ring-closing metathesis

REDAL	sodium bis(2-methoxyethoxy)aluminum hydride
ref	reference
R_f	retention factor
RNA	ribonucleic acid
s	singlet or seconds
s	selectivity factor = $k_{\text{rel(fast/slow)}} = \ln[(1 - C)(1 - ee)]/\ln[(1 - C)(1 + ee)]$, where C = conversion
S	sinister
sat.	saturated
SEM	2-(trimethylsilyl)ethoxymethyl
SOD	superoxide dismutase
Su	succinimide
t	triplet
T	thymine
TBAF	tetra- <i>n</i> -butylammonium fluoride
TBAT	tetra- <i>n</i> -butylammonium difluorotriphenylsilicate
TBDPS	<i>tert</i> -butyldiphenylsilyl
TBHP	<i>tert</i> -butyl hydroperoxide
TBS	<i>tert</i> -butyldimethylsilyl
TCA	trichloroacetic acid
temp	temperature
TES	triethylsilyl
Tf	trifluoromethanesulfonyl
TFA	trifluoroacetic acid

TFAA	trifluoroacetic anhydride
TFE	2,2,2-trifluoroethanol
THF	tetrahydrofuran
THIQ	tetrahydroisoquinoline
TIPS	triisopropylsilyl
TLC	thin layer chromatography
TMEDA	<i>N,N,N',N'</i> -tetramethylethylenediamine
TMP	2,2,6,6-tetramethylpiperidine
TMS	trimethylsilyl
TOF	time-of-flight
tol	tolyl
Tr	triphenylmethane (trityl)
Troc	2,2,2-trichloroethoxycarbonyl
Ts	<i>para</i> -toluenesulfonyl (tosyl)
UV	ultraviolet
w/v	weight per volume
v/v	volume per volume
X	anionic ligand or halide
Z	cis (zusammen) olefin geometry

CHAPTER 1

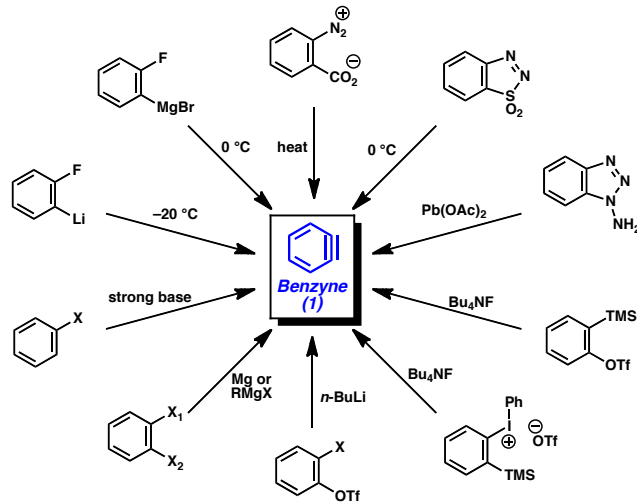
The Acyl-Amidation of Arynes

1.1 Introduction

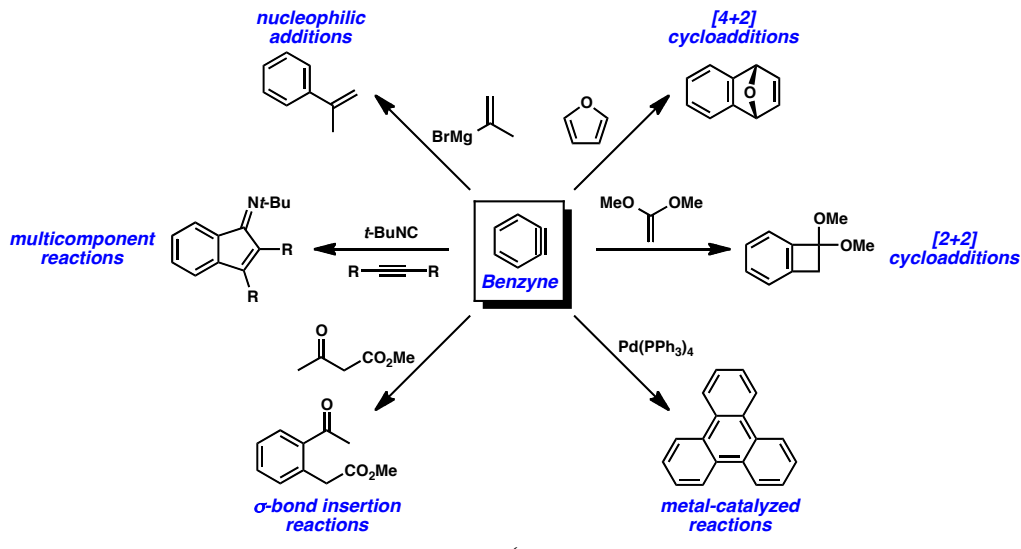
Arynes have long been of interest to both physical organic and synthetic chemists. The structure of benzyne was first elucidated by J. D. Roberts in 1953 and since that time a number of methods to generate these reactive intermediates have been realized (Scheme 1.1).¹ Many of these procedures require high temperature or strong base such as *n*-butyllithium or sodium amide.² In 1983, Kobayashi and co-workers reported the *in situ* generation of arynes from corresponding *o*-silyl aryl triflates.³ This has proven to be one of the mildest and most synthetically useful ways of generating arynes. Desilylation upon treatment of the *o*-silyl aryl triflate with fluoride ion induces an elimination of the triflate to furnish the highly strained triple bond characteristic of arynes. This method can be performed under ambient conditions and with a wide variety of fluoride sources. While these intermediates cannot be isolated and are difficult to observe

spectroscopically, they can be harnessed in a variety of reaction pathways to afford interesting and important architectures, often forming multiple carbon–carbon or carbon–heteroatom bonds in a single operation (Scheme 1.2).⁴

Scheme 1.1. *In situ* generation of benzyne.



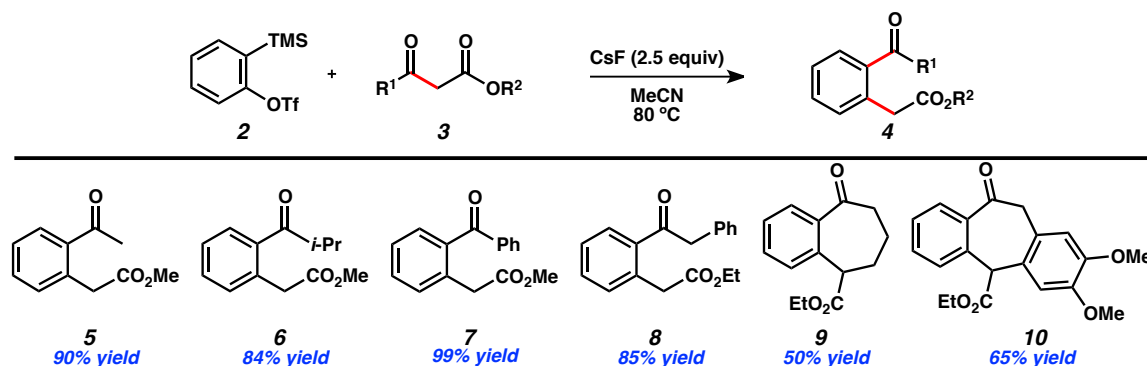
Scheme 1.2. Representative reactions of benzyne (1).



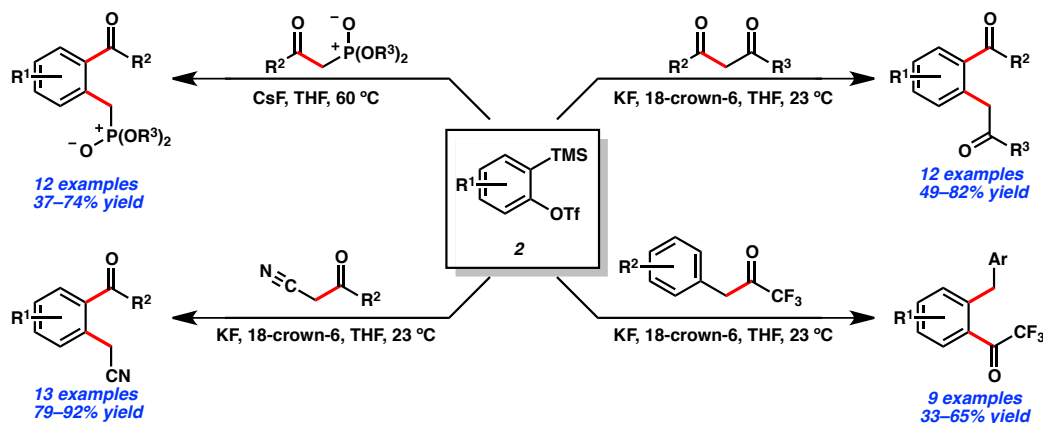
The Stoltz group has been interested in the synthetic utility of arynes for a number of years. In 2005, Tambar and Stoltz reported on the first acyl alkylation of arynes using β -ketoesters (Scheme 1.3).⁵ Aryne insertion into the alpha, beta carbon–carbon bond of

β -ketoesters is thought to proceed through a formal [2+2] cycloaddition followed by fragmentation to afford acyl-alkylated products **5–10** in good yield. Since the Stoltz group's initial studies, aryne insertion into carbon–carbon bonds bearing electron withdrawing groups has been extended to a variety of substrate classes, including 1,3-diketones,⁶ α -ketonitriles,⁷ β -ketophosphonates,⁸ and trifluoromethyl ketones,⁹ among others (Scheme 1.3).¹⁰ More recently, the Garg lab developed a procedure for embedding heteroarenes into cyclic ureas in order to probe the inherent regioselectivity of such reactions.¹¹

Scheme 1.3. The direct acyl alkylation of arynes.

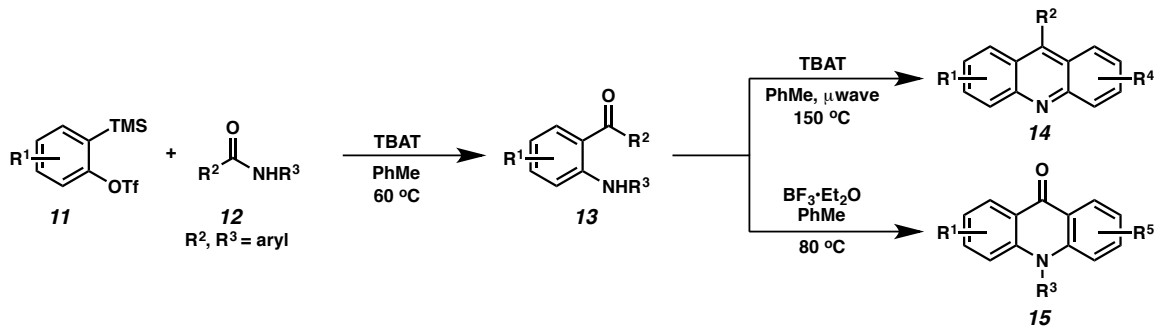


Scheme 1.4. Insertion of arynes into C–C σ bonds.

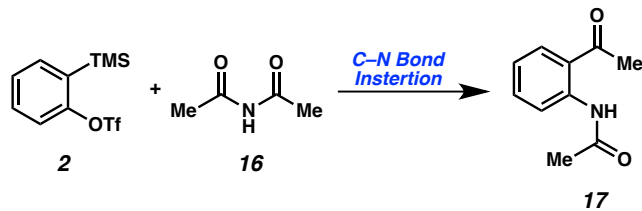


Previous work by the Greaney group demonstrated that the insertion of amides into arynes could afford similar acyl-aminated products (Scheme 1.5).¹² However, the scope of their method was focused on *N*-aryl benzamides substrates (**12**), which significantly limited further derivatization of the insertion products (**13**). These *N*-aryl *ortho*-acyl anilines (**13**) could be reacted further to prepare tricyclic polyaromatic systems, namely acridines (**14**) and acridones (**15**). We sought to address this limitation by developing a method of the insertion of arynes into the C–N bonds of imides (**16**) (Scheme 1.6). These *N*-acyl anilines (**17**) would be far more amenable to derivation therefore provide access to an array of important chemical motifs, such as indoles, quinolones and *ortho*-acyl anilines.

Scheme 1.5. Greaney’s Acyl-Amination and Derivatives.



Scheme 1.6. Acyl-Amidation of Arynes.



1.2 Acyl-Amidation of Arynes

We initiated our synthetic studies by optimizing conditions for the insertion reaction. Using acetylacetamide (**16**) as a model imide substrate and *ortho*-silylaryl triflate **2** as the aryne precursor, we observed the best yields for the insertion reaction in toluene at 60 °C and TBAT as a fluoride source (Table 1.1).

With optimized parameters in hand, we next set out to explore the substrate scope. Our method showed tolerance to imide substrates possessing both aliphatic and aromatic substituents, with yields ranging from modest to very good. Substrates bearing carbamate functionalities were also compatible, albeit with reduced yields (entries 7 and 8).

Table 1.1. Scope of the Imide.

		18		19	
Entry	R	R ₁	X	Yield (%)	
1	Me	Me	NH	89	
2	Et	Et	NH	88	
3	1-Ad	1-Ad	NH	84	
4	Ph	Ph	NH	68	
5	<i>i</i> -Pr	<i>i</i> -Pr	NH	78	
6	<i>i</i> -Bu	<i>i</i> -Bu	NH	79	
7	OMe	Bn	NH	24	
8	OBn	Me	NH	31	
9	CH ₂ CH ₂ Ph	CH ₂ CH ₂ Ph	NH	74	
10	Me	Me	O	54	

Having explored the substrate scope of this reaction with respect to the imide, we next investigated its tolerance with respect to the aryne precursor used (Table 1.2).

Although substituted phenyl ring systems provided fair to good yields, precursors bearing nitrogen (i.e. indolyne and pyridyne) fared poorly.

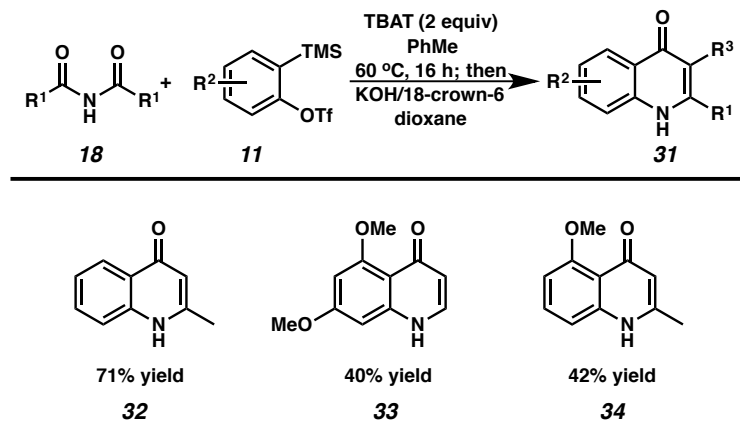
Table 1.2. Substituted Aryne Precursors.

Entry	Aryne	Product	Yield (%)
1			31
2			44
3			65
4			47
5			47

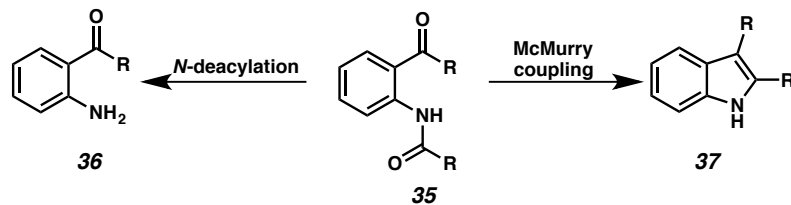
Following previous research conducted by the Buchwald group,¹³ we found that acylamide insertion products could be elaborated to substituted quinolone products by a base-initiated Camps cyclization in a two-step, one-pot sequence (see Table 1.3).

Additionally, these aryl ketoamides have previously been converted to indoles via McMurry couplings. *N*-deacylation of these ketoamides affords ketoanilines. Similarly, ketoester insertion products can be elaborated to chromones *via* base-initiated cyclization followed by condensation (Scheme 1.7). or to 1,3 diketones through Baker–Venkataraman rearrangements.¹⁴ Our lab is making on-going efforts to explore the scope of this reaction and its potential in developing other valuable synthetic transformations.

Table 1.3. Camps Cyclization of Ketoamide Insertion Products.



Scheme 1.7. Derivatization of *ortho*-acyl anilides.



1.3 Conclusion

To summarize, we have discovered a method for inserting arenes into C–N and C–O σ bonds of imides and anhydrides, respectively to generate 1,2-ketoamide and ketoester products. These compounds are capable of further derivatization to provide a broad array of synthetically useful compounds. Our lab is making ongoing efforts to explore the scope of this reaction and its potential in developing other valuable synthetic transformations.

1.4 Experimental Procedures

1.4.1 Materials and Methods.

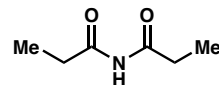
Unless otherwise stated, reactions were performed in flame-dried glassware under nitrogen atmosphere using dry, deoxygenated solvents (distilled or passed over a column of activated alumina). Reaction temperatures were controlled by an IKAmag temperature modulator. Thin layer chromatography (TLC) was performed using E. Merck silica gel 60 F254 precoated plates (0.25 mm) and visualized by UV fluorescence quenching. SiliaFlash P60 Academic Silica gel (particle size 0.040-0.063 mm) was used for flash chromatography. ^1H and ^{13}C NMR spectra were recorded on a Varian Inova 500 (500 MHz and 125 MHz, respectively) and are reported relative to Me₄Si (δ 0.0). IR spectra were recorded on a Perkin Elmer Paragon 1000 Spectrometer and are reported in frequency of absorption (cm⁻¹). HRMS were acquired using an Agilent 6200 Series TOF with an Agilent G1978A Multimode source in electrospray ionization (ESI), atmospheric pressure chemical ionization (APCI) or mixed (MM) ionization mode.

1.4.2 Representative Procedure for Acyl-amidation

A 2-dram vial equipped with a magnetic stir bar was charged with TBAT and acetylacetamide. The vial was purged with nitrogen, and PhMe was added via syringe followed by silylaryltriflate. The vial was sealed and placed in an aluminum block preheated to 60 °C. The reaction mixture was stirred at this temperature for 16 h, then it was allowed to cool to 23 °C. The mixture was concentrated in vacuo and purified by column chromatography (10% EtOAc in hexanes) to afford a white solid. Characterization data match those previously reported.

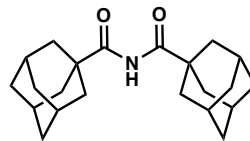
1.4.3 Spectroscopic Data

The spectroscopic data for compounds **18-1**,¹⁵ **18-4**,¹⁵ **19-1**,¹⁶ **19-2**,¹⁷ **19-10**, **30**,¹⁸ **32**,¹⁹ **33**¹⁸ were identical to those previously reported.



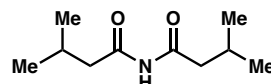
N-propionylpropionamide (**18-2**)

¹H NMR (500 MHz, CDCl₃) δ 7.73 (s, 1H), 2.62 (q, *J* = 7.4 Hz, 3H), 1.18 (t, *J* = 7.4 Hz, 4H); ¹³C NMR (126 MHz, CDCl₃) δ 175.17, 30.87, 8.52; IR (NaCl/Film) 3266.83, 3175.24, 2978.35, 1736.17, 1503.45, 1421.79, 1181.11, 1072.97, 729.68 cm⁻¹; HRMS



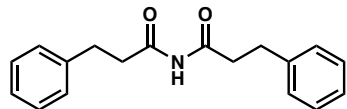
Di-1-adamantanecarboxamide (18-3)

¹H NMR (500 MHz, CDCl₃) δ 2.04 (dd, *J* = 7.4, 2.6 Hz, 6H), 1.93 (d, *J* = 2.9 Hz, 12H), 1.73 (m, 12H); IR (NaCl/Film) 2906.06, 2851.48, 1693.63, 1453.93, 1325.17, 1284.81, 1250.94, 1102.93, 952.74, 743.88.



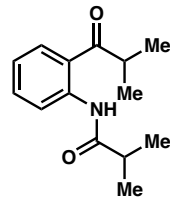
3-methyl-N-(3-methylbutanoyl)butanamide (18-6)

¹H NMR (300 MHz, CDCl₃) δ 8.72 (br s, 1H), 2.47 (d, *J* = , 4H), 2.14 (heptet, *J* = , 2H); ¹³C (125 MHz, CDCl₃) δ 173.9, 46.3, 25.2, 22.4; IR (NaCl/Film); HRMS (MM: ESI-APCI) *m/z* calc'd for C₁₀H₁₉NO₂ [M+H]⁺ = 186.1494, found 186.1500.



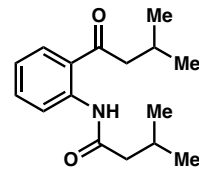
3-phenyl-N-(3-phenylpropanoyl)propanamide (18-9)

^1H NMR (500 MHz, CDCl_3) δ 8.10 (s, 1H), 7.25 (m, 10H), 2.95 (m, 8H); ^{13}C NMR (126 MHz, CDCl_3) δ 173.09, 140.33, 128.71, 128.54, 126.52, 39.20, 30.39; IR (NaCl/Film) 3147.72, 1675.04, 1494.86, 1453.56, 1380.88, 1311.33, 1199.44, 1146.83, 981.74, 725.51, 697.04 cm^{-1} ; (MM: ESI-APCI) m/z calc'd for $\text{C}_{18}\text{H}_{19}\text{NO}_2$ $[\text{M}+\text{H}]^+$ = 282.1489, found 282.1489.



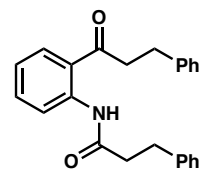
***N*-(2-isobutryrylphenyl)isobutyramide (19-5)**

^1H NMR (300 MHz, CDCl_3) δ 11.80 (br s, 1H), 8.79 (d, J = 6 Hz, 1H), 7.93 (d, J = 6 Hz, 1H), 7.53 (t, J = 4.5 Hz, 1H), 7.10 (t, J = 6 Hz, 1H), 3.65 (sept, J = 6 Hz, 1H), 2.62 (sept, J = 6 Hz, 1H), 1.28 (d, J = 6 Hz, 6H), 1.22; ^{13}C (75 MHz, CDCl_3) δ 209.2, 176.6, 141.7, 134.8, 130.6, 122.2, 121.1, 120.7, 37.6, 36.3, 19.6 (2 unresolved signals); IR (Neat Film, NaCl); HRMS (MM: ESI-APCI) m/z calc'd for $\text{C}_{14}\text{H}_{19}\text{NO}_2$ $[\text{M}+\text{H}]^+$ = 234.1489, found 234.1490.



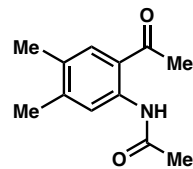
3-methyl-N-(2-(3-methylbutanoyl)phenyl)butanamide (19-6)

^1H NMR (300 MHz) δ 11.73 (br s, 1H), 8.77 (d, J = , 1H), 7.90 (d, J = , 1H), 7.53 (t, J = , 1H), 7.10 (t, J = , 1H), 2.88 (d, J = , 2H), 2.33–2.19 (m, 4H), 1.03–0.99 (m, 12H); ^{13}C (126 MHz) 205.0, 172.1, 141.0, 134.9, 130.4, 122.2, 121.92, 120.9, 49.0, 48.1, 26.3, 25.6, 22.7, 22.5. IR (Neat Film, NaCl); HRMS (MM: ESI-APCI) m/z calc'd for $\text{C}_{16}\text{H}_{23}\text{NO}_2$ $[\text{M}+\text{H}]^+$ = 262.1802 , found 262.1804.



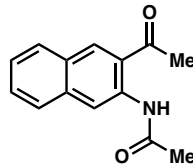
3-phenyl-N-(2-(3-phenylpropanoyl)phenyl)propanamide (19-9)

Observed as rotomers, major rotomer reported. ^1H NMR (500 MHz, CDCl_3) δ 11.71 (s, 1H), 8.76 (dd, J = 8.5, 1.1 Hz, 1H), 7.89 (dd, J = 8.2, 1.5 Hz, 1H), 7.55 (m, 1H), 7.40 (m, 1H), 7.26 (m, 10H), 3.35 (m, 2H), 3.09 (m, 2H), 3.03 (dd, J = 8.4, 7.1 Hz, 2H); IR (NaCl/Film) 3026.46, 2925.93, 1696.65, 1651.11, 1604.35, 1583.56, 1519.16, 1450.30, 1360.55, 1297.79, 1194.79, 1194.90, 976.10, 751.87, 698.56 cm^{-1} ; HRMS (MM: ESI-APCI) m/z calc'd for $\text{C}_{24}\text{H}_{23}\text{NO}_2$ $[\text{M}+\text{H}]^+$ = 358.1802, found 358.1812.



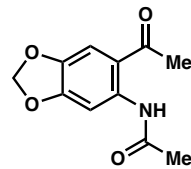
***N*-(2-acetyl-4,5-dimethylphenyl)acetamide (22)**

^1H NMR (300 MHz, CDCl_3) δ 11.63 (br s, 1H), 8.53 (s, 1H), 7.61 (s, 1H), 2.63 (s, 3H), 2.31 (s, 3H), 2.26 (s, 3H), 2.21 (s, 3H); ^{13}C (75 MHz, CDCl_3) δ 202.4 (C), 169.4 (C), 145.3, 139.1 (C), 132.4 (CH), 130.6 (C), 121.5 (CH), 119.8 (C), 28.6 (CH_3), 25.6 (CH_3), 20.6 (CH_3), 19.4 (CH_3); IR (Neat Film/NaCl); HRMS (MM: ESI-APCI) m/z calc'd for $\text{C}_{12}\text{H}_{15}\text{NO}_2$ $[\text{M}+\text{H}]^+$ = 206.1176, found 206.1171.



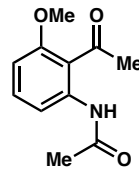
***N*-(3-acetylnaphthalen-2-yl)acetamide (24)**

^1H NMR (300 MHz, CDCl_3) δ 11.5 (br s, 1H), 9.12, (s, 1H), 8.44 (s, 1H), 7.83 (d, J = 9.0 Hz, 2H), 7.57 (t, J = 7.5 Hz, 1H), 7.43 (t, J = 7.5 Hz, 1H), 2.80 (s, 3H), 2.27 (s, 3H); ^{13}C (75 MHz, CDCl_3) 203.0 (C), 169.3 (C), 136.7 (C), 136.1 (C), 134.3 (CH), 129.7 (CH), 128.9 (CH), 128.2 (C), 127.7 (CH), 125.6 (CH), 122.7 (C), 117.7 (CH), 28.7 (CH_3), 25.6 (CH_3). IR (Neat Film, NaCl); HRMS (MM: ESI-APCI) m/z calc'd for $\text{C}_{14}\text{H}_{13}\text{NO}_2$ $[\text{M}+\text{H}]^+$ = 228.1019, found 228.1022.



***N*-(6-acetylbenzo[*d*][1,3]dioxol-5-yl)acetamide (26)**

¹H NMR (300 MHz, CDCl₃) δ 12.08 (br s, 1H), 8.37 (s, 1H), 7.25 (s, 1H), 6.02 (s, 2H), 2.57 (s, 3H), 2.20 (s, 3H); ¹³C NMR (75 MHz, CDCl₃) δ 200.6 (C), 169.5 (C), 152.9 (C), 142.4 (C), 139.3 (C), 115.1 (C), 109.6 (CH), 102.1 (CH), 101.5 (CH₂), 28.8 (CH₃), 25.6 (CH₃). IR (Neat Film, NaCl); HRMS (MM: ESI-APCI) *m/z* calc'd for C₁₁H₁₁NO₄ [M+H]⁺ = 222.0761, found 222.0766.



***N*-(2-acetyl-3-methoxyphenyl)acetamide (30)**

¹H NMR (500 MHz, CDCl₃) δ 10.49 (s, 1H), 8.07 (d, *J* = 8.3 Hz, 1H), 7.40 (td, *J* = 8.4, 0.5 Hz, 1H), 6.69 (dd, *J* = 8.4, 0.9 Hz, 1H), 3.90 (s, 3H), 2.61 (s, 3H), 2.17 (s, 3H); ¹³C NMR (126 MHz, CDCl₃) δ 204.58, 169.20, 160.00, 139.40, 133.90, 114.14, 106.31, 55.83, 33.73, 25.48; IR (NaCl/Film) 3086.81, 2947.73, 1698.62, 1639.62, 1634.03, 1528.84, 1470.57, 1470.57, 1403.54, 1273.11, 1243.38, 1195.89, 1093.22, 1017.32, 967.43, 802.27, 735.19, 610.77 cm⁻¹; HRMS (MM: ESI-APCI) *m/z* calc'd for C₁₁H₁₃NO₃ [M+H]⁺ = 262.1802, found 262.1804.

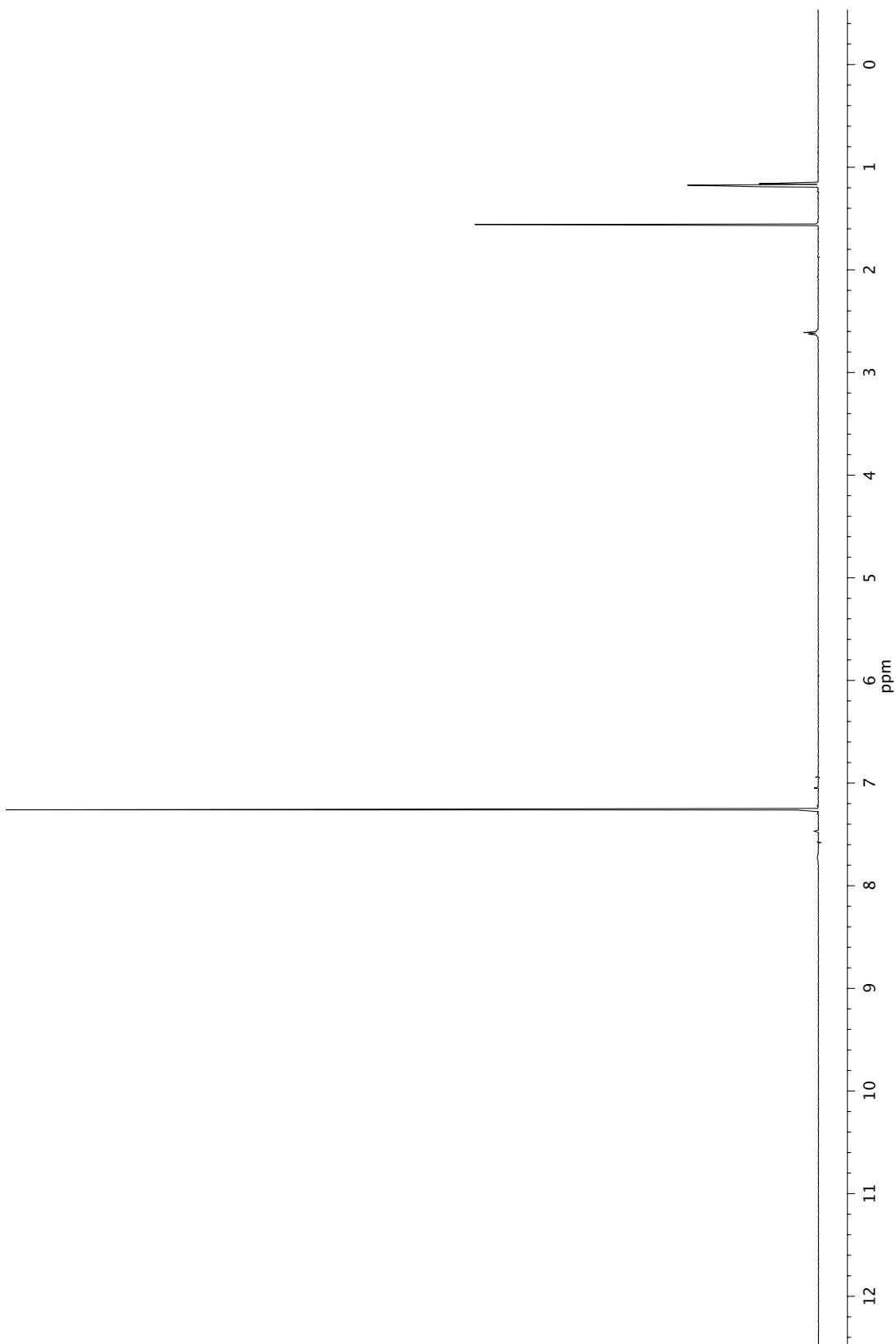
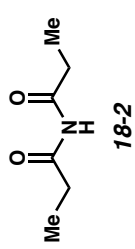
1.5 References

1. Roberts, J. D.; Simmons, H. E., Jr.; Carlsmith, L. A.; Vaughan, C. W. *J. Am. Chem. Soc.* **1953**, *75*, 3290–3291.
2. For methods of benzyne generation, see: a) Kitamura, T.; Yamane, M. *J. Chem. Soc. Chem. Commun.* **1995**, 983–984. b) Campbell, C. D.; Rees, C. W. *J. Chem. Soc. (C)* **1969**, 742–747. c) Matsumoto, T.; Hosoya, T.; Katsuki, M.; Suzuki, K. *Tetrahedron Lett.* **1991**, *32*, 6735–6736. d) Friedman, L.; Logullo, F. M. *J. Am. Chem. Soc.* **1963**, *85*, 1792–1797. e) Logullo, F. M.; Seitz, A. H.; Friedman, L. *Org. Synth.* **1968**, *48*, 12–17. f) Wittig, G.; Hoffmann, R. W. *Org. Synth.* **1967**, *47*, 4–8. g) Hoffmann, R. W. *Dehydrobenzene and Cycloalkynes*; Academic Press: New York, 1967.
3. Himeshima, Y.; Sonoda, T.; Kobayashi, H. *Chem. Lett.* **1983**, 1211–1214.
4. For examples of the reactivity highlighted in Scheme 2, see: a) Liu, Z.; Larock, R. C. *Org. Lett.* **2003**, *5*, 4673–4675. b) Allan, K. M.; Gilmore, C. D.; Stoltz, B. M. *Angew. Chem., Int. Ed.* **2011**, *50*, 4488–4491. c) Wittig, G.; Pohmer, L. *Chem. Ber.* **1956**, *89*, 1334–1351. d) Stevens, R. V.; Bisacchi, G. S. *J. Org. Chem.* **1982**, *47*, 2393–2396. e) Peña, D.; Escudero, S.; Pérez, D.; Guitián, E.; Castedo, L. *Angew. Chem., Int. Ed.* **1998**, *37*, 2659–2661.
5. Tambar, U. K.; Stoltz, B. M. *J. Am. Chem. Soc.* **2005**, *127*, 5340–5341.
6. Yoshida, H.; Watanabe, M.; Ohshita, J.; Kunai, A. *Chem. Commun.* **2005**, 3292–3294.
7. Yoshida, H.; Watanabe, M.; Ohshita, J.; Kunai, A. *Tetrahedron Lett.* **2005**, *45*, 6729–6731.
8. Liu, Y.-L.; Liang, Y.; Pi, S.-F.; Li, J.-H. *J. Org. Chem.* **2009**, *74*, 5691–5694.

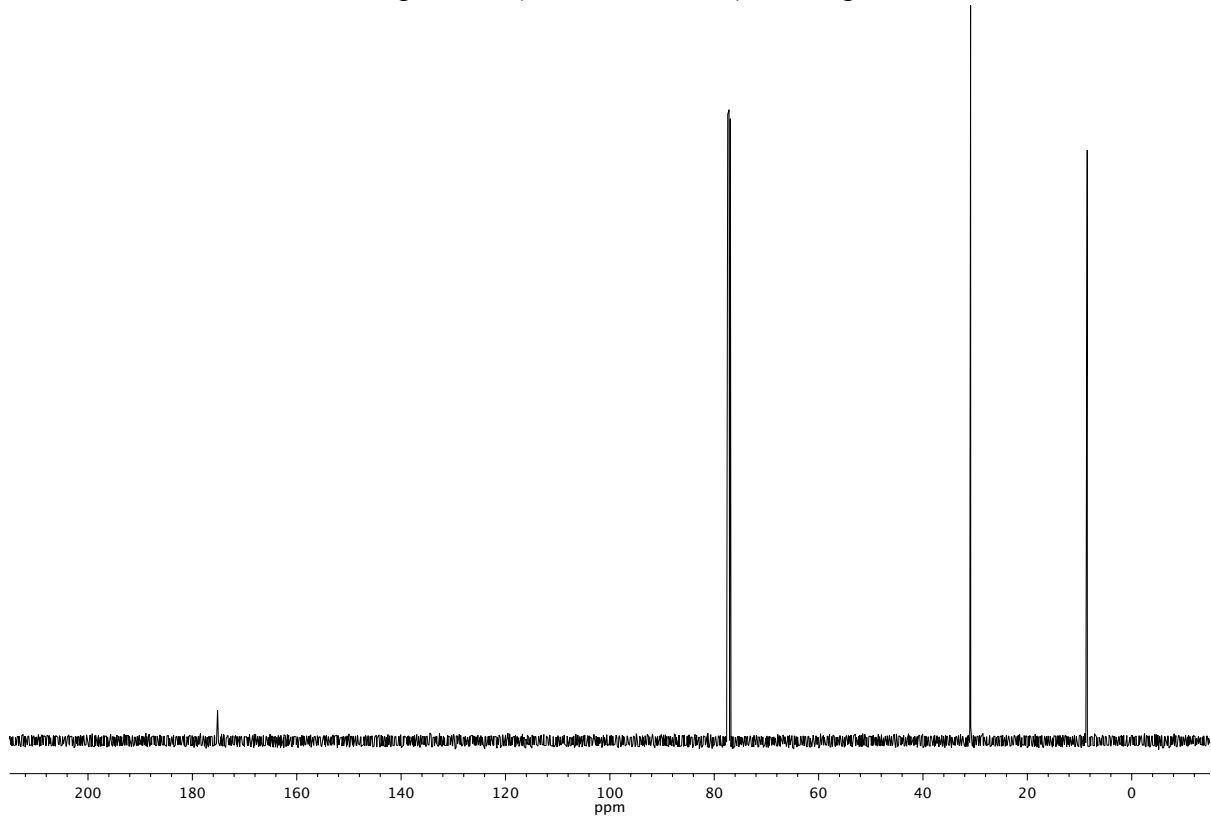
9. Yoshida, H.; Ito, Y.; Yoshikawa, Y.; Ohshita, J.; Takaki, K. *Chem. Commun.*, **2011**, 8664–8666.
10. Bhunia, A.; Yetra, S. R.; Biju, A. T. *Chem. Soc. Rev.* **2012**, *41*, 3140–3152.
11. Garg, N. K.; Goetz, A. E. *J. Org. Chem.* **2014**, *79*, 846–851.
12. Pintori, D. G.; Greaney, M. F. *Org. Lett.* **2010**, *12*, 168–171.
13. Jones, C. P.; Anderson, K. W.; Buchwald, S. L. *J. Org. Chem.* **2007**, *72*, 7968–7973.
14. a) Baker, W. *J. Chem. Soc.*, **1933**, 1381–1389 b) Mahal, H. S.; Venkataraman, K. *J. Chem. Soc.*, **1934**, 1767–1769.
15. Lee, J.; Hong, M.; Jung, Y.; Cho, E. J.; Rhee, H. *Tetrahedron* **2012**, *68*, 2045–2051.
16. Pialat, A.; Liégault, B.; Marc Taillefer, M. *Org. Lett.* **2013**, *15*, 1764–1767.
17. Canonne, P.; Boulanger, R.; Chantegrel, B. *Tetrahedron* **1987**, *43*, 663–668.
18. Liu, G.-B.; Xu, J.-L.; He, C. C.; Chen, G.; Qiang Xu, Q.; Xu, H.-X.; Jian-Xin Li, J.-X. *Bioorg. Med. Chem.* **2009**, *17*, 5433–5441.
19. Cross, R. M.; Manetsch, R. *J. Org. Chem.* **2010**, *24*, 8654–8657.

Appendix 1

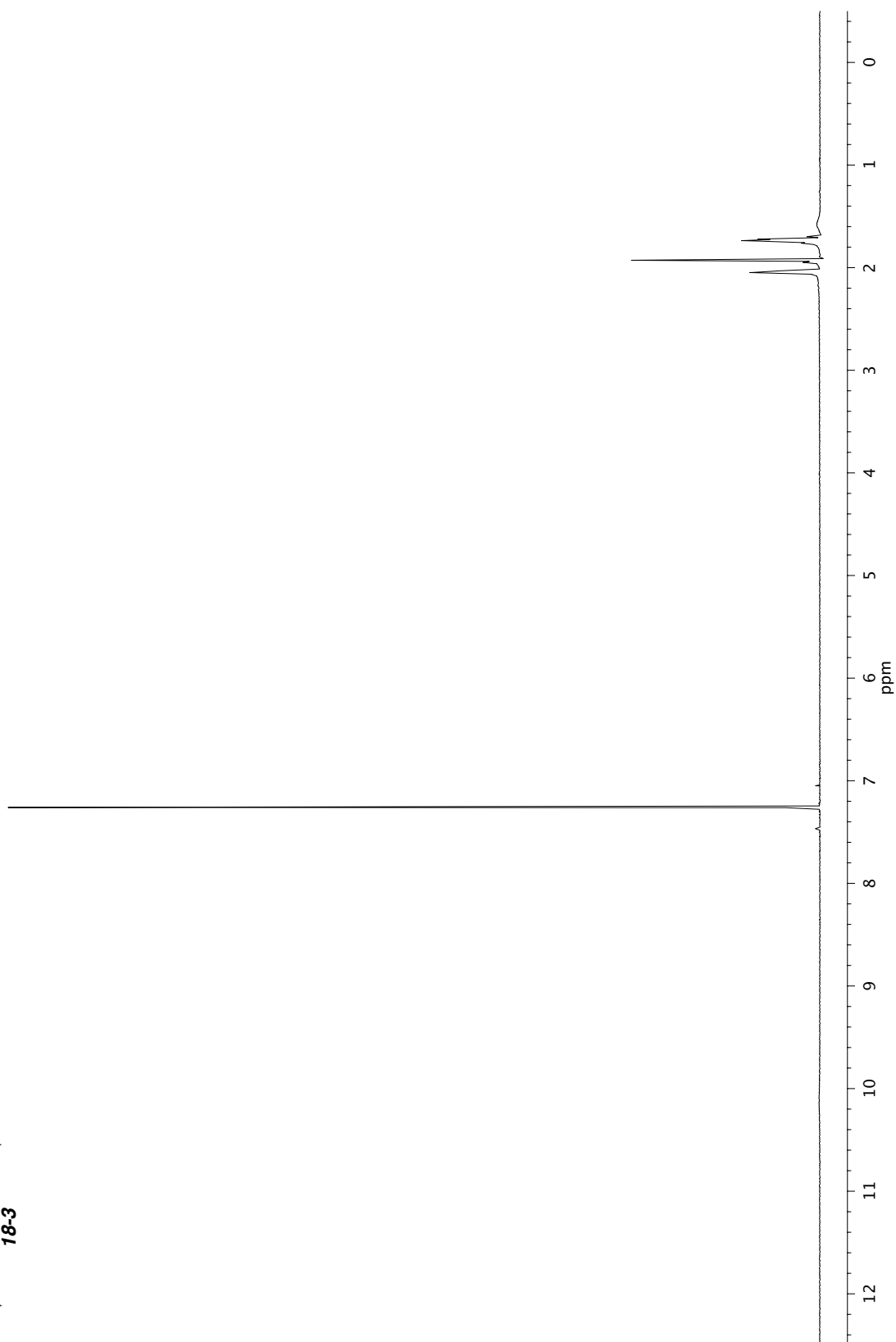
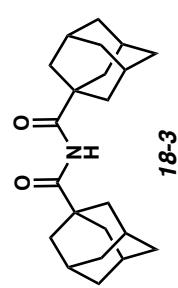
Spectra Relevant to Chapter 1



Infrared spectrum (Thin Film, NaCl) of compound **18-2**.



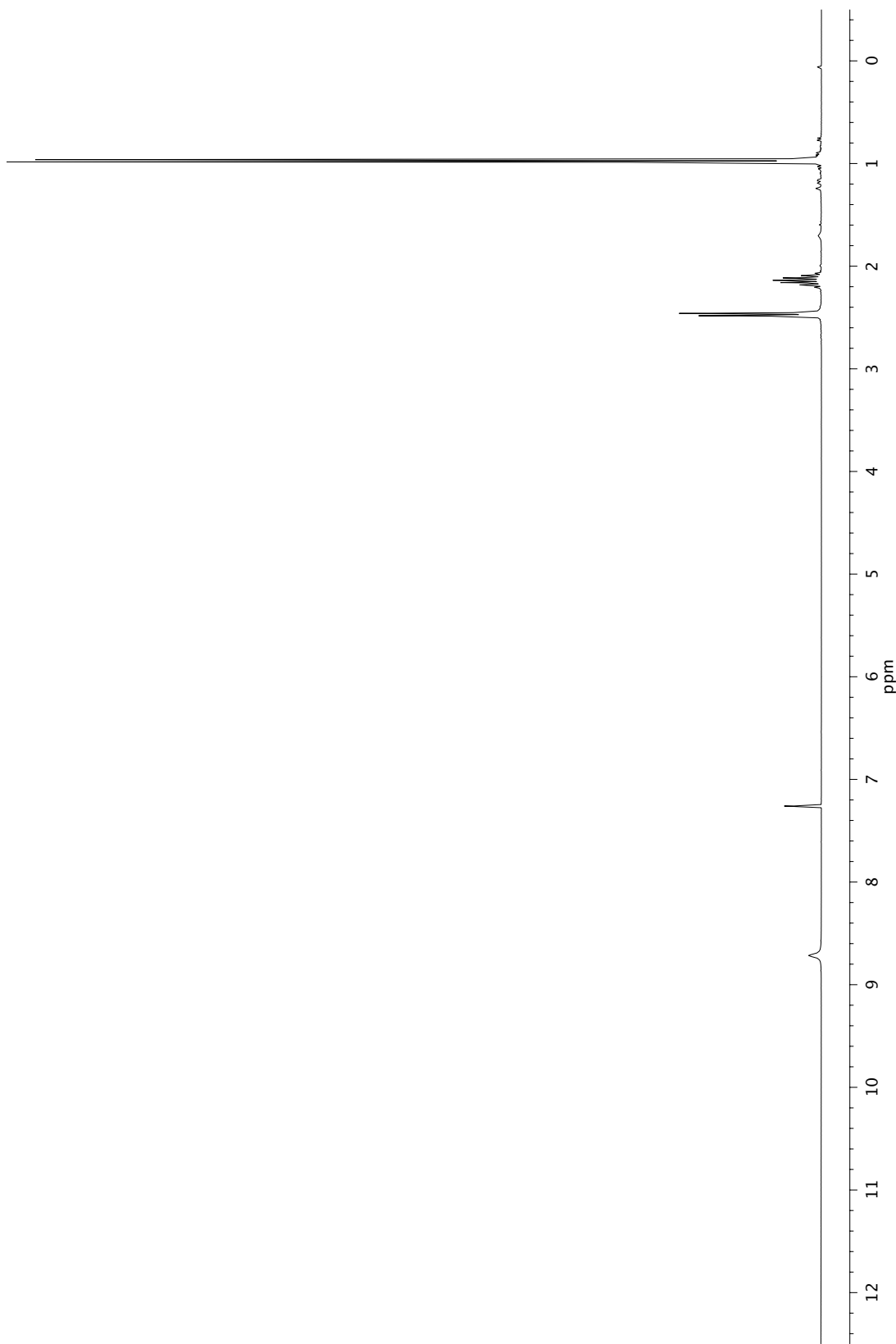
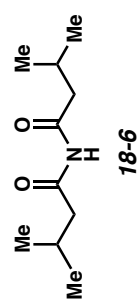
^{13}C NMR (126 MHz, CDCl_3) of compound **18-2**.



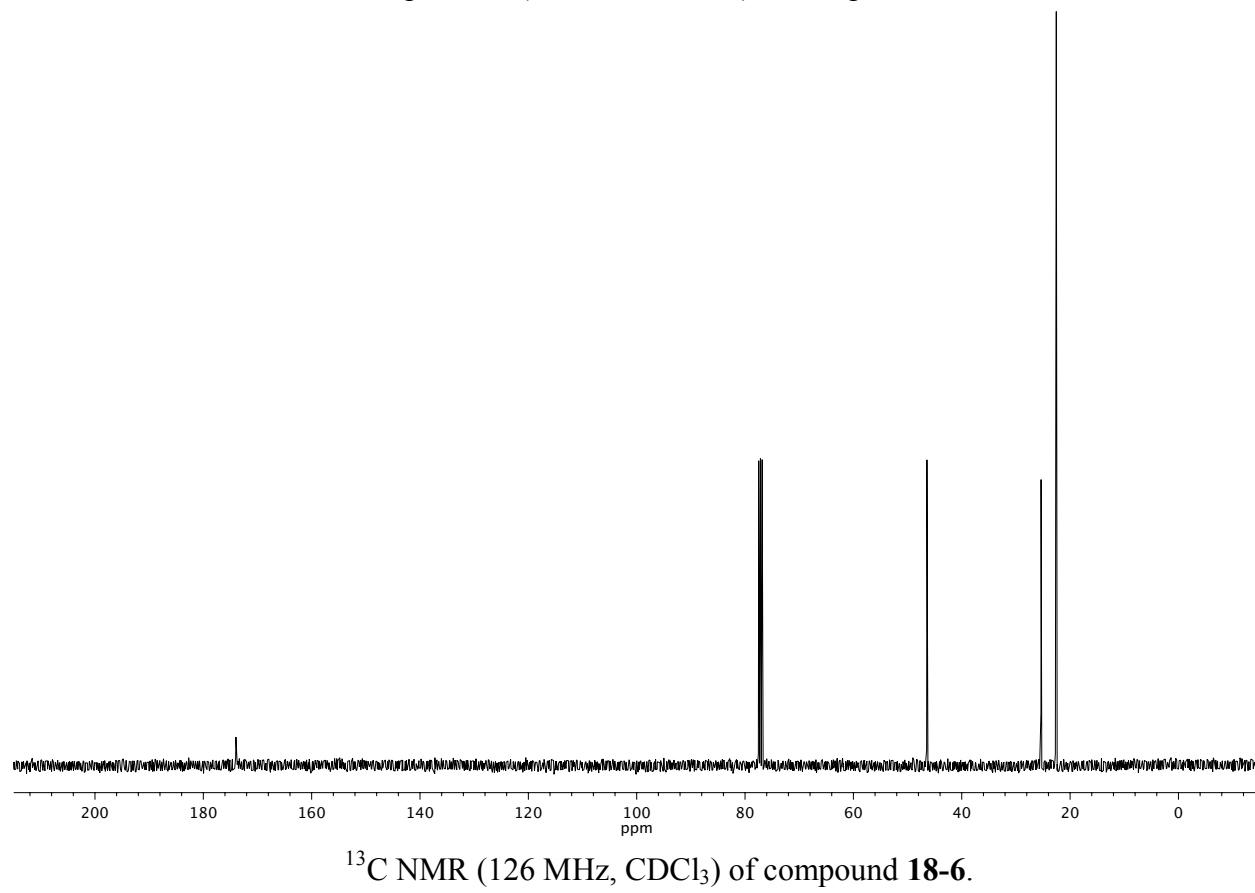
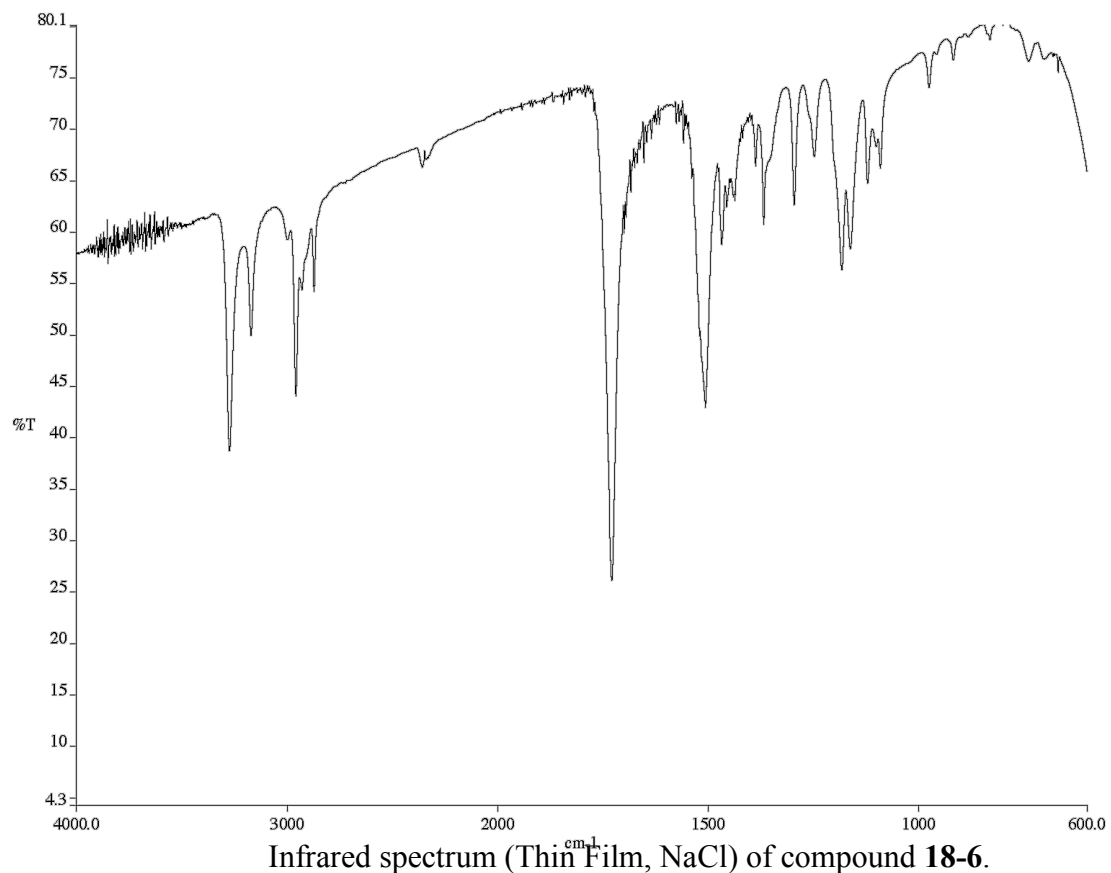
¹H NMR (500 MHz, CDCl₃) of compound 18-3.

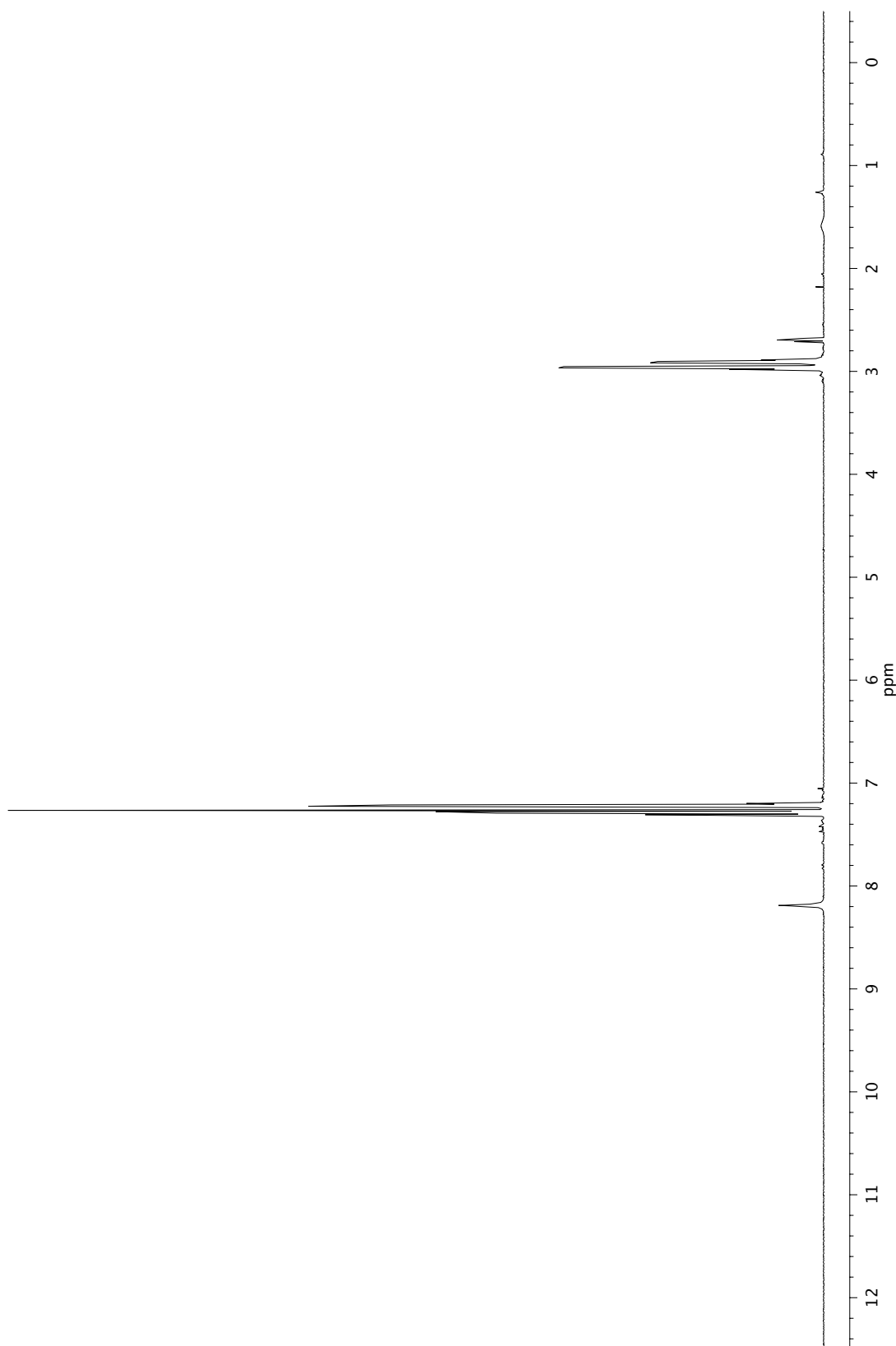
Infrared spectrum (Thin Film, NaCl) of compound **18-3**.

^{13}C NMR (126 MHz, CDCl_3) of compound **18-3**.

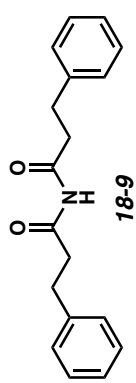


¹H NMR (300 MHz, CDCl₃) of compound 18-6.

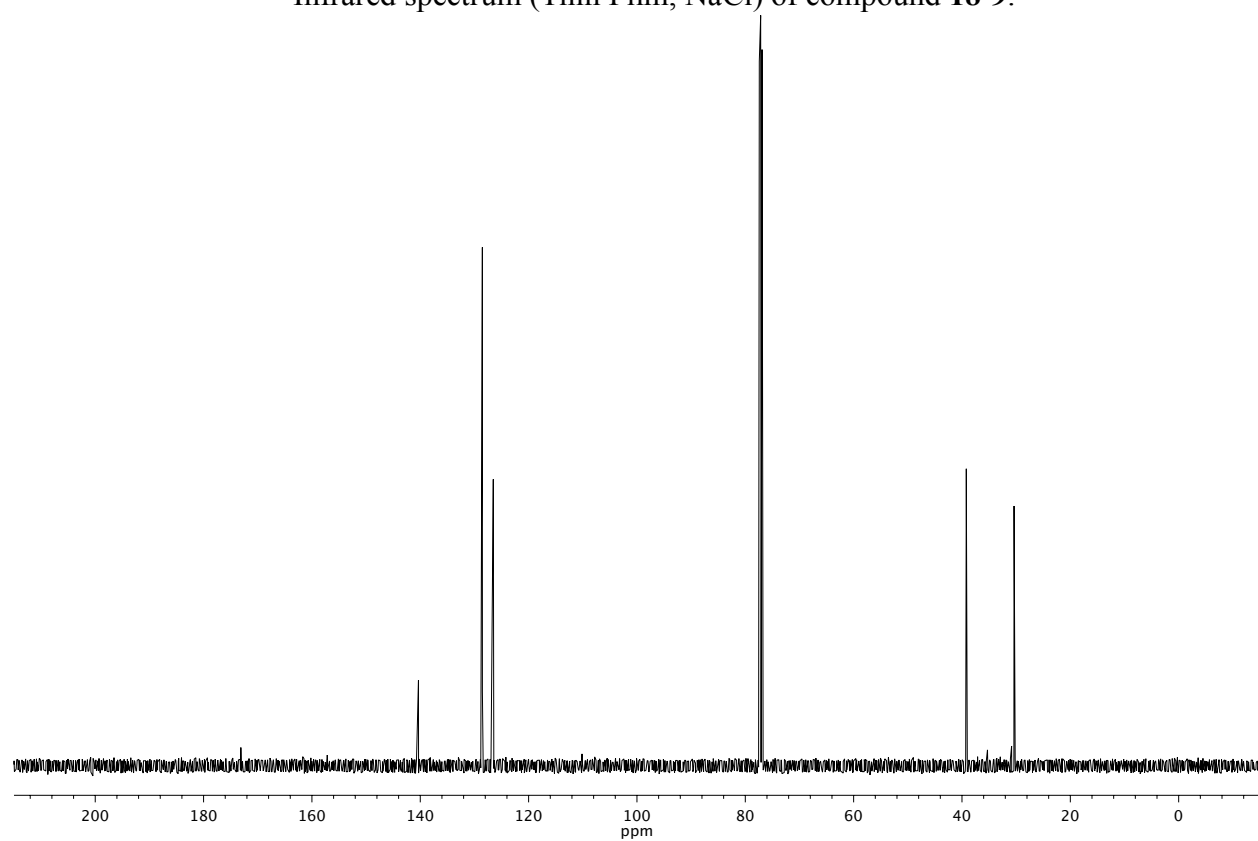




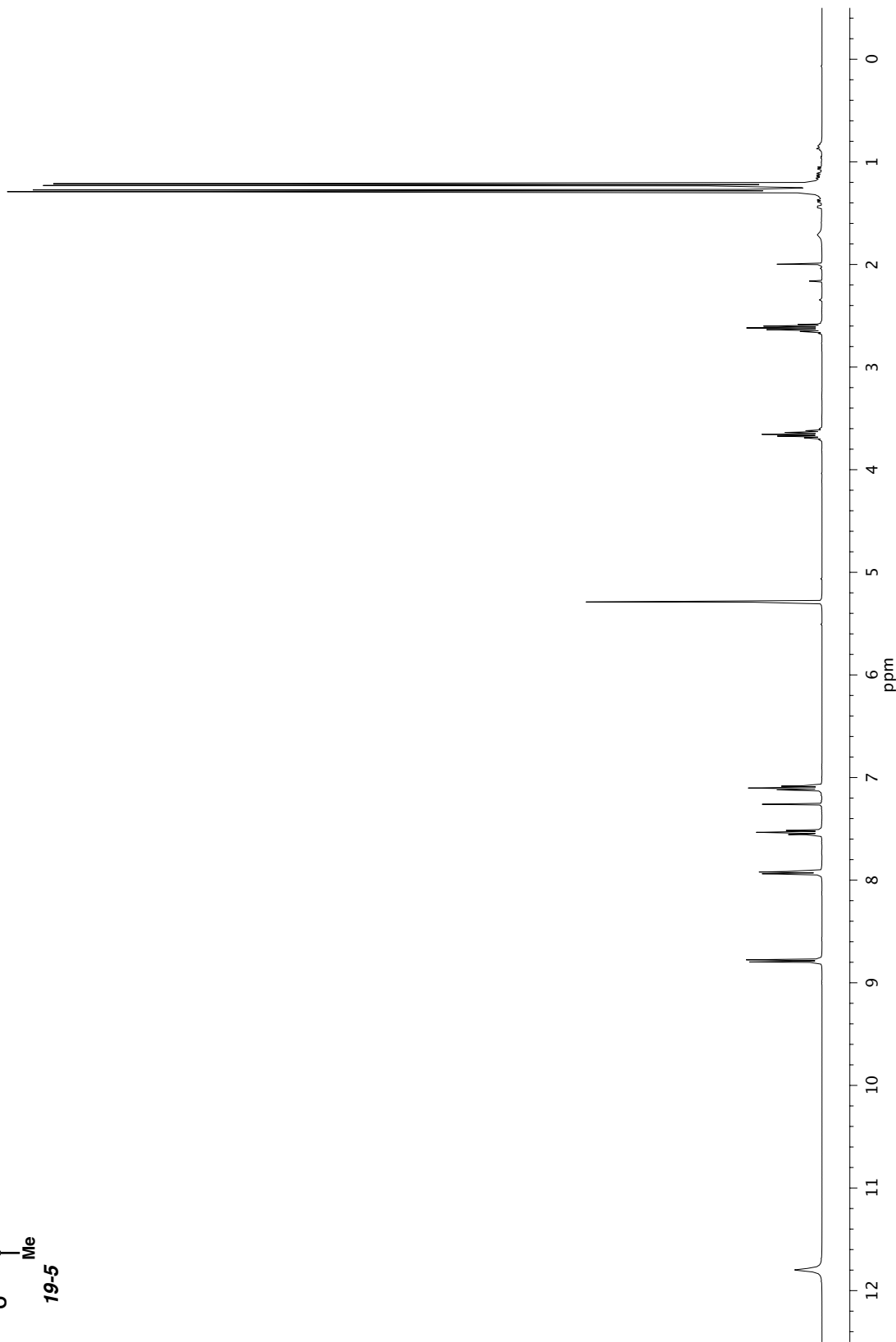
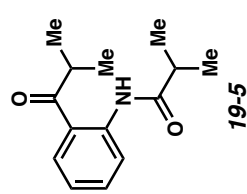
^1H NMR (500 MHz, CDCl_3) of compound **18-6**.



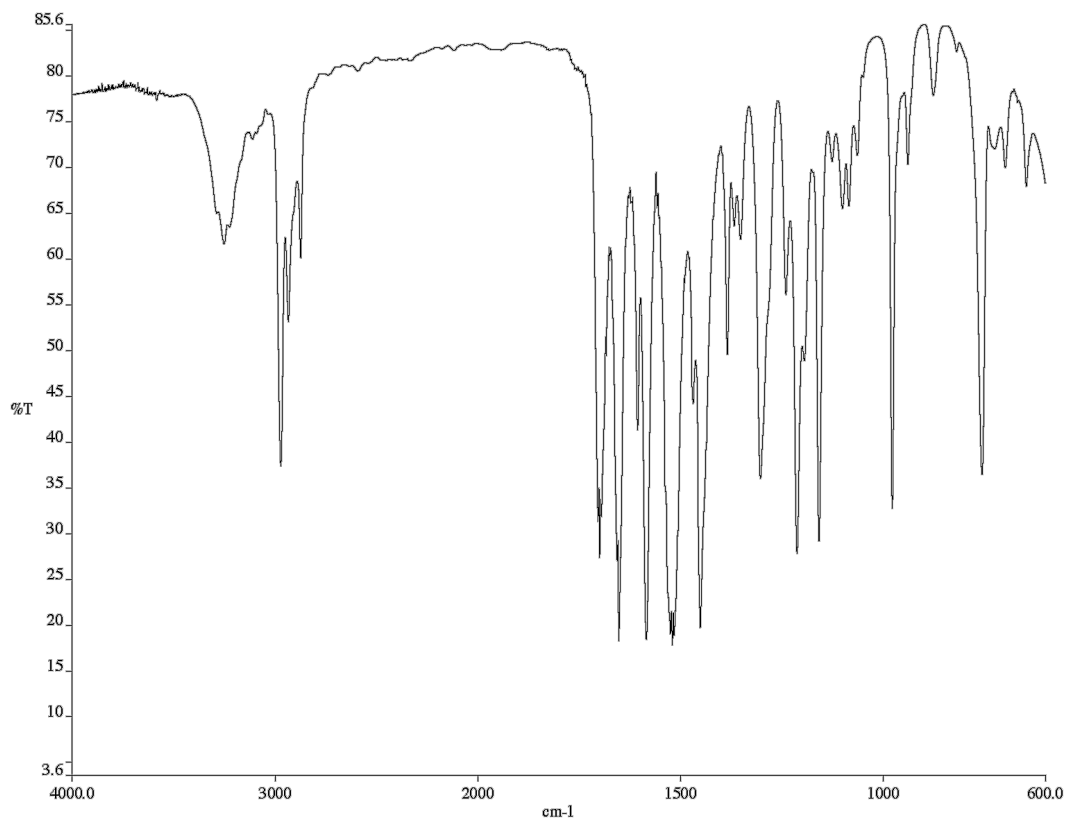
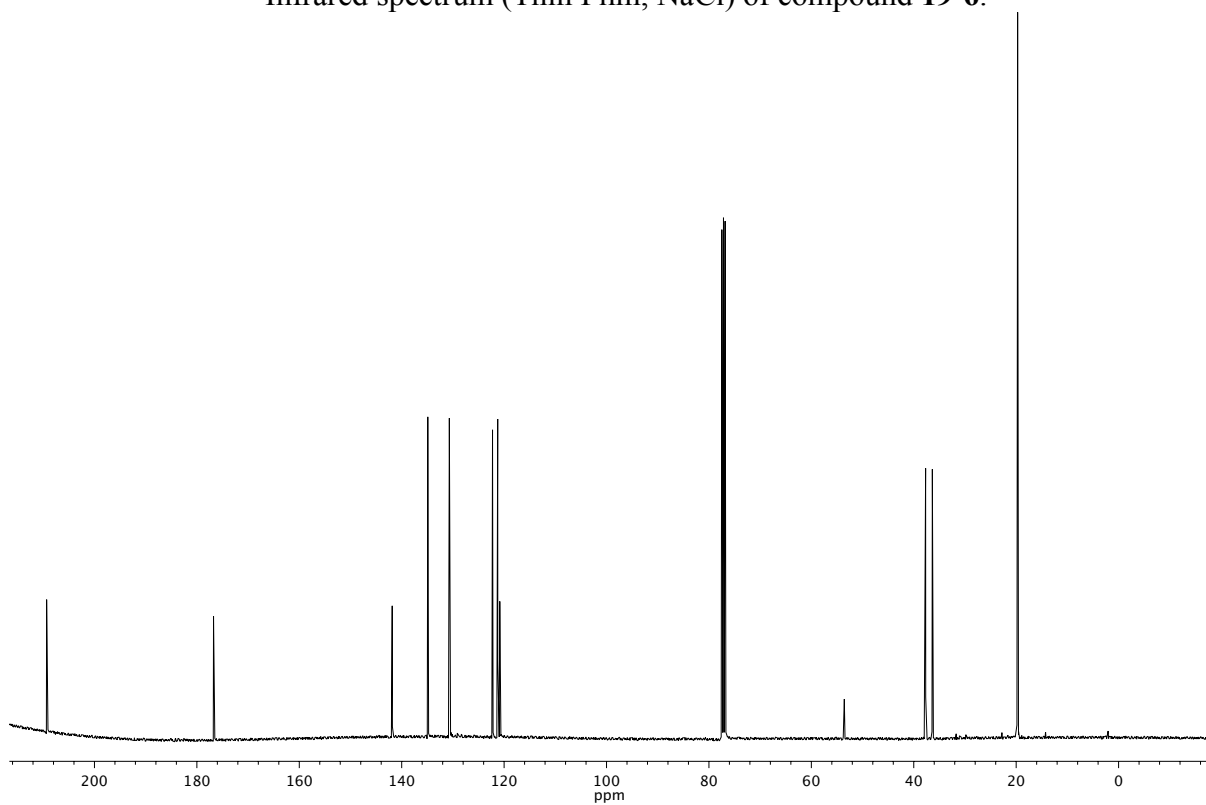
Infrared spectrum (Thin Film, NaCl) of compound **18-9**.

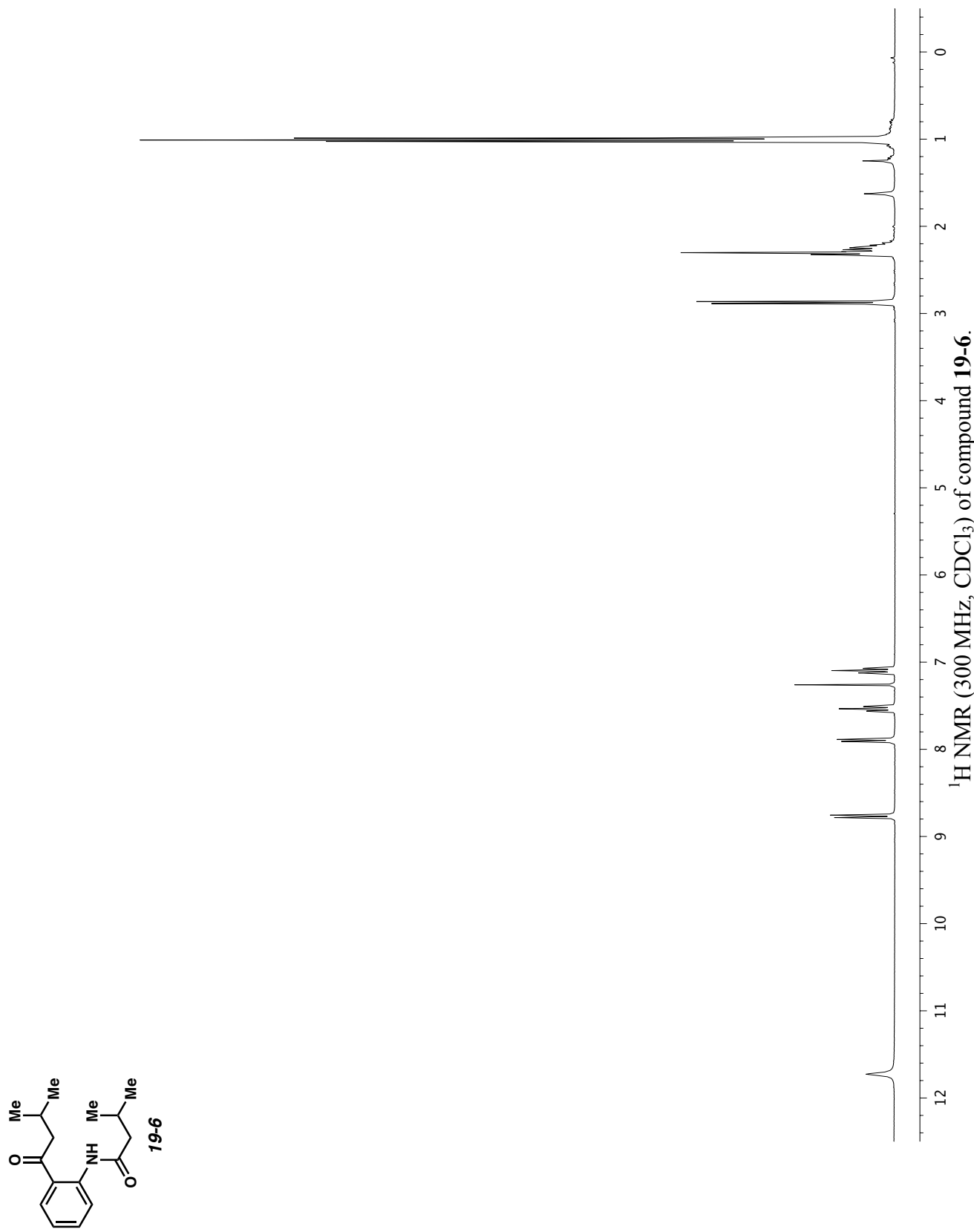


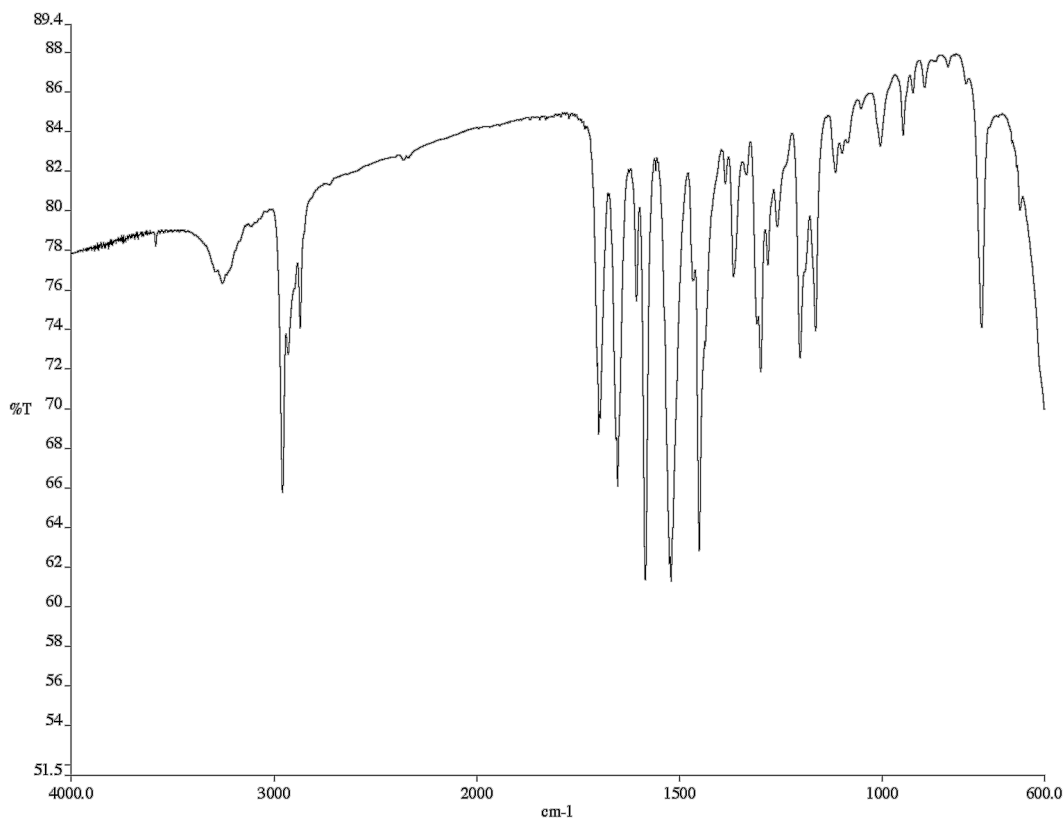
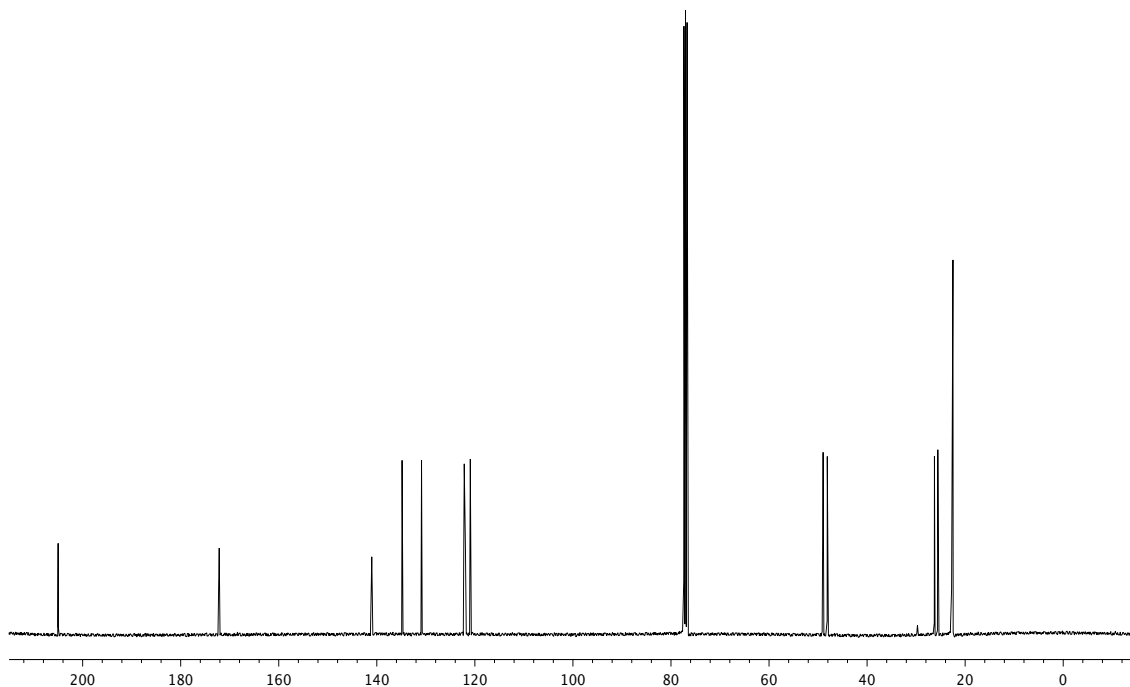
¹³C NMR (126 MHz, CDCl₃) of compound **18-6**.

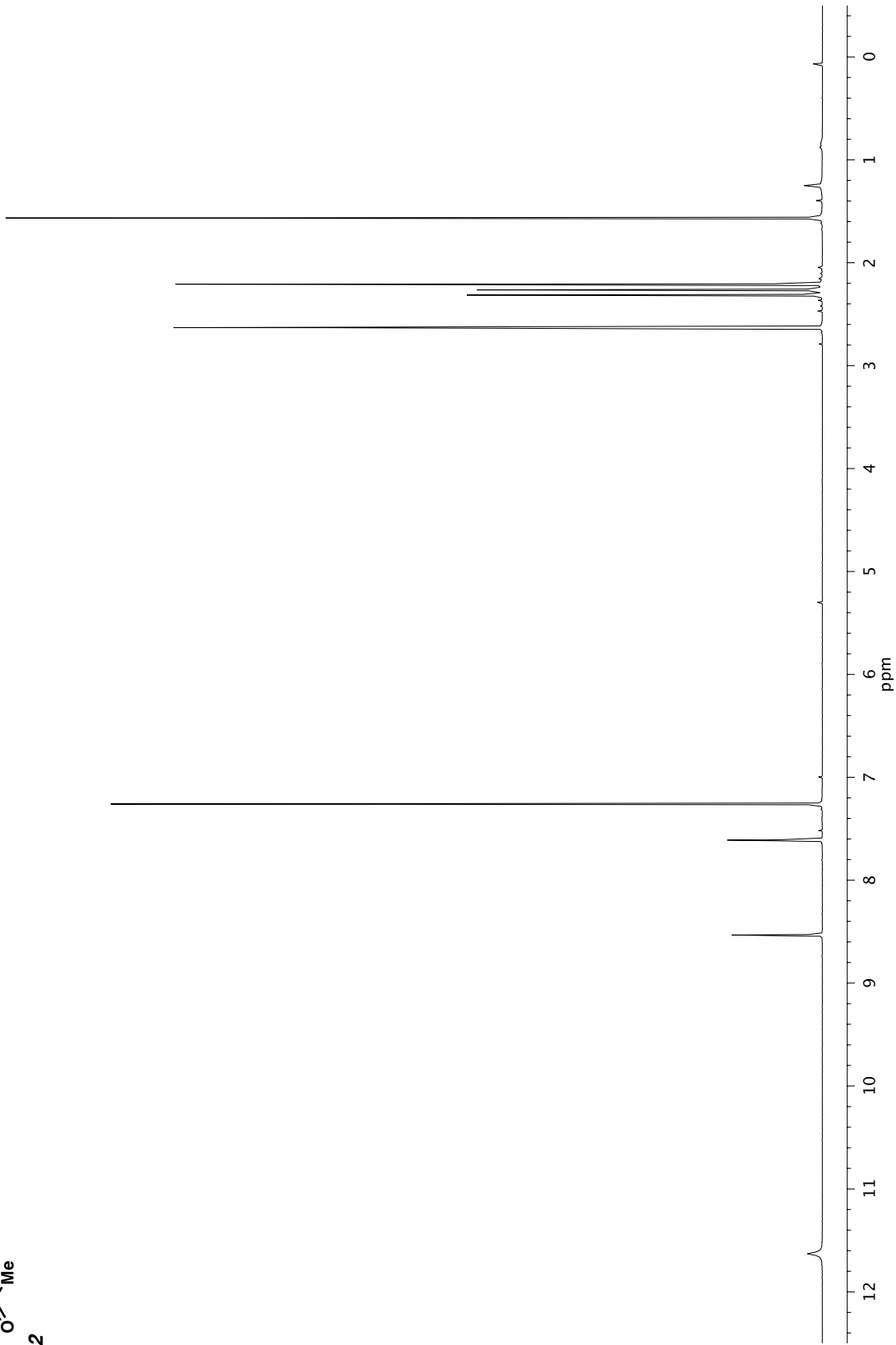
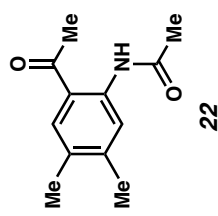


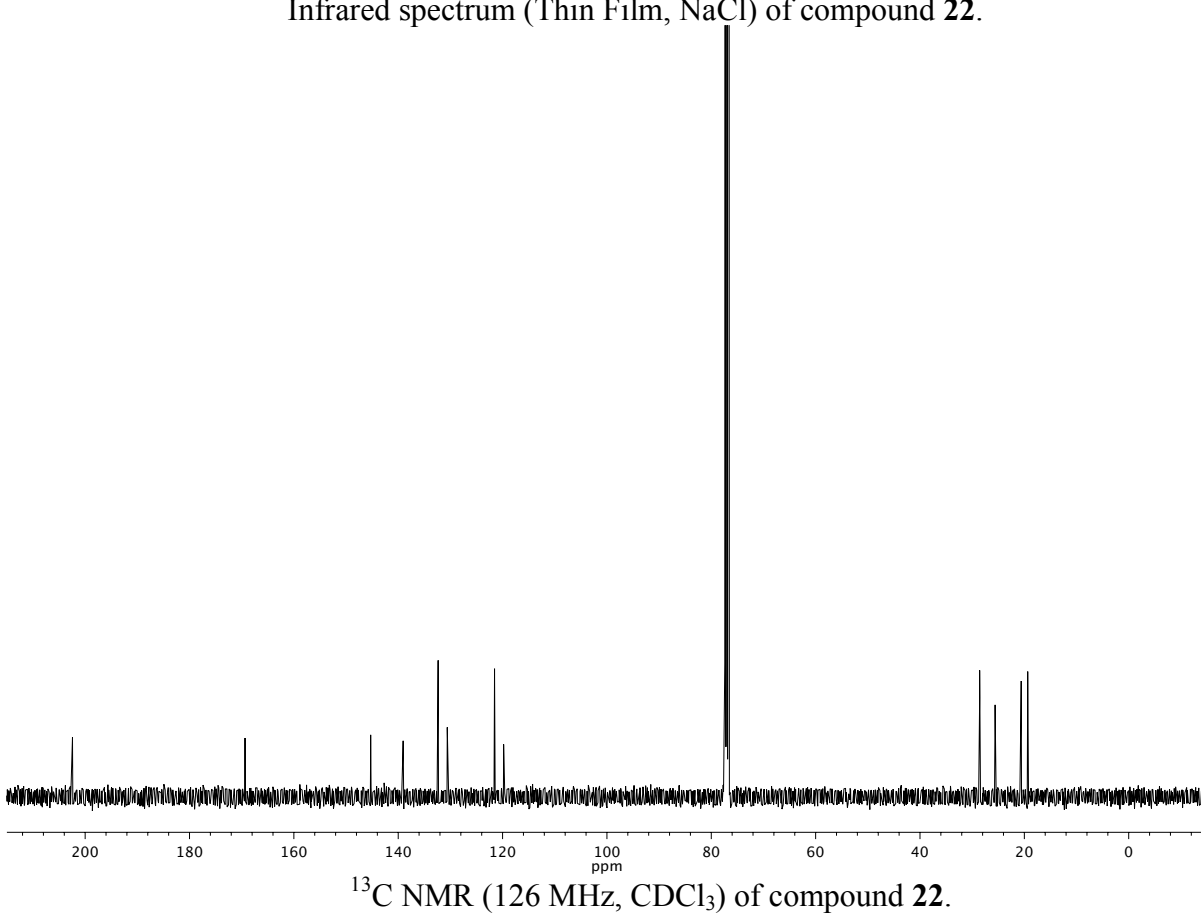
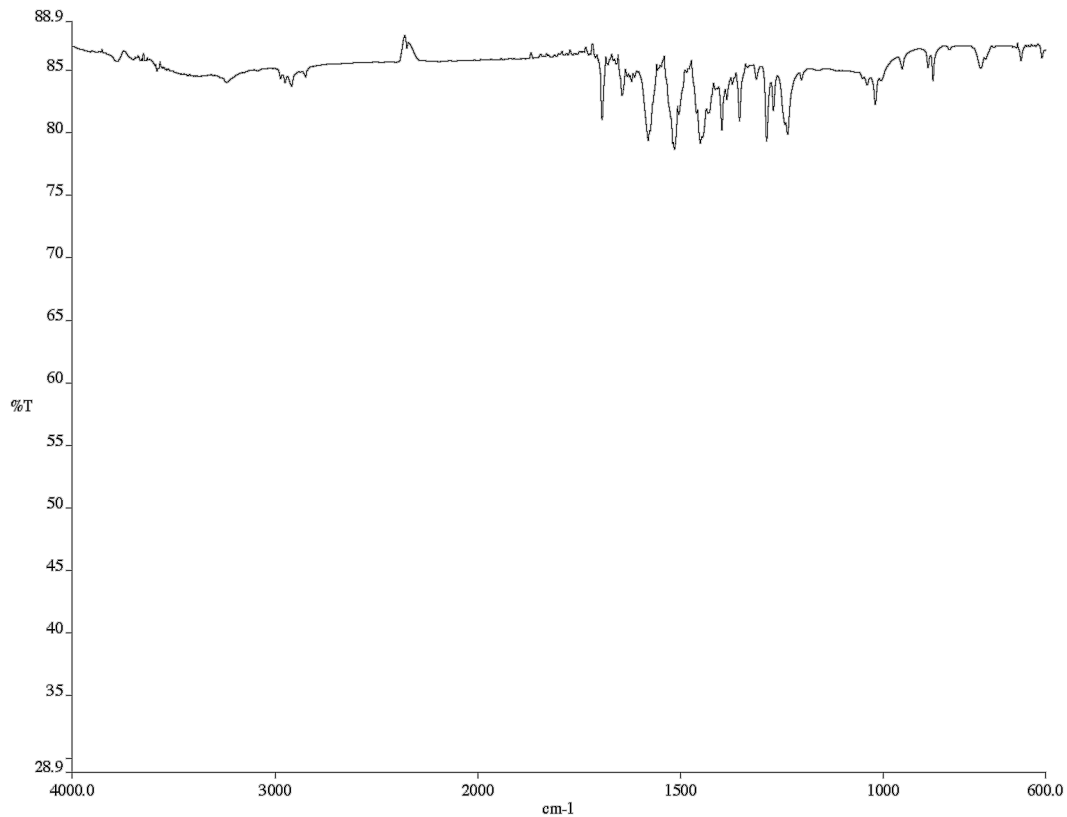
^1H NMR (300 MHz, CDCl_3) of compound 19-5.

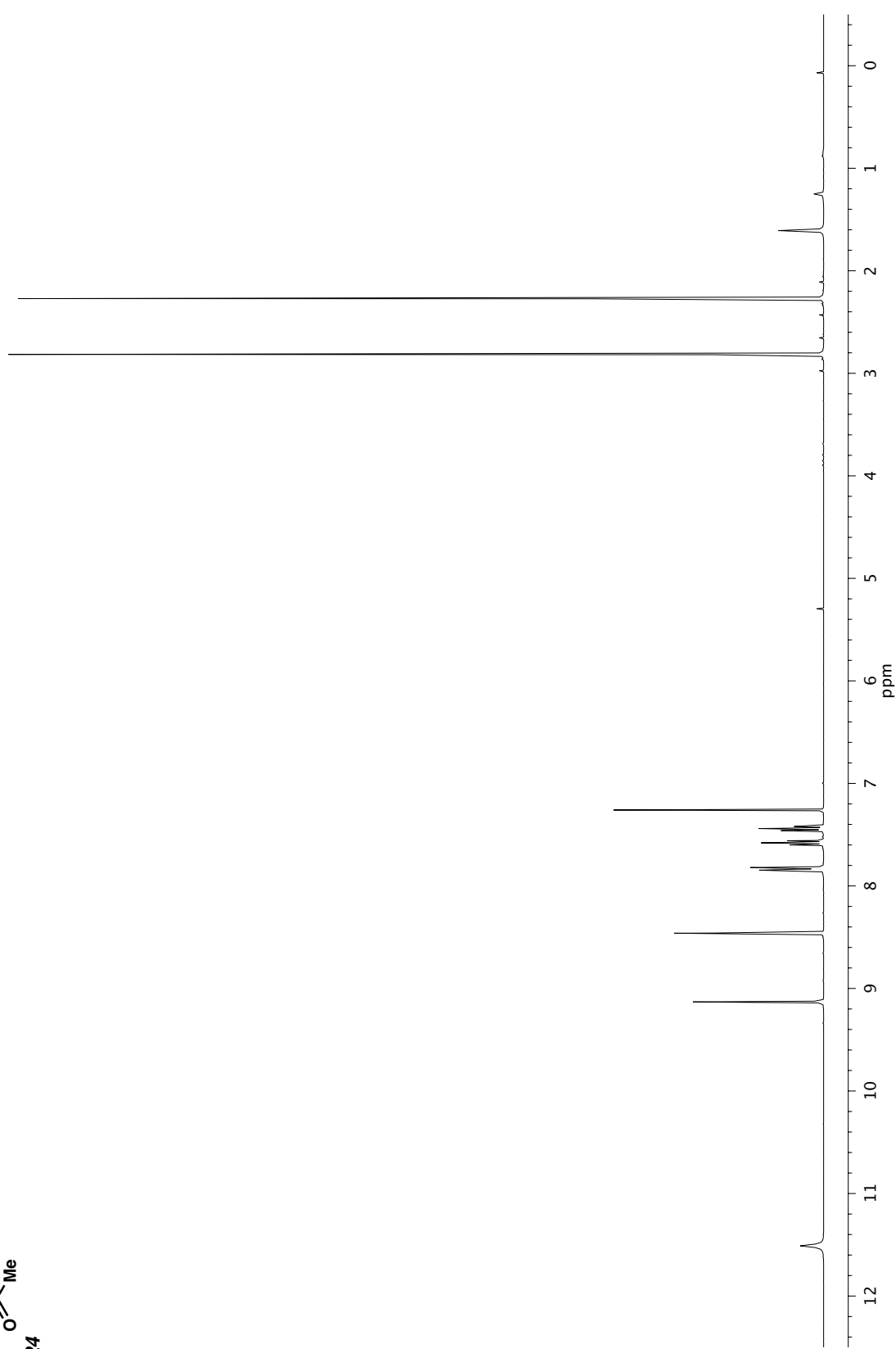
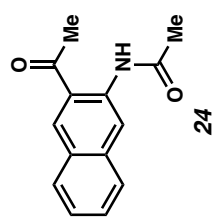
Infrared spectrum (Thin Film, NaCl) of compound **19-6**.¹³C NMR (126 MHz, CDCl₃) of compound **19-6**.



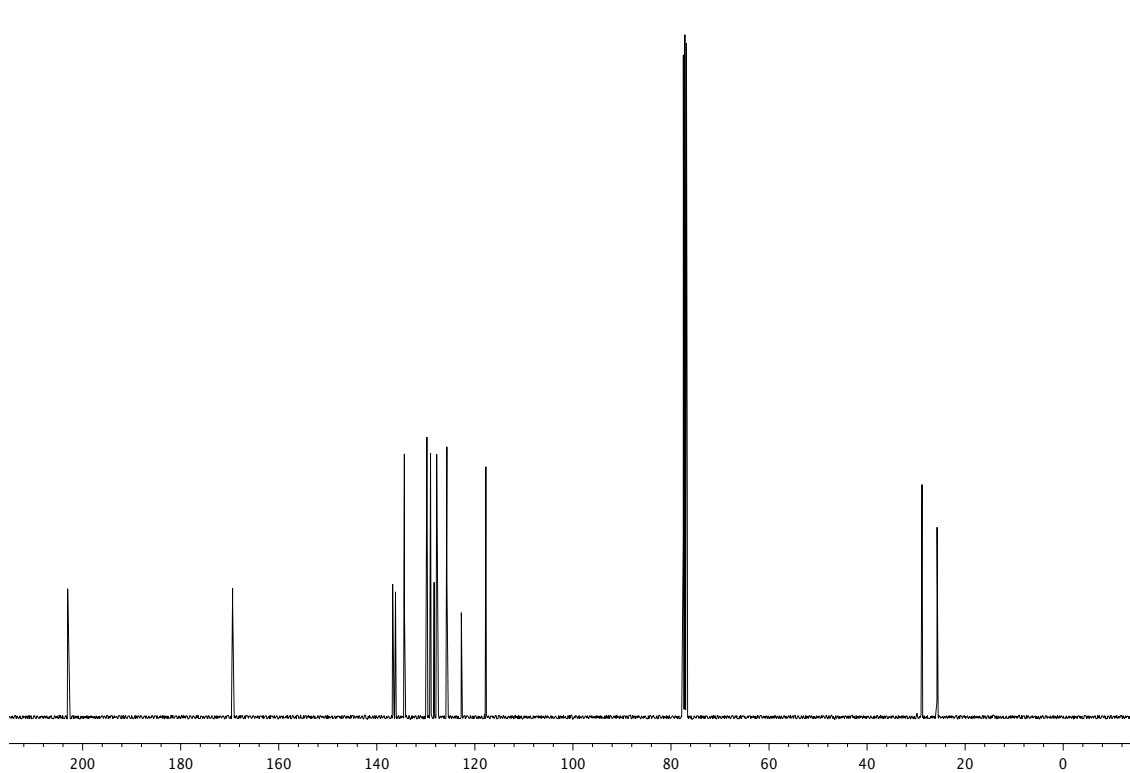
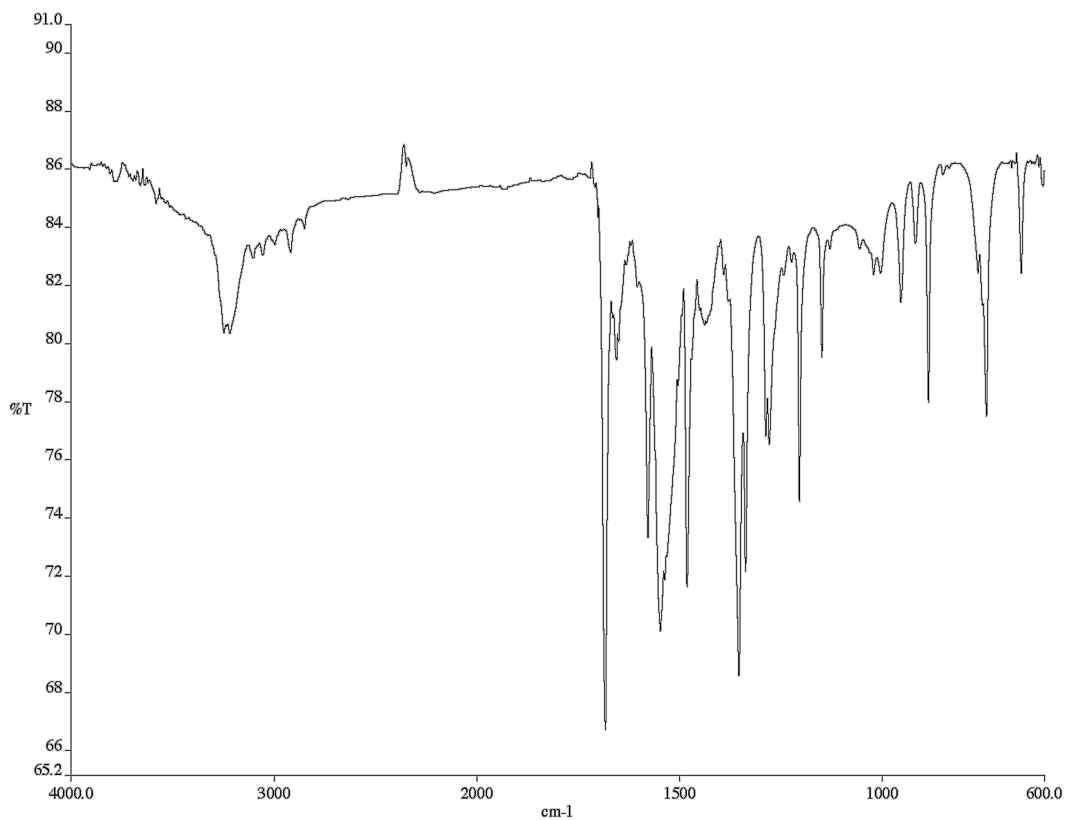
Infrared spectrum (Thin Film, NaCl) of compound **19-6**.¹³C NMR (126 MHz, CDCl₃) of compound **19-6**.

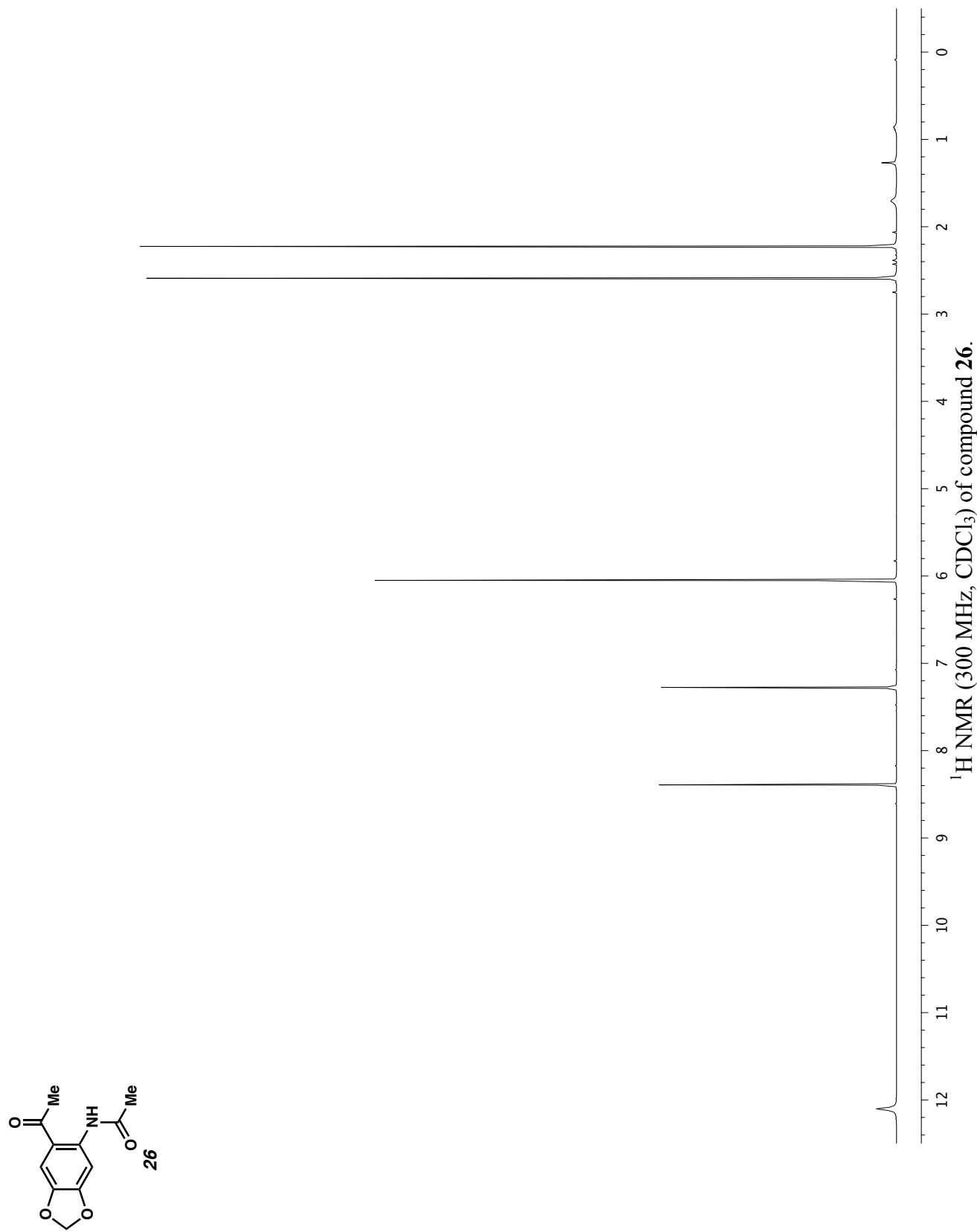


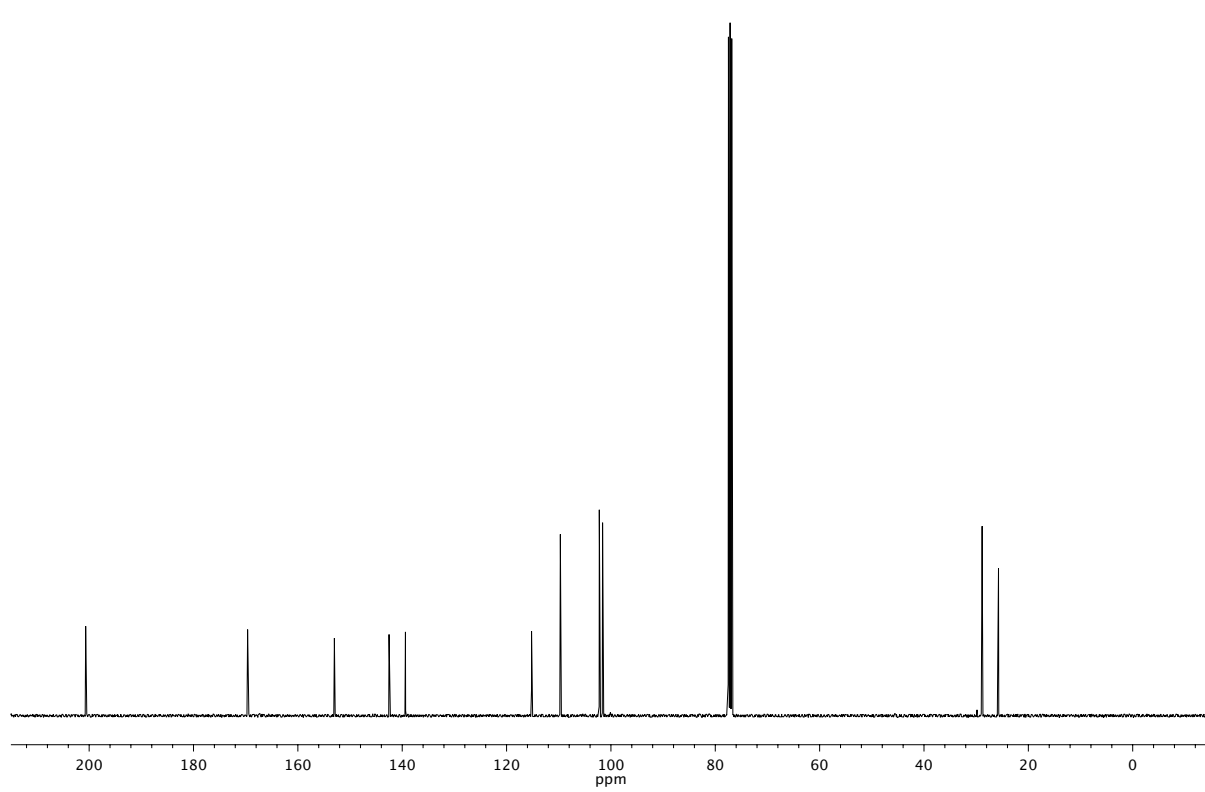
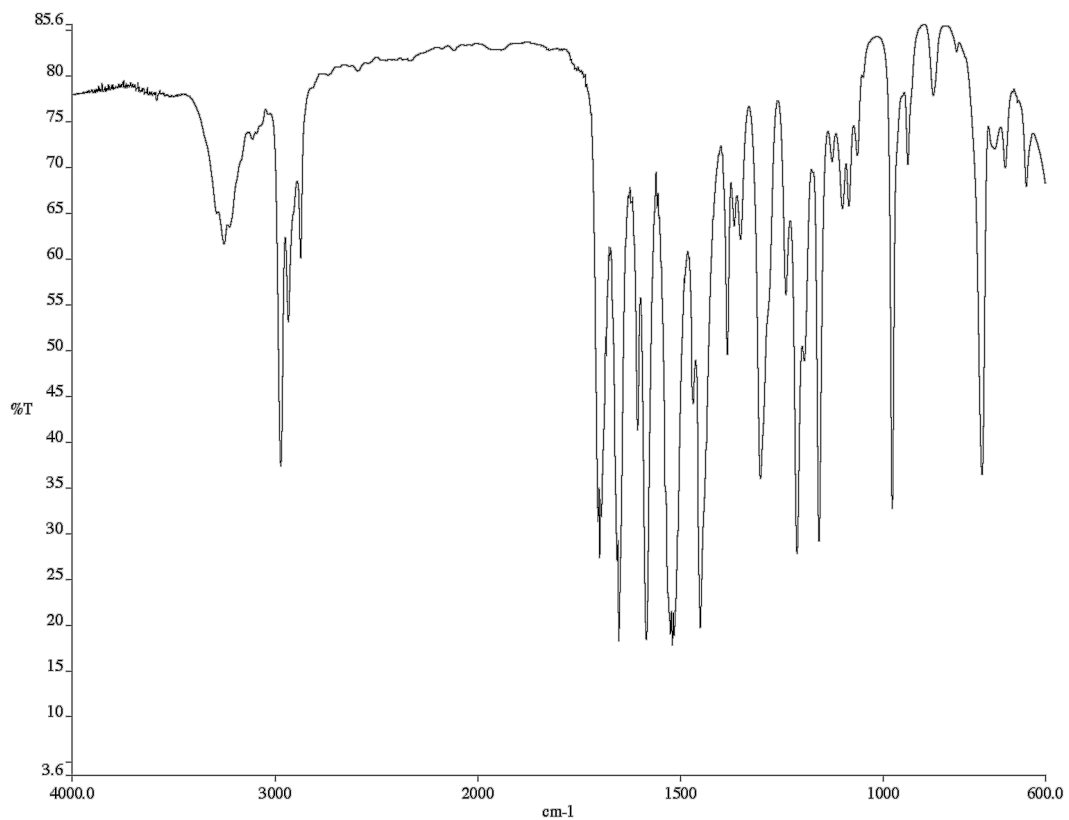


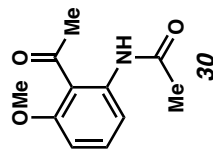
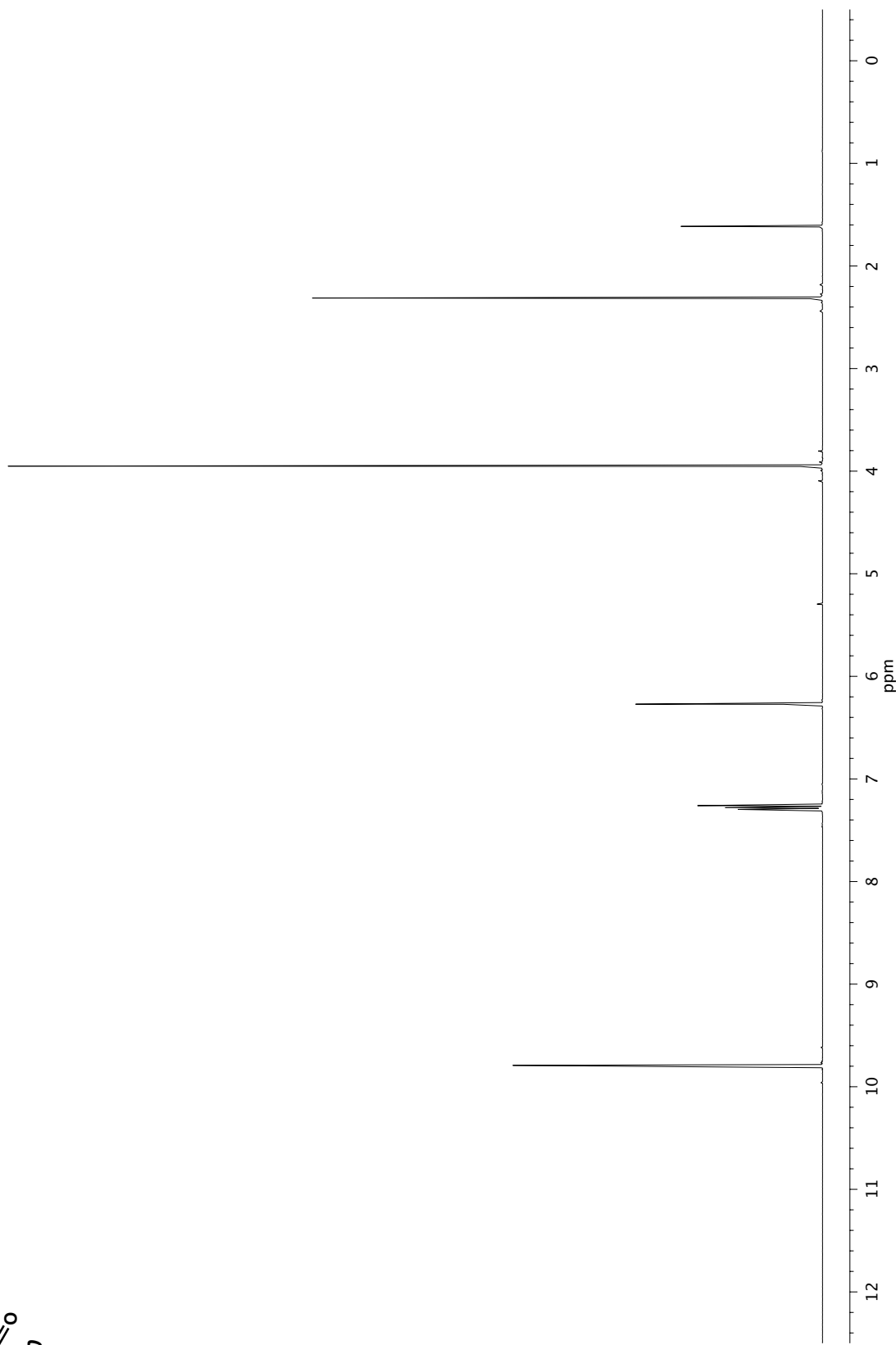


¹H NMR (300 MHz, CDCl₃) of compound 24.

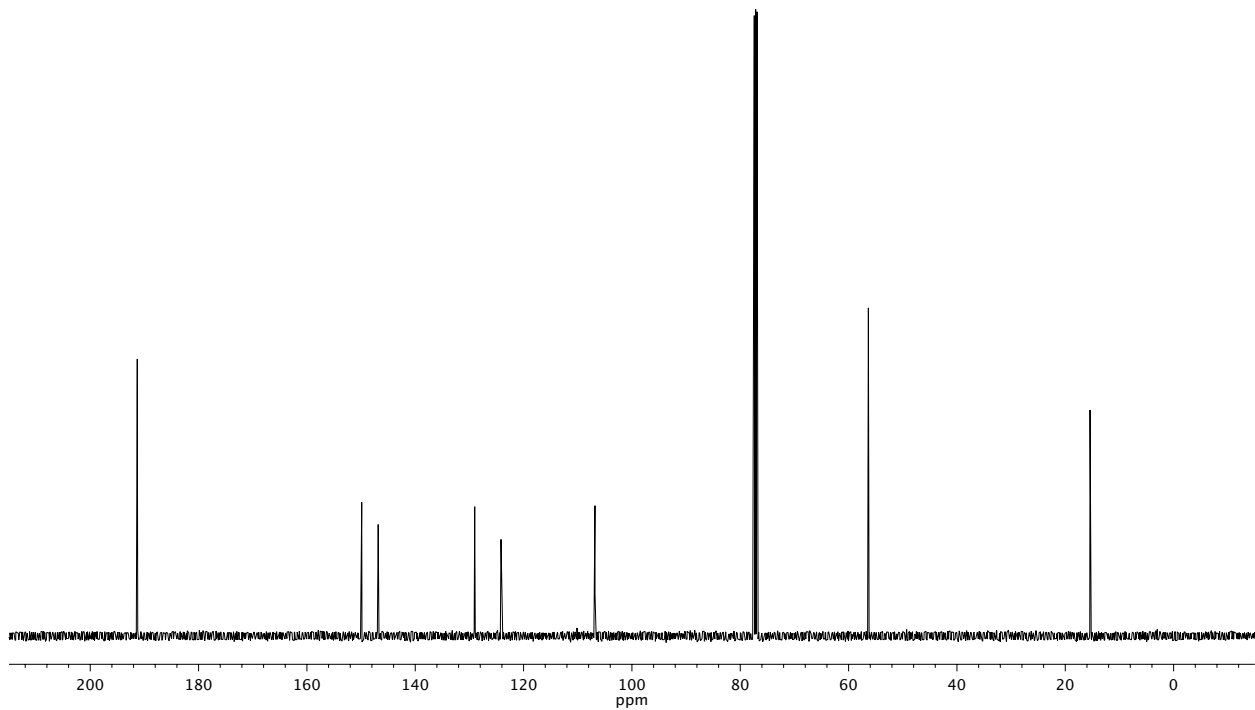








Infrared spectrum (Thin Film, NaCl) of compound **3g**.



^{13}C NMR (126 MHz, CDCl_3) of compound **3g**.

CHAPTER 2

Progress Toward the Total Synthesis of Jorumycin

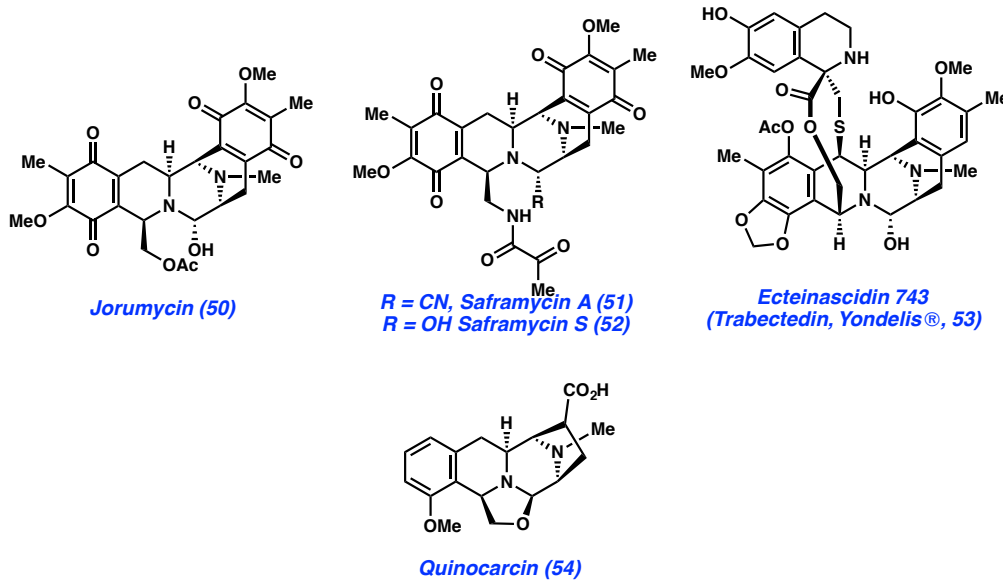
2.1 Introduction

Over the past decades, the tetrahydroisoquinoline (THIQ) alkaloids have piqued the attention of medicinal, biological, and chemical communities due to their novel biochemical modes of action, the potent biological properties they exhibit, and the complex molecular architectures characteristic of these molecules (Figure 1).¹ With more than 60 naturally occurring representatives, this family of compounds boasts a remarkable degree of structural diversity that translates into a wide array of antineoplastic/antiproliferative properties. For example, jorumycin (**50**) inhibits the growth of A549 human lung carcinoma and HT29 human colon carcinoma cell lines at extremely low concentrations ($IC_{50} = 0.24$ nM).² Saframycins A (**51**) and S (**52**) display nanomolar cytotoxicity toward L1210 leukemia cell lines ($IC_{50} = 5.6$, 5.3 nM, respectively). The therapeutic potential of these molecules is perhaps best conveyed by those members that have advanced through human clinical trials. Ecteinascidin 743

(Trabectedin, Yondelis, **53**) is approved in Europe, Russia, and South Korea for the treatment of soft tissue sarcomas and has been granted priority review by the FDA within the U.S. as a treatment for patients with advanced soft tissue sarcoma (STS), including liposarcoma and leiomyosarcoma subtypes, and phase III trials were recently completed.³

^{4a} In addition to their various antineoplastic properties, the THIQ alkaloids also possess broad-spectrum antibiotic activity against the Gram-positive and Gram-negative bacterial strains responsible for infectious diseases such as meningitis, pneumonia, strep throat, and diphtheria.⁵

Figure 2.1. Tetrahydroisoquinoline natural products.



While the numerous biological properties of the THIQ alkaloids make them ideal targets for pharmaceutical development, the isolation of material from natural sources is often expensive and low yielding.¹ Fortunately, in such cases, chemical synthesis can provide an alternative means to produce the quantities necessary for advanced biological testing. It is therefore of critical to develop synthetic methods that assemble these

important molecules in a concise and efficient manner. In 2010, we published on the total synthesis of quinocarcin (**54**), a mono-THIQ, and have recently turned our attention to the preparation of the related bis-THIQ alkaloids. In pursuit of this goal, we devised a general technique to rapidly construct the core of the THIQ alkaloids while providing avenues to introduce the varying peripheral functionality that make up this large and diverse class of natural products.

As the first such molecule to investigate, we selected joramycin (**50**), a bioactive isolate from the sea slug *Jorunna funebris*.^{6,7} Taking into account the fundamental structural features that joramycin (**50**) shares with other members of the class of bis-THIQ natural products containing the potent saframycins, safracins, renieramycins and cibrostatins, we believe that joramycin will serve as the cornerstone for a general, convergent, and concise strategy to its relatives.^{2,8,9}

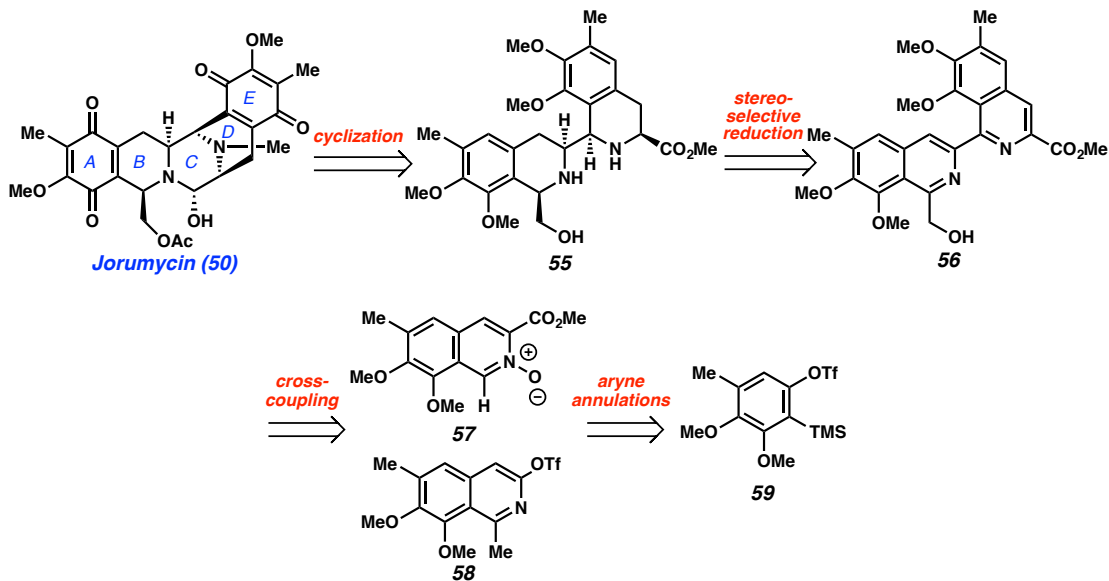
Herein, we have devised a synthetic route, which obviates such a need. Instead, our route to joramycin hinges on a diastereoselective reduction of a bis-tetrahydroisoquinoline, which itself can be prepared from a highly convergent cross-coupling of two isoquinoline subunits.

2.2 Retrosynthetic Analysis of Joramycin

Retrosynthetically, we envisioned that the pentacyclic bis-THIQ core of joramycin (**50**) could be accessed by late-stage assembly of the central C-ring piperazine. Consequently, we are targeted bis-THIQ **55**, which could undergo cyclization to form the pentacyclic core of joramycin. To construct this intermediate, we planned to reduce bis-isoquinoline **56** by a diastereoselective tetra-hydrogenative pathway. We believed that

this bis-isoquinoline could be furnished by an $\text{Csp}^2\text{-H/Csp}^2\text{-OTf}$ cross-coupling of two component isoquinolines (**57** and **58**), each of which could be prepared by methods previously developed in our laboratories from a single aryne precursor **59**.¹⁰ This highly modular approach distinguishes itself from previous syntheses by convergently generating the carbon framework of the bis-THIQ alkaloids in a regio- and stereoselective manner without the use of one or more Pictet-Spengler reactions in a linear sequence.¹ Strategies utilizing the Pictet-Spengler reaction necessitate the use of electron-rich arenes. Our approach eliminates this need and allows one to envision access to an array of THIQ analogs, simply by varying the aryne precursor.

Scheme 2.1. Retrosynthetic Analysis of Jorumycin.

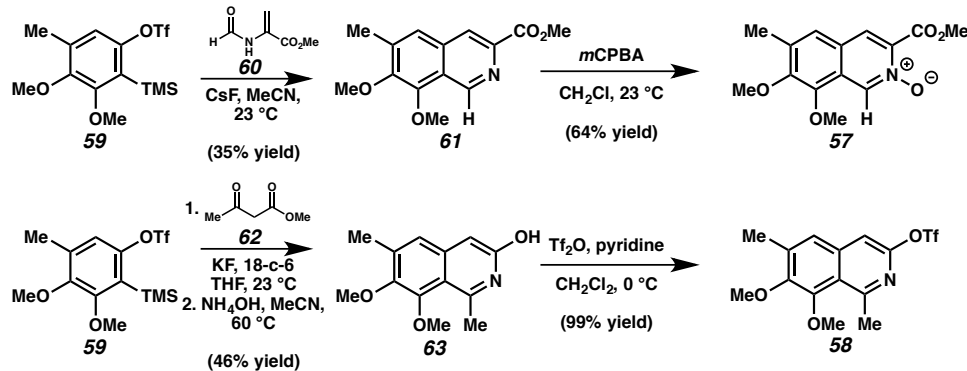


2.3 Synthesis of Jorumycin

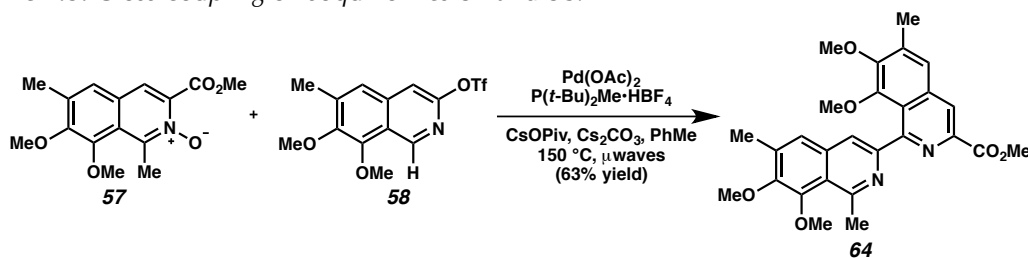
We began our synthesis of jorumycin by looking to prepare isoquinolines **57** and **58** (Scheme 2.2). Our lab has developed two methods for the regioselective synthesis of

highly substituted isoquinolines.¹⁰ The *N*-oxide coupling partner **57** was attained through the annulation of silyl aryl triflate **58** with methyl 2-formamidoacrylate (**60**). Subsequent oxidation using *m*CPBA affords the Csp²–H coupling partner **57**. We next turned our attention to 3-isoquinoline triflate **58**. Acyl-alkylation of the same silyl aryl triflate **58** was accomplished upon exposure to KF and methyl acetoacetate (**62**). Subsequent condensation with ammonium hydroxide furnished 3-hydroxy isoquinoline **63**, which was quantitatively triflated using triflic anhydride to afford our desired isoquinoline Csp²–OTf coupling partner (**58**).

Scheme 2.2. Preparation of isoquinolines **57** and **58**.

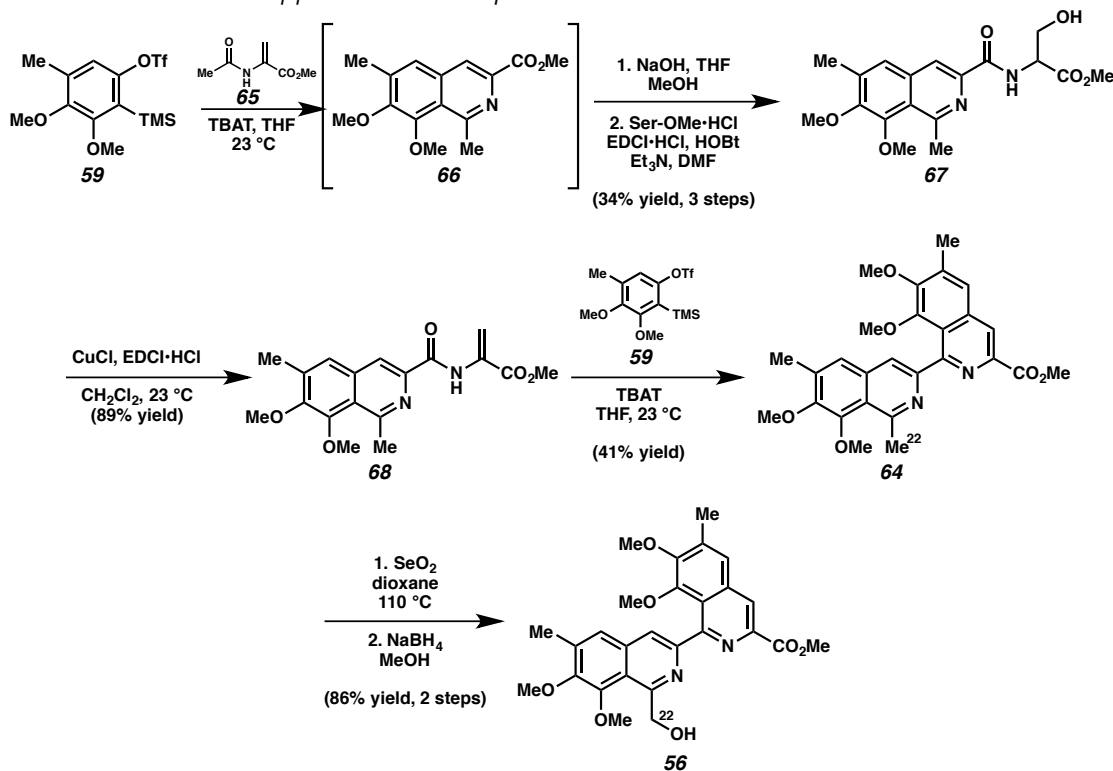


We next examined the convergent coupling of the two isoquinoline fragments. To this end, we investigated Pd-catalyzed oxidative coupling reactions, originally reported by Fagnou, that enable the coupling of aryl halides and heterocyclic *N*-oxides by C–H functionalization.¹¹ In the event, isoquinoline *N*-oxide **57** and triflate **58** were successfully coupled to furnish bis-isoquinoline **64** using modified Fagnou conditions (Scheme 2.3).

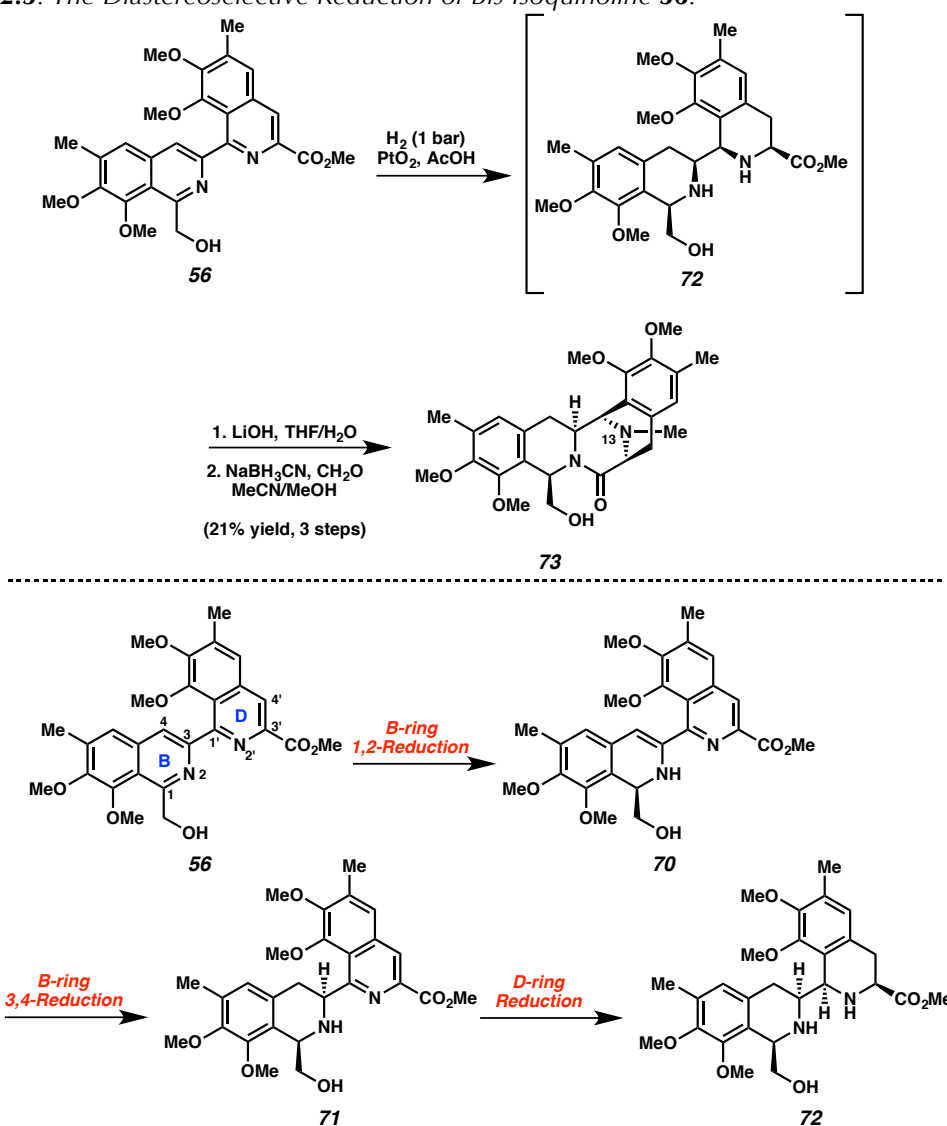
Scheme 2.3. Cross-coupling of isoquinolines **57** and **58**.

While the cross-coupling of our two isoquinoline quinolone fragments represents a highly convergent route to the bis-THIQ, the scalability of our aryne annulation reaction to prepare isoquinoline ester **61** was not ideal (22% yield from **59** to **57**) and led us to devise an alternative route to bis-isoquinoline **64**. While methyl 2-formamidoacrylate (**65**) proved to be a difficult substrate for our aryne annulation methodology, methyl 2-acetamidoacrylate (**65**) has been a robust annulation partner. We therefore pursued a sequence in which aryne annulation, saponification and amide formation furnishes serine derivative **67** (Scheme 2.4). Dehydration affords amidoacrylate **68**, which we can use in a second regio-selective aryne annulation reaction thus providing bis-isoquinoline **64**. While this route provides a similar overall yield to the cross-coupling strategy, it has proven to be more scalable, providing greater quantities of bis-isoquinoline **64**.

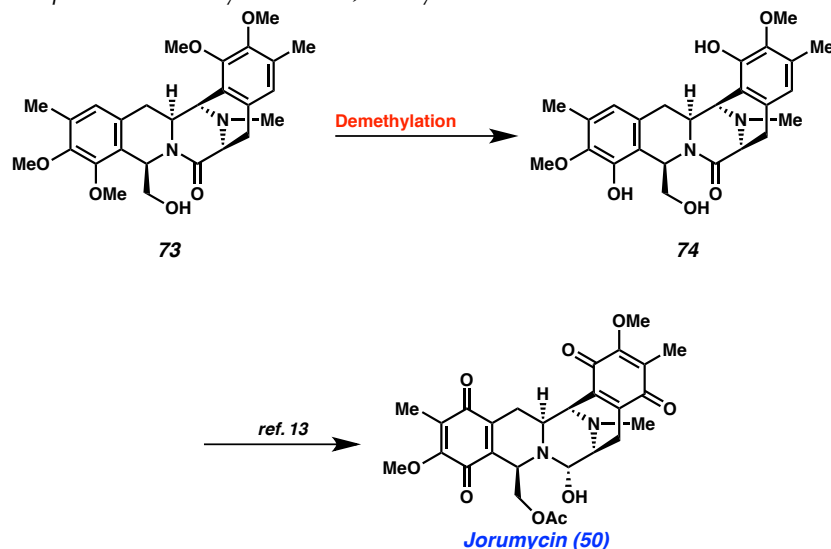
With a robust method for the preparation of bis-isoquinoline **64** available, we turned our attention to the latter steps of the synthesis, namely oxidation of C(22), tetrahydrogenation of the bis-isoquinoline core and C-ring formation. Initially, we found that bis-isoquinoline **11** undergoes smooth benzylic oxidation upon treatment with SeO₂ at C(22) and subsequent reduction of the resultant aldehyde to afford the hydroxymethyl bis-isoquinoline **7** in 86% yield (Scheme 2.4).

Scheme 2.4. Alternative approach to bis-isoquinoline **64**.

With bis-isoquinoline **56** in hand, we turned our attention to the key reduction of this intermediate.¹² After extensive experimentation we discovered that exposure of bis-isoquinoline **56** to Adams' catalyst, hydrogen gas, and acetic acid, followed by LiOH-induced cyclization provides a pentacyclic lactam. This compound was treated with formaldehyde and NaBH3CN to install a CH₃ at N(12) with the desired all *cis* stereochemistry (Scheme 2.5). This allowed for the isolation of THIQ **73** in 21% yield overall yield. Although the isolated yield of THIQ **73** is moderate, it is the only characterizable bis-THIQ structure that we have been able to isolate to date. Given the complexity of the tetrahydrogenation reaction, it is remarkable that the process proceeds with good diastereoselectivity. We believe this diastereoselectivity is a function of a self-reinforcing situation, wherein each hydrogenation enhances the stereoselectivity of the subsequent event (Scheme 2.5).

Scheme 2.5. The Diastereoselective Reduction of Bis-Isoquinoline **56**.

With this highly diastereoselective reduction/cyclization sequence, we have accessed the core of the bis-THIQ alkaloid natural products in a highly convergent and rapid manner in 9 steps from aryne precursor **59**. Selective bis-demethylation of pentacycle **73** provides bis-phenol **74**, which can be advanced to several bis-THIQ alkaloids by known sequences of minimal steps. In the case of jorumycin (**1**), 4 steps are needed for intermediate **74**.¹³

Scheme 2.6. Completion of the Synthesis of Jorumycin.

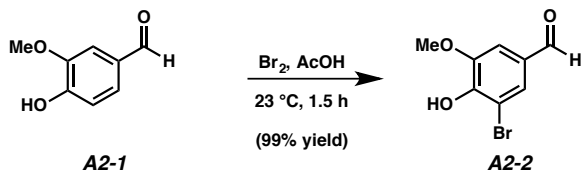
A highly convergent synthesis of (\pm) -jorumycin has been achieved. Unlike previous syntheses, our approach relies on the convergent cross-coupling of two isoquinoline subunits followed by a highly diastereoselective reduction and cyclization sequence to access the pentacyclic core, eliminating the need for electron-rich arenes to perform electrophilic aromatic substitution reactions. Our laboratory is currently using this strategy to prepare other members of this important class of natural products along with non-natural derivatives thereof.

2.4 EXPERIMENTAL SECTION

2.4.1 Materials and Methods

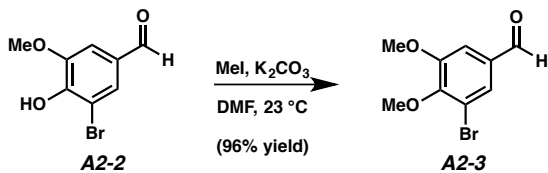
Unless stated otherwise, reactions were performed in flame-dried glassware under an argon or nitrogen atmosphere using dry, deoxygenated solvents (distilled or passed over a column of activated alumina). Commercially obtained reagents were used as received. Reaction temperatures were controlled by an IKA mag temperature modulator. Thin-layer chromatography (TLC) was performed using E. Merck silica gel 60 F254 precoated plates (0.25 mm) and visualized by UV fluorescence quenching, potassium permanganate, or CAM staining. SiliaFlash P60 Academic Silica gel (particle size 0.040-0.063 mm) was used for flash chromatography. ^1H and ^{13}C NMR spectra were recorded on a Varian 500 (at 500 MHz and 125 MHz, respectively) and are reported relative to CHCl_3 (δ 7.24). Data for ^1H NMR spectra are reported as follows: chemical shift (δ ppm) (multiplicity, coupling constant (Hz), integration). Data for ^{13}C spectra are reported in terms of chemical shift relative to CHCl_3 (δ 77.23). IR spectra were recorded on a Perkin Elmer Paragon 1000 Spectrometer and are reported in frequency of absorption (cm^{-1}). HRMS were acquired using an Agilent 6200 Series TOF with an Agilent G1978A Multimode source in electrospray ionization (ESI), atmospheric pressure chemical ionization (APCI) or mixed (MM) ionization mode.

2.4.2 Preparative Procedures Spectroscopic Data



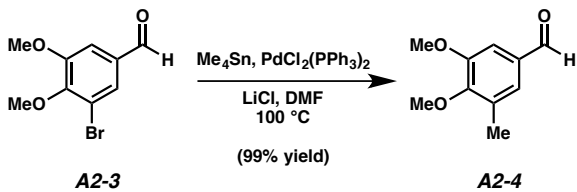
3-Bromovanillin (A2-2)

The following procedure was adopted from a literature report by Rao and Stuber.¹⁴ A single-neck, 2 L round-bottom flask was charged with vanillin (A2-1, 50 g, 328.6 mmol). Glacial acetic acid was added (1.1 L, 3.0 M). Following this, a mechanical stirrer was affixed to the flask through the neck and, with vigorous but even stirring, the vanillin dissolved to form a pale yellow solution. At this point, neat bromine (16.84 mL, 361.5 mmol) was added in a rapid dropwise fashion to the stirring solution through the flask neck to produce a deep red-orange solution. Following addition, the reaction was maintained with vigorous stirring for 90 minutes, after which time TLC analysis indicated formation of the product ($R_f = 0.32$, 15% ethyl acetate in hexanes). The reaction also results in the formation of a bright orange-yellow precipitate when nearing completion. Upon completion of the reaction, the mechanical stirrer was disengaged and the contents of the reaction flask were poured onto chilled deionized water (0 °C, 600 mL), resulting in further precipitation of a pale yellow solid from the bright orange aqueous layer. The reaction flask was washed into this flask with more chilled water. While still cooled, the contents of the 1 L Erlenmeyer flask were filtered over a glass frit to separate the desired solid product. The isolated solid product (A2-2, 75.25 g, 99% yield) was transferred to a flask and dried under vacuum for a period of 8 hours.



3-bromo-4,5-dimethoxy benzaldehyde (A2-3)

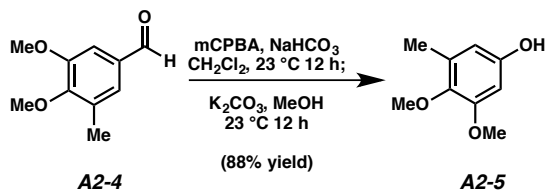
To a 1 L round-bottom flask was added anhydrous K_2CO_3 (113.56 g, 821.6 mmol), followed by a solution of bromobenzaldehyde **A2-2** (75.25 g, 325.66 mmol) in reagent grade acetone (700 mL). A mechanical stirrer was affixed to the reaction flask, and vigorous stirring was required to generate an evenly distributed, maroon suspension. To this stirring mixture was added Me_2SO_4 (77.74 mL, 821.69 mmol) over 1 minute via funnel. The reaction was left to stir vigorously at 25 °C for 8 hours, at which point TLC analysis confirmed the conversion of phenol **A2-2** to a less polar product. The reaction contents were then vacuum filtered over a glass frit to separate residual solid K_2CO_3 . The filtered solid was washed with acetone (2 x 100 mL) and methanol (100 mL). The organic filtrate was concentrated to an orange oil and purified by flash chromatography (5% → 50% ethyl acetate in hexanes eluent) to yield bromobenzaldehyde **A2-3** (76.6 g, 96% yield), which was isolated as a white powder: R_f = 0.56 (30% ethyl acetate in hexanes); ^1H NMR (500 MHz, CDCl_3) δ 9.86 (s, 1H), 7.67 (d, J = 1.80 Hz, 1H), 7.40 (d, J = 1.85 Hz, 1H), 3.96 (s, 3H), 3.95 (s, 3H); ^{13}C NMR (125 MHz, CDCl_3) δ 189.83, 154.17, 151.81, 133.03, 128.77, 117.92, 110.09, 60.83, 56.25; IR (NaCl/film) 2945, 2860, 1692, 1588, 1566, 1486, 1469, 1452, 1420, 1393, 1380, 1312, 1281, 1240, 1212, 1144, 1133, 1048, 993, 855, 840 cm^{-1} ; HRMS (MM: ESI-APCI) m/z calc'd for $\text{C}_9\text{H}_9\text{BrO}_3$ [M] $^+$: 243.9735, found 243.9731.



3,4-dimethoxy-5-methylbenzaldehyde (A2-4)

A 250 mL round-bottom flask was charged with lithium chloride (4.32 g, 102.00 mmol) and then flame dried. To this flask was added a solution of benzaldehyde **A2-3** (5.0 g, 20.40 mmol) in *N,N*-dimethylformamide (200 mL) that had been rigorously sparged with argon. Next, $\text{PdCl}_2(\text{PPh}_3)_2$ (0.358 g, 0.51 mmol) was added to the stirring mixture, producing a bright yellow-orange solution that was stirred vigorously. A reflux condenser was affixed to the top of the reaction flask before adding, dropwise, neat tetramethyltin (7.06 mL, 51.0 mmol). The reaction vessel was sealed under an argon atmosphere and heated to reflux in 100 °C oil bath. The reaction was maintained at reflux for 3 hours; during this period the color of the solution changed to dark red-orange.¹⁵ TLC analysis of the reaction after this period showed full consumption of the starting material. The reaction was cooled to room temperature and then quenched by the addition of H_2O (200 mL). The aqueous layer was thoroughly extracted with ethyl acetate (5 x 200 mL), and the combined organic layers were washed with brine (150 mL). The organic extract was dried over MgSO_4 , concentrated under vacuum, and purified by flash chromatography (5% ethyl acetate in hexanes eluent) to furnish benzaldehyde **A2-4** as a colorless oil (3.63 g, 99% yield): R_f = 0.42 (10% ethyl acetate in hexanes); ^1H NMR (500 MHz, CDCl_3) δ 9.85 (s, 1H), 7.17 (d, J = 1.71 Hz, 1H), 7.16 (d, J = 0.60 Hz, 1H), 3.78 (s, 3H), 3.77 (s, 3H), 2.19 (s, 3H); ^{13}C NMR (125 MHz, CDCl_3) δ 191.14, 153.02,

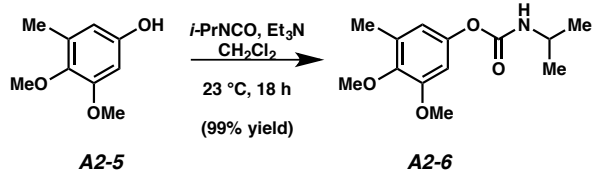
152.70, 126.95, 108.79, 60.05, 55.65, 15.75; IR (NaCl/film) 2939, 2833, 1693, 1586, 1491, 1465, 1422, 1387, 1329, 1299, 1233, 1140, 1096, 1003, 856 cm^{-1} ; HRMS (MM: ESI-APCI) m/z calc'd for $\text{C}_{10}\text{H}_{12}\text{O}_3$ [M] $^+$: 180.0786, found 180.0779.



3,4-dimethoxy-5-methylphenol (A2-5)

A 250 mL round-bottom flask was charged with anhydrous NaHCO_3 (0.467 g, 0.56 mmol). To this, was added a solution of benzaldehyde **A2-4** (1.00 g, 5.55 mmol) in CH_2Cl_2 (11 mL). This mixture was vigorously stirred until the NaHCO_3 fully dissolved. At this point, *m*-CPBA (1.92 g, 11.10 mmol) was added as a solid in a single portion to the pale yellow solution. Immediately, the solution turned bright yellow, and was maintained with stirring at 25 °C under an atmosphere of N_2 . Notable accumulation of precipitate resulted in increasing turbidity of the solution, and after 6 hours, TLC analysis indicated formation of a new product ($R_f = 0.22$, hexanes) and consumption of benzaldehyde **A2-4**. At this time, methanol (110 mL) and anhydrous K_2CO_3 (2.30 g, 16.65 mmol) were added, and the solution turned maroon in color. The reaction was maintained at 25 °C for 12 hours, resulting in formation of a new polar product. The reaction was stopped by concentration under vacuum to yield a dark maroon solid. This solid was dissolved in H_2O (100 mL), and then neutralized with concentrated aqueous HCl (6 mL). **Warning:** vigorous gas evolution. The resulting suspension was extracted with CH_2Cl_2 (5 x 100 mL), and the combined organic extracts were washed with

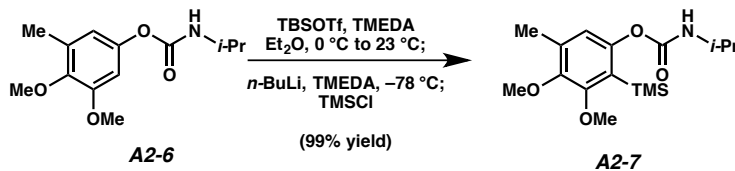
saturated aqueous NaHCO_3 (2×200 mL) to remove benzoate byproducts. The organic layers were dried with Na_2SO_4 , concentrated under vacuum, and purified by flash chromatography (30% ethyl acetate in hexanes eluent) to provide phenol **A2-5** (0.822 g, 4.89 mmol, 88% yield) as a white solid: $R_f = 0.30$ (30% ethyl acetate in hexanes); ^1H NMR (500 MHz, CDCl_3) δ 6.29 (d, $J = 2.80$ Hz, 1H), 6.20 (d, $J = 2.80$ Hz, 1H), 4.53 (s, 1H), 3.81 (s, 3H), 3.73 (s, 3H), 2.21 (s, 3H); ^{13}C NMR (125 MHz, CDCl_3) δ 153.36, 151.78, 141.12, 132.41, 108.36, 98.17, 60.35, 55.69, 15.85; IR (NaCl/film) 3272, 2957, 1614, 1483, 1463, 1440, 1430, 1348, 1268, 1226, 1219, 1196, 1181, 1154, 1096, 1001, 854, 772, 737 cm^{-1} ; HRMS (MM: ESI-APCI) m/z calc'd for $\text{C}_9\text{H}_{12}\text{O}_3$ $[\text{M}]^+$: 168.0786, found 168.0753.



Isopropyl carbamate **A2-6**

This procedure was adopted from the literature procedure reported by Bronner, et al.¹⁶ A 100 mL round-bottom flask was charged with a solution of phenol **A2-5** (1.696 g, 10.08 mmol) in CH_2Cl_2 (35 mL). The solution was stirred at 25 °C under an atmosphere of N_2 before neat isopropyl isocyanate (1.483 mL, 15.12 mmol) was added via syringe. The solution turned orange, and after 5 minutes of stirring, freshly distilled Et_3N (0.281 mL, 2.02 mmol) was added via syringe to effect the formation of a dark purple solution. The reaction was maintained with stirring for 18 hours at 25 °C. Following this period, TLC analysis showed conversion of phenol **A2-5** to a single product. The reaction was

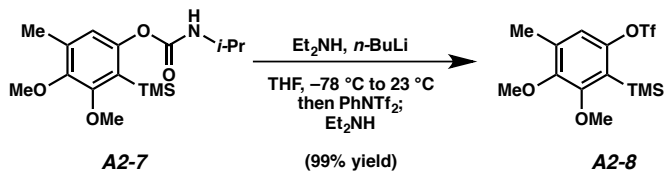
concentrated to an orange-brown residue and purified by flash chromatography (5% ethyl acetate in hexanes eluent) to provide isopropyl carbamate **A2-6** as a clear, pale yellow oil (2.553 g, 10.08 mmol, 99% yield): R_f = 0.48 (30% ethyl acetate in hexanes); ^1H NMR (500 MHz, CDCl_3) δ 6.55 (d, J = 2.65 Hz, 1H), 6.54 (d, J = 2.65 Hz, 1H), 2.79 (s, 1H), 3.87 (m, 1H), 3.82 (s, 3H), 3.76 (s, 3H), 2.24 (s, 3H), 1.23 (d, J = 7.25 Hz, 6H); ^{13}C NMR (125 MHz, CDCl_3) δ 153.92, 152.87, 146.66, 144.62, 115.29, 104.21, 60.15, 55.78, 43.44, 22.93, 15.91; IR (NaCl/film) 3326, 2972, 2936, 1715, 1604, 1529, 1490, 1466, 1422, 1332, 1220, 1190, 1175, 1142, 1095, 1050, 1009, 936, 854, 773 cm^{-1} ; HRMS (MM: ESI-APCI) m/z calc'd for $\text{C}_{13}\text{H}_{19}\text{NO}_4$ [M] $^+$: 253.1314, found 253.1319.



TMS carbamate **A2-7**

This procedure was adopted from the literature procedure reported by Bronner, et al.³ To a solution of isopropyl carbamate **A2-6** (9.10 g, 35.9 mmol) in diethyl ether (180 mL) was added freshly distilled TMEDA (5.90 mL, 39.5 mmol). The solution was cooled to 0 °C. Distilled TBSOTf (9.00 mL, 39.5 mmol) was then added. The resulting solution was maintained for 10 minutes at 0 °C and then the flask was allowed to warm to 23 °C over 30 minutes. Additional TMEDA was then added to the mixture (21.5 mL, 144 mmol). The reaction was then cooled to –78 °C with vigorous stirring to avoid aggregation of triflate salts. Next, *n*-BuLi (2.5 M in hexanes, 58.0 mL, 144 mmol) was added dropwise. The solution was maintained with stirring at –78 °C for 4 hours, after which time freshly distilled TMSCl (32.0 mL, 251 mmol) was added dropwise. The

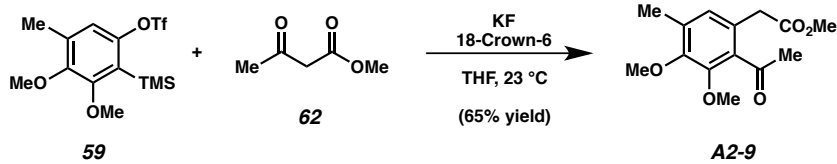
reaction vessel was allowed to warm to 23 °C over the course of two hours. At this point, TLC analysis indicated the presence of a single, new product. Saturated aqueous NaHSO₄ solution (150 mL) was added and stirred with the reaction mixture for 0.5 hour. The layers were separated and the organic layer was washed with an additional 150 mL of the NaHSO₄ solution. The combined aqueous layers were then extracted with diethyl ether (3 x 250mL). The combined organic extracts were washed with brine (250 mL), dried with Na₂SO₄, and then concentrated under vacuum to a colorless crystalline solid. Purification via flash chromatography (5% → 15% ethyl acetate in hexanes eluent) provided pure TMS carbamate **A2-7** (11.6 g, 99% yield): *R*_f = 0.63 (15% ethyl acetate in hexanes); ¹H NMR (500 MHz, CDCl₃) δ 6.62 (s, 1H), 4.69 (d, *J* = 7.08 Hz, 1H), 3.89 (m, 1H), 3.83 (s, 3H), 3.76 (s, 3H), 2.23 (s, 3H), 1.23 (d, *J* = 6.75, 6H), 0.29 (s, 9H); ¹³C NMR (125 MHz, CDCl₃) δ 156.69, 153.00, 149.33, 147.28, 133.33, 121.79, 118.88, 59.19, 58.54, 42.27, 21.88, 14.83, 0.13; IR (NaCl/film) 3326, 2971, 2937, 1710, 1601, 1530, 1464, 1384, 1370, 1324, 1247, 1220, 1193, 1179, 1080, 1026, 987, 844, 810, 759 cm⁻¹; HRMS (MM: ESI-APCI) *m/z* calc'd for C₁₆H₂₇NO₄Si [M+H]⁺: 326.1734, found 326.1725.



Silyl aryl triflate **A2-8**

To a solution of TMS carbamate **A2-7** (13.2 g, 40.5 mmol) in THF (160 mL) at –78 °C was added diethylamine (6.30 mL, 60.8 mmol), followed by *n*-BuLi (2.5 M in hexanes, 24.3 mL, 60.8 mmol). After 20 minutes, the reaction was allowed to warm to 23 °C for

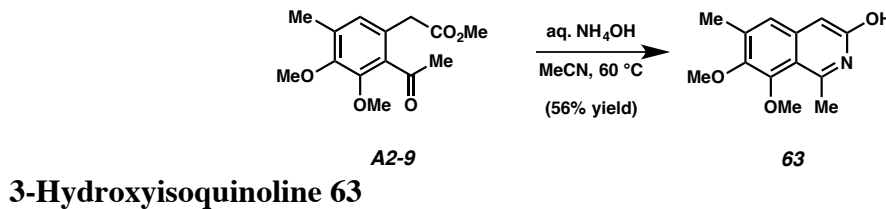
30 minutes. PhNTf₂ (21.7 g, 60.8 mmol) was then added in one portion. The reaction was maintained with stirring for 4 hours at 23 °C, after which point more diethylamine was added (7.50 mL, 72.9 mmol). The reaction was stirred at 23 °C for 12 hours. The reaction was then filtered on a silica pad, and washed with 25% EtOAc in hexanes. Evaporation of the solvent, followed by purification via flash chromatography (2% ethyl acetate in hexanes eluent) yielded silyl aryl triflate **A2-8** (14.9 g, 99% yield) as a pale yellow oil that crystallized upon cooling: R_f = 0.68 (15% ethyl acetate in hexanes); ¹H NMR (500 MHz, CDCl₃) δ 6.87 (s, 1H), 3.86 (s, 3H), 3.77 (s, 3H), 2.27 (s, 3H), 0.36 (s, 9H); ¹³C NMR (125 MHz, CDCl₃) δ 158.72, 150.74, 149.21, 135.84, 117.49 (q, J = 320 Hz), 124.53, 117.96, 60.79, 60.03, 16.43, 1.41; ¹⁹F NMR (282 MHz, CDCl₃) δ –73.10; IR (NaCl/film) 2956, 2858, 1600, 1464, 1420, 1383, 1368, 1292, 1248, 1213, 1179, 1142, 1068, 1023, 982, 930, 873, 846, 764 cm^{–1}; HRMS (MM: ESI-APCI) *m/z* calc'd for C₁₃H₁₉F₃O₅SSi [M]⁺: 372.0675, found 372.0674.



Ketoester **A2-9**

To a solution of silyl aryl triflate **59** (1.86 g, 5.00 mmol) in THF (50 mL) was added methyl acetoacetate (**62**, 0.54 mL, 5.00 mmol), KF (872 mg, 15.0 mmol) and 18-crown-6 (4.00 g, 15.0 mmol) at 23 °C. The reaction was maintained at this temperature for 16 hours, at which time TLC analysis indicated complete consumption of silyl aryl triflate **59**. The solution was diluted with diethyl ether (150 mL) and water (150 mL). The

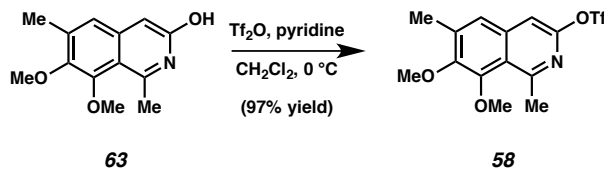
aqueous layer was extracted with diethyl ether (3 x 150 mL), and the combined organic layers were dried over Na_2SO_4 , filtered and concentrated. Purification of this residue by flash chromatography (10% EtOAc in hexanes eluent) furnished ketoester **A2-9** (860 mg, 65% yield) as a colorless solid: R_f = 0.49 (4:1 hexanes:ethyl acetate) along with the corresponding α -arylation bi-product (170 mg, 13% yield, not characterized); ^1H NMR (500 MHz, CDCl_3) δ 6.76 (s, 1H), 3.85 (s, 3H), 3.80 (s, 3H), 3.66 (s, 3H), 3.60 (s, 2H), 2.53 (s, 3H), 2.23 (s, 3H); ^{13}C NMR (125 MHz, CDCl_3) δ 204.67, 172.20, 150.95, 150.51, 134.57, 134.26, 128.77, 126.84, 61.37, 60.28, 52.20, 37.96, 32.46, 16.09; IR (NaCl/film) 2951, 2849, 1740, 1692, 1604, 1568, 1484, 1451, 1437, 1400, 1351, 1306, 1269, 1200, 1167, 1147, 1078, 1040, 1012 cm^{-1} ; HRMS (MM: ESI-APCI) m/z calc'd for $\text{C}_{11}\text{H}_{10}\text{O}_2\text{N}$ [M+H] $^+$: 267.1227, found 267.1233.



3-Hydroxyisoquinoline **63**

Ketoester **A2-9** (735 mg, 2.76 mmol) was dissolved in MeCN (2 mL) in a pressure flask with a sealable top. To this was added 28–30% aqueous ammonium hydroxide (4 mL), and the flask was sealed. The reaction was maintained at 60 °C with vigorous stirring for 18 hours. At this point, a yellow solid was generated and TLC analysis indicated the complete consumption of the starting material. The reaction mixture was then cooled to 23 °C, and the solid was filtered and washed with water. The resulting yellow residue was analytically pure 3-hydroxyisoquinoline **63** (324 mg, 1.32 mmol). The filtrate was diluted with dichloromethane (5 mL), NH_4Cl saturated solution

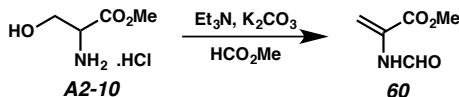
was added (10 mL) and the phase were separated. The aqueous layer was further extracted with CH_2Cl_2 (5x 15 mL). The organic layers were dried on Na_2SO_4 , filtered and concentrated. Purification of this residue by flash chromatography (5% MeOH in CH_2Cl_2 eluent) furnished 3-hydroxyisoquinoline **63** (51 mg, 0.22 mmol). Overall, 3-hydroxyisoquinoline **63** (375 mg, 1.54 mmol, 56% yield) was obtained as a yellow solid: $R_f = 0.10$ (95:5 CH_2Cl_2 :MeOH); ^1H NMR (500 MHz, CDCl_3) δ 7.17 (s, 1H), 6.94 (s, 1H), 6.52 (s, 1H), 3.91 (s, 3H), 3.82 (s, 3H), 3.01 (s, 3H), 2.29 (s, 3H); ^{13}C NMR (125 MHz, CDCl_3) δ 161.99, 149.63, 149.62, 146.04, 142.71, 140.48, 121.54, 113.27, 104.86, 60.63, 60.35, 21.23, 17.43; IR (NaCl/film) 2938, 1690, 1458, 1324 cm^{-1} ; HRMS (MM: ESI-APCI) m/z calc'd for $\text{C}_{13}\text{H}_{16}\text{O}_3\text{N} [\text{M}+\text{H}]^+$: 234.1125, found 234.1125.



Isoquinoline triflate **58**

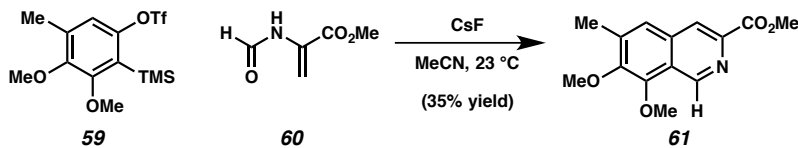
3-Hydroxyisoquinoline **163** was dissolved in dry CH_2Cl_2 (6 mL). To this solution, was added pyridine (1.00 mL, 12.2 mmol), and the reaction was cooled to 0 °C. Triflic anhydride (0.31 mL, 1.83 mmol) was added dropwise to the cold solution, which was maintained at 0 °C for 40 minutes. At this time, TLC analysis indicated complete consumption of the starting material. The reaction was quenched at 0 °C by the addition of saturated aqueous NaHCO_3 (10 mL) followed by warming to 23 °C. The mixture was extracted with CH_2Cl_2 (3 x 30 mL), and the combined organic extracts were dried over Na_2SO_4 and concentrated under vaccuum. The resulting residue was purified by flash chromatography (5% ethyl acetate in hexanes eluent) to furnish isoquinoline triflate **58**

(433 mg, 97% yield): R_f = 0.83 (hexanes:ethyl acetate 1:1); ^1H NMR (500 MHz, CDCl_3) δ 7.37 (s, 1H), 7.19 (s, 1H), 3.96 (s, 3H), 3.91 (s, 3H), 3.05 (s, 3H), 2.42 (s, 3H); ^{13}C NMR (125 MHz, CDCl_3) δ 158.84, 151.22, 150.68, 150.09, 139.41, 137.00, 123.79, 123.11, 118.97 (q, J = 320 Hz), 107.83, 60.99, 60.38, 26.91, 17.20; IR (NaCl/film) 2961, 2924, 2853, 1604, 1552, 1452, 1413, 1377, 1352, 1332, 1260, 1208, 1094, 1059, 1016, 966, 940, 799, 699 cm^{-1} ; HRMS (MM: ESI-APCI) m/z calc'd for $\text{C}_{11}\text{H}_{10}\text{O}_2\text{N}$ [M+H] $^+$: 366.0618, found 366.0637.



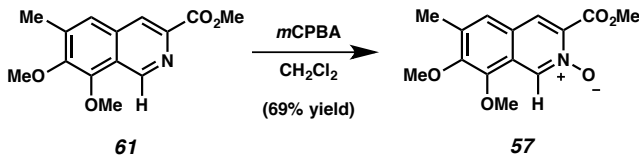
2-(Formamido)acrylic acid methyl ester **60**¹⁷

A mixture of serine methyl ester hydrochloric salt **A2-10** (15.6 g, 100 mmol), K_2CO_3 (55.3 g, 400 mmol), and a catalytic amount of Et_3N (160 μL) in methyl formate (320 mL) was stirred for 16 h at 23 °C. The salts were filtered, and the solvent was removed under reduced pressure. Quick purification by column chromatography (hexanes-ethyl acetate 40:60) afforded the desired product **60** (7.15 g, 55%). White solid, R_f 0.56 (hexanes:ethyl acetate 1:1), trans:cis 88:12. ^1H NMR (300 MHz, CDCl_3) δ 8.55 (d, J = 11.2 Hz, 1H, cis), 8.39 (s, 1H, trans), 7.79 (br, 1H, trans), 7.52 (br, 1H, cis), 6.62 (s, 1H, trans), 5.95 (s, 1H, trans), 5.67 (s, 1H, cis), 5.42 (s, 1H, cis), 3.84 (s, 3H). ^{13}C NMR (125 MHz, CDCl_3) δ 164.34, 161.14 (*cis*), 159.65 (*trans*), 130.35, 110.58 (*trans*), 104.80 (*cis*), 53.25.



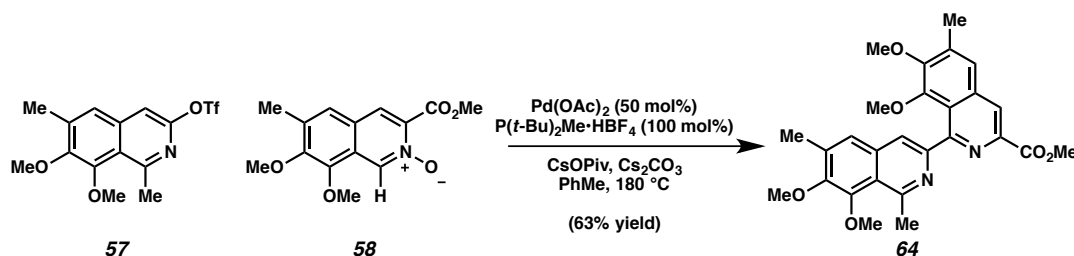
Isoquinoline **57**¹⁸

To silyl aryl triflate **59** (37 mg, 0.10 mmol) and methyl-2-formamidoacrylate (**60**, 39 mg, 0.30 mmol) stirring in MeCN (10 mL) at 23 °C was added CsF (92 mg, 0.60 mmol). The flask was maintained at 23 °C for 6 hours. Afterward, HCl 1N (1 mL) was added and the reaction was further stirred for 15 min. The mixture was then basified with NaHCO₃ saturated solution and EtOAc was added. The phases were separated, and the aqueous layer was extracted with EtOAc (3x 20 mL). The organic layers were dried on Na₂SO₄, filtered and concentrated. The resulting red residue was purified by flash chromatography (25% ethyl acetate in hexanes eluent) to furnish isoquinoline **61** (10 mg, 36% yield) as a red solid: *R*_f = 0.35 (1:1 hexanes:ethyl acetate); ¹H NMR (500 MHz, CDCl₃) δ 9.48 (s, 1H), 8.42 (s, 1H), 7.49 (s, 1H), 4.04 (s, 3H), 4.03 (s, 3H), 3.99 (s, 3H), 2.45 (s, 3H); ¹³C NMR (125 MHz, CDCl₃) δ 166.72, 151.15, 147.65, 147.35, 141.05, 139.42, 132.91, 125.02, 124.29, 123.24, 61.80, 60.69, 53.01, 17.56; IR (NaCl/Film) 2949, 2855, 1738, 1717, 1620, 1570, 1483, 1456, 1418, 1386, 1321, 1285, 1257, 1196, 1141, 1105, 1085, 1006, 984, 906, 818, 802, 777 cm⁻¹; HRMS (MM: ESI-APCI) *m/z* calc'd for C₁₁H₁₀O₂N [M+H]⁺: 262.1074, found 262.1070.



Isoquinoline N-oxide 57

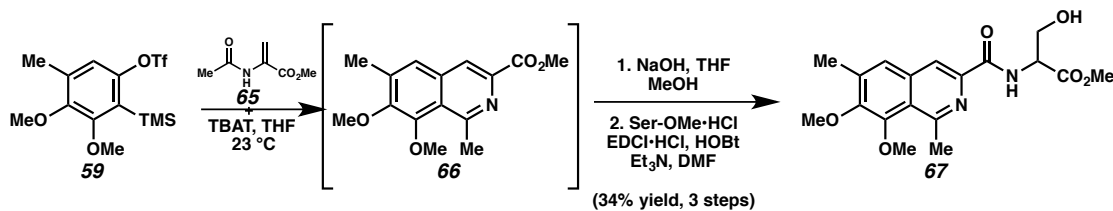
To a solution of isoquinoline **61** (575 mg, 2.20 mmol) in dichloromethane (22 mL) at 0 °C was added *m*CPBA (1.10 g, 4.40 mmol, 70% w/w). The reaction was allowed to reach 23 °C and was further stirred for 24 hours. After this time, TLC analysis indicated complete consumption of the isoquinoline. The reaction mixture was directly purified by flash chromatography (10% acetone in dichloromethane to 10% acetone/ 2% MeOH in dichloromethane eluent) providing isoquinoline *N*-oxide **57** (421 mg, 69% yield): R_f = 0.12 (1:1 hexanes:ethyl acetate); ^1H NMR (500 MHz, CDCl_3) δ 8.95 (s, 1H), 7.86 (s, 1H), 7.33 (s, 1H), 4.01 (s, 3H), 3.96 (s, 3H), 3.95 (s, 3H), 2.38 (s, 3H); ^{13}C NMR (125 MHz, CDCl_3) δ 162.65, 152.03, 144.45, 137.97, 137.41, 133.29, 125.77, 125.17, 125.13, 123.72, 61.53, 60.66, 53.52, 17.14. IR (NaCl/film) 2951, 2850, 1742, 1623, 1607, 1558, 1475, 1447, 1418, 1374, 1277, 1258, 1209, 1144, 1100, 1073, 1002, 958, 936, 828 cm^{-1} ; HRMS (MM: ESI-APCI) m/z calc'd for $\text{C}_{11}\text{H}_{10}\text{O}_2\text{N} [\text{M}+\text{H}]^+$: 278.1028, found 278.1034.



Bis-isoquinoline 64

Palladium acetate (34 mg, 0.15 mmol) was added to a flame-dried high pressure glassware containing cesium carbonate (280 mg, 0.86 mmol), cesium pivalate (136 mg, 0.58 mmol) and di-*tert*-butylmethylphosphonium tetrafluoroborate (72 mg, 0.29 mmol). The vessel was sealed. The vessel evacuated and backfilled with nitrogen atmosphere three times. Next, toluene (5 mL) was added to the reaction vial, which was subsequently heated to 60°C in an oil bath. The suspension was maintained at this temperature for 1 hour with vigorous stirring. Concomitant to this step, isoquinoline triflate **95** (106 mg, 0.29 mmol) was added to a flask containing isoquinoline *N*-oxide **94** (240 mg, 0.86 mmol). Toluene (10 mL) was added to the flask under an argon atmosphere. Upon cooling the palladium solution to room temperature, the isoquinolines solution was added. Next, the sealed tube was heated at 180°C for 4 hours. At the completion of this step, the content was filtered over a short plug of celite, the plug was washed with CH_2Cl_2 and acetone. Removal of the solvent and purification of the crude residue by flash chromatography (25% ethyl acetate in hexanes to 50% ethyl acetate in hexanes to 10% acetone/ 2% MeOH in dichloromethane) yielded bis-isoquinoline **64** (87 mg, 63% yield) as a white solid, along with isoquinoline **61** (56 mg, 25% yield recovered) and isoquinoline *N*-oxide **57** (70 mg, 30% yield recovered). Bis-isoquinoline : R_f = 0.16 (1:1 EtOAc:Hexanes) ; ^1H NMR (500 MHz, CDCl_3) δ 8.46 (s, 1H), 7.59 (s, 1H), 7.57 (s, 1H),

7.38 (s, 1H), 3.99 (s, 3H), 3.97 (s, 3H), 3.96 (s, 3H), 3.79 (s, 3H), 3.37 (s, 3H), 3.11 (s, 3H), 2.45 (s, 3H), 2.43 (s, 3H); ^{13}C NMR (125 MHz, CDCl_3) δ 166.82, 157.67, 155.46, 152.70, 152.52, 150.55, 149.71, 149.08, 139.81, 138.99, 137.18, 135.16, 134.85, 124.78, 124.21, 123.84, 123.52, 122.02, 117.04, 61.03, 60.72, 60.44, 60.24, 53.00, 27.04, 17.30, 17.20; IR (NaCl/film) 2930, 1719, 1555, 1395, 1318, 1262, 1121, 1096 cm^{-1} ; HRMS (MM: ESI-APCI) m/z calc'd for $\text{C}_{27}\text{H}_{29}\text{O}_6\text{N}_2$ [M+H] $^+$: 477.2020, found 477.2030.



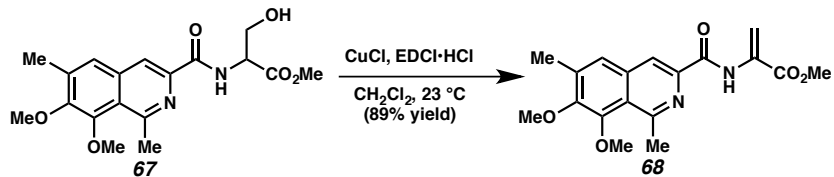
Isoquinoline 67

TBAT (1.450 g, 2.686 mmol) was added to a flame-dried round bottom flask equipped with a magnetic stir bar. The flask was sealed with a septum, evacuated and back-filled with N_2 . THF (6.0 mL) and methyl 2-acetamidoacrylate **65** (576.6 mg, 4.027 mmol) were sequentially added via syringe. To the solution was then added a solution of aryne precursor **59** (500.0 g, 1.343 mmol) in THF (7.0 mL), and the reaction mixture was stirred at room temperature for 20 hours. The mixture was evaporated in *vaccum* and the resulting residue was purified by silica gel flash column chromatography (0% ethyl acetate in hexanes to 50% ethyl acetate in hexanes) to give a mixture of isoquinoline **66** and methyl 2-acetamidoacrylate (**65**) as a brown solid.

The mixture was dissolved with THF (9.0 mL) and methanol (9.0 mL). To the solution was added 2 M aqueous sodium hydroxide solution (9.06 mL, 18.12 mmol), and the reaction mixture was warmed up to 50 °C and stirred at 50 °C for one hour. The

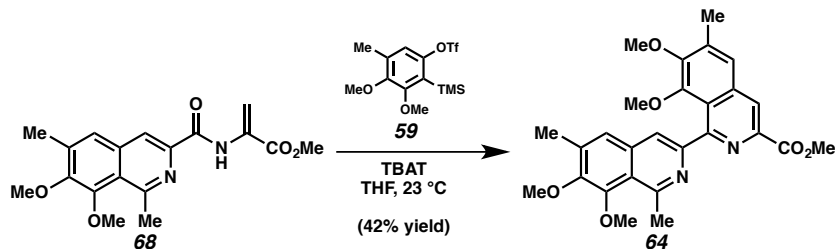
reaction mixture was allowed to cool to room temperature and acidified with 10% citric acid in water. The mixture was extracted with dichloromethane/2-propanol (10:1, v/v). The combined organic layers were dried over anhydrous sodium sulfate, filtered and concentrated under reduced pressure to give a crude isoquinoline the carboxylic acid as a brown solid.

The crude carboxylic acid, DL-serine methyl ester hydrochloride (355.2 mg, 2.283 mmol), 1-hydroxybenzotriazole (HOBr) hydrate (235.9 mg, 1.746 mmol), triethylamine (0.49 mL, 3.49 mmol), 1-ethyl-3-(3-dimethylaminopropyl)carbodiimide (EDCI) hydrochloride (437.7 mg, 2.283 mmol) and *N,N*-dimethylformamide (DMF, 4.0 mL) were stirred at room temperature for 13 hours. Saturated aqueous sodium bicarbonate solution (20 mL) and water (10 mL) were added to the reaction mixture. The mixture was then extracted with ethyl acetate (2 x 30 mL, 1 x 20 mL). The organic layers were combined, washed with brine, dried over anhydrous sodium sulfate, filtered and evaporated under reduced pressure. The resulting residue was purified by silica gel flash column chromatography (50% ethyl acetate in hexanes) to give **67** (174.3 mg, 0.4810 mmol, 36% yield from **59**) as a tan foam: R_f = 0.23 (50% ethyl acetate in hexanes); ^1H NMR (500 MHz, CDCl_3) δ 9.12 (d, J = 7.5 Hz, 1H), 8.24 (s, 1H), 7.49 (d, J = 1.2 Hz, 1H), 4.94 (dt, J = 7.7, 4.0 Hz, 1H), 4.16 (t, J = 3.9 Hz, 2H), 4.00 (s, 3H), 3.99 (s, 3H), 3.87 (s, 3H), 3.29 (s, 1H), 3.12 (s, 3H). ^{13}C NMR (126 MHz, CDCl_3) δ 171.02, 165.30, 156.09, 151.70, 149.48, 140.25, 137.64, 134.02, 125.05, 123.51, 118.36, 77.46, 77.21, 76.95, 63.10, 60.61, 60.01, 55.03, 52.59, 26.95, 16.77 cm^{-1} ; HRMS (MM: ESI-APCI) m/z calc'd for $\text{C}_{18}\text{H}_{22}\text{N}_2\text{O}_6$ $[\text{M}+\text{H}]^+$: 363.1551, found 363.1551.



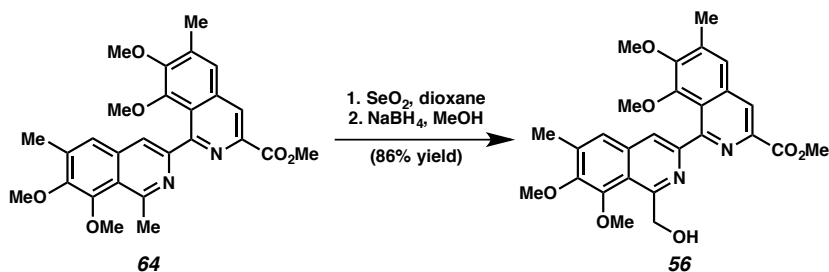
Acrylate 68

To a solution of methyl isoquinoline **67** (542.5 mg, 1.497 mmol) in dichloromethane (18.7 mL) were added EDCI hydrochloride (717.4 mg, 3.743 mmol) and copper (I) chloride (44.5 mg, 0.449 mmol). The reaction mixture was stirred at room temperature for 5 hours. To the reaction mixture were then added saturated aqueous sodium bicarbonate (25 mL) and water (40 mL), and the mixture was extracted with dichloromethane. The organic layers were combined, dried over anhydrous sodium sulfate, filtered and evaporated in *vaccum*. The resulting residue was purified by silica gel flash column chromatography (dichloromethane as eluent) to give **68** (457.1 mg, 1.327 mmol 89% yield) as a white solid: R_f = 0.82 (50% ethyl acetate in hexanes); mp 155.0 – 156.0 °C (from dichloromethane and hexanes); ^1H NMR (500 MHz, CDCl_3) δ 10.79 (s, 1H), 8.32 (m, 1H), 7.56 (dd, J = 0.9, 0.5 Hz, 1H), 6.89 (s, 1H), 6.06 (d, J = 1.6 Hz, 1H), 4.03 (s, 3H), 4.00 (s, 3H), 3.97 (s, 3H), 3.20 (s, 3H), 2.51 (s, 3H); ^{13}C NMR (126 MHz, CDCl_3) δ 164.60, 163.87, 156.31, 152.03, 149.81, 140.83, 138.03, 134.43, 131.37, 125.23, 123.89, 118.47, 108.73, 77.28, 77.02, 76.77, 60.77, 60.15, 52.89, 27.32, 16.89 cm^{-1} ; HRMS (MM: ESI-APCI) m/z calc'd for $\text{C}_{18}\text{H}_{20}\text{N}_2\text{O}_5$ $[\text{M}+\text{H}]^+$: 345.1445, found 345.1430.



Bis-isoquinoline 64

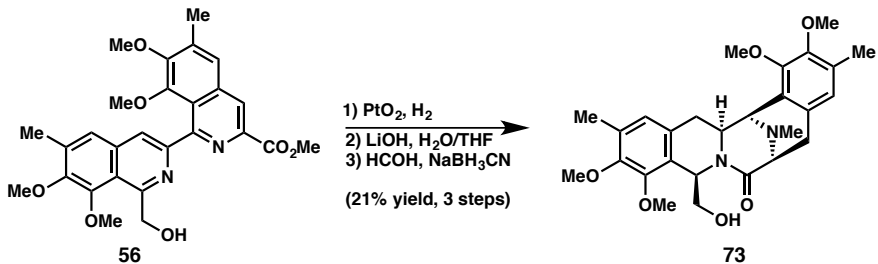
TBAT (8.114 g, 15.03 mmol) was added to a flame-dried round bottom flask equipped with a magnetic stir bar. The flask was sealed with a septum, evacuated and back-filled with N₂. THF (8.0 mL) and a solution of acrylate **26** (862.8 mg, 2.505 mmol) in THF (8.0 mL) were sequentially added via syringe. A solution of aryne precursor **7b** (2.799 g, 7.515 mmol) in THF (8.0 mL) was then added to the reaction mixture, which was stirred at room temperature for 20 hours. The volatiles of the reaction mixture were removed in vacuo, and the resulting residue was purified by silica gel flash column chromatography (0% ethyl acetate in hexanes to 70% ethyl acetate in hexanes) to give **22** (494.9 mg, 1.038 mmol 42% yield) spectroscopic data can be found above.



Bis-isoquinoline alcohol 56

Selenium dioxide (17 mg, 0.150 mmol) was added to a solution of **93** (35 mg, 0.075 mmol) in dioxane (1.5 mL). The reaction mixture was subsequently heated to 110 °C for 4 hours. After this time, the solution was filtered on celite and washed with

EtOAc. The solvent was removed, and MeOH (4 mL) was added. NaBH₄ (17 mg, 0.45 mmol) was subsequently added and the reaction was stirred for 12 h. At which time another portion of NaBH₄ (17 mg, 0.45 mmol) was added, and the reaction was kept at 23 °C for another 4 h. After this period of time, water and EtOAc were added and the organic phases were separated. Extraction of the aqueous layer with EtOAc, followed by drying the organic layers with Na₂SO₄, filtration and concentration gave the crude residue which was purified by flash chromatography (50% ethyl acetate in hexanes) yielded bis-isoquinoline **56** (32 mg, 86% yield) as a off-white solid: R_f = 0.46 (60:40 EtOAc:Hexanes); ¹H NMR (500 MHz, CDCl₃) δ 8.49 (s, 1H), 7.77 (s, 1H), 7.60 (s, 1H), 7.46 (s, 1H), 5.28 (d, *J* = 2.6 Hz, 2H), 4.01 (s, 3H), 3.99 (s, 3H), 3.94 (s, 3H), 3.81 (s, 3H), 3.32 (s, 3H), 2.47 (s, 3H), 2.45 (s, 3H); ¹³C NMR (125 MHz, CDCl₃) δ 166.65, 156.97, 155.30, 152.62, 151.17, 150.44, 149.21, 148.86, 139.67, 139.23, 138.05, 135.08, 134.64, 124.76, 124.22, 123.75, 123.62, 119.92, 117.86, 64.30, 60.98, 60.78, 60.42, 60.33, 53.03, 17.31, 17.19; IR (NaCl/film) 3350, 2947, 2853, 1722, 1557, 1454, 1394, 1323, 1263, 1121, 1098, 1009 cm⁻¹; HRMS (MM: ESI-APCI) *m/z* calc'd for C₂₇H₂₉O₇N₂ [M+H]⁺: 493.1969, found 493.1994.



Bis-terahydroisoquinoline 73

To bis-isoquinoline **56** (18 mg, 0.036 mmol) in acetic acid (1.5 mL) was added PtO_2 (4 mg, 0.016 mmol). The reaction mixture was putted under a hydrogen atmosphere and stirred at 23 °C for 24 h. Upon complete conversion of the bis-isoquinoline by LC-MS, the mixture was treated with NaOH 1N and dilute with dichloromethane. The aqueous layer was further extracted with dichloromethane (4x), the organic phase dried on Na_2SO_4 , filtered, concentrated. The crude residue was then diluted in THF (1.5 mL) and H_2O (1.5 mL), and lithium hydroxide was added (15 mg, 0.640 mmol). The reaction mixture was stirred at 23 °C for 20 h and was followed by LC-MS. Upon completion, the reaction mixture was diluted with water and dichloromethane. The phases were separated, and the aqueous layer was further extracted with dichloromethane (4x), the organic phases dried on Na_2SO_4 , filtered, concentrated. The residue was then diluted in MeCN (2 mL) and formaldehyde (0.15 mL, 37% w/w) was added. The mixture was stirred for 15 minute at 23 °C. Afterward, NaBH_3CN (20 mg, 0.320 mmol) was added and the reaction kept at 23°C for 30 min. HCl 2N (2 mL) was added and the solution stirred for 24 h. The mixture was then poured in NaHCO_3 saturated solution, dichloromethane was added and the phases separated. The aqueous phase was washed 4x with dichloromethane, and the organic phases were dried on Na_2SO_4 , filtered and concentrated. The residue was purified by prep TLC (4% MeOH/1% Et_3N / 95%

CH_2Cl_2), affording the bis-tetrahydroisoquinoline intermediate **73** (4 mg, 21% yield); ^1H NMR (500 MHz, CDCl_3) δ 6.73 (s, 1H), 6.70 (s, 1H), 5.74 (dd, J = 6.2, 3.8 Hz, 1H), 4.14 (dd, J = 3.8, 1.3 Hz, 1H), 3.99 (dt, J = 12.7, 2.9 Hz, 1H), 3.88 (s, 3H), 3.86 (s, 3H), 3.74 (s, 6H), 3.68 (dt, J = 6.8, 1.2 Hz, 1H), 3.43 (dt, J = 9.9, 4.5 Hz, 1H), 3.26-3.17 (m, 2H), 3.05 (s, 1H), 2.93 (dd, J = 15.2, 2.5 Hz, 1H), 2.87 (d, J = 17.2 Hz, 1H), 2.45 (s, 3H), 2.26 (dd, J = 15.2, 12.7 Hz, 1H), 2.21 (s, 6H); ^{13}C NMR (125 MHz, CDCl_3) δ 173.43, 150.89, 149.90, 149.64, 149.41, 132.22, 132.12, 131.66, 128.87, 126.20, 125.04, 124.73, 122.28, 69.22, 60.73, 60.51, 60.26, 60.17, 60.09, 59.10, 55.82, 53.00, 40.36, 31.88, 28.99, 16.03, 15.93.

2.5 References and Notes

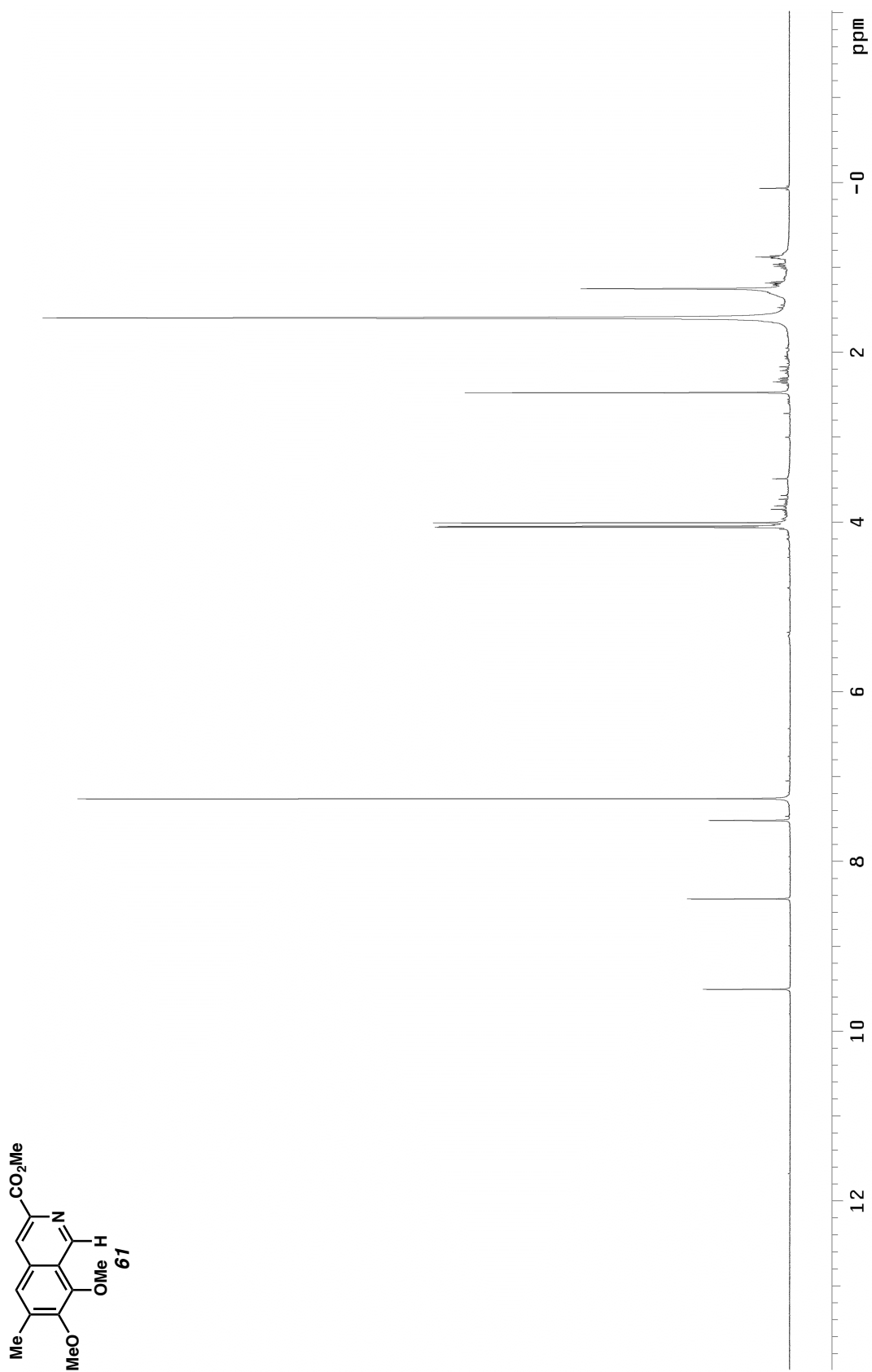
1. Scott, J. D.; Williams, R. M. *Chem. Rev.* **2002**, *102*, 1669–1730.
2. Lane, J. W.; Chen, Y.; Williams, R. M. *J. Am. Chem. Soc.* **2005**, *127*, 12684–12690.
3. Carter, N.; Keam, S. J. Trabectedin. *Drugs*, **2010**, *70*, 355–376.
4. a) U.S. FDA Grants Priority Review for YONDELIS® (trabectedin) for the Treatment of Patients with Advanced Soft Tissue Sarcoma.
<http://www.jnj.com/news/all/US-FDA-Grants-Priority-Review-for-YONDELIS-trabectedin-for-the-Treatment-of-Patients-with-Advanced-Soft-Tissue-Sarcoma>
(accessed July 13, 2015). b) Trabectedin Improves Disease Control in Patients with Advanced Soft Tissue Sarcoma. <http://www.jnj.com/news/all/Trabectedin-Improves-Disease-Control-in-Patients-with-Advanced-Soft-Tissue-Sarcoma> (accessed July 13, 2015).
5. a) Asaoka, T.; Yazawa, K.; Mikami, Y.; Arai, T. *J. Antibiot.* **1982**, *35*, 1708-1710.
b) Tomita, F.; Takahashi, K.; Shimizu, K.-I. *J. Antibiot.* **1983**, *36*, 463-467. c) Frincke, J. M.; Faulkner, D. J. *J. Am. Chem. Soc.* **1982**, *104*, 265-269. d) Ikeda, Y.; Shimada, Y.; Honjo, K.; Okumoto, T.; Munakata, T. *J. Antibiot.* **1983**, *36*, 1290-1294.
6. Fontana, A.; Cavaliere, P.; Wahidulla, S.; Naik, C. G.; Cimino, G. *Tetrahedron* **2000**, *56*, 7305–7308.
7. Charupant, K.; Daikuhara, N.; Saito, E.; Amnuoypol, S.; Suwanborirux, K.; Owa, T.; Saito, N. *Bioorg. Med. Chem.* **2009**, *17*, 4548–4558.
8. Wu, Y.-C.; Zhu, J. *Org. Lett.* **2009**, *11*, 5558–5561.

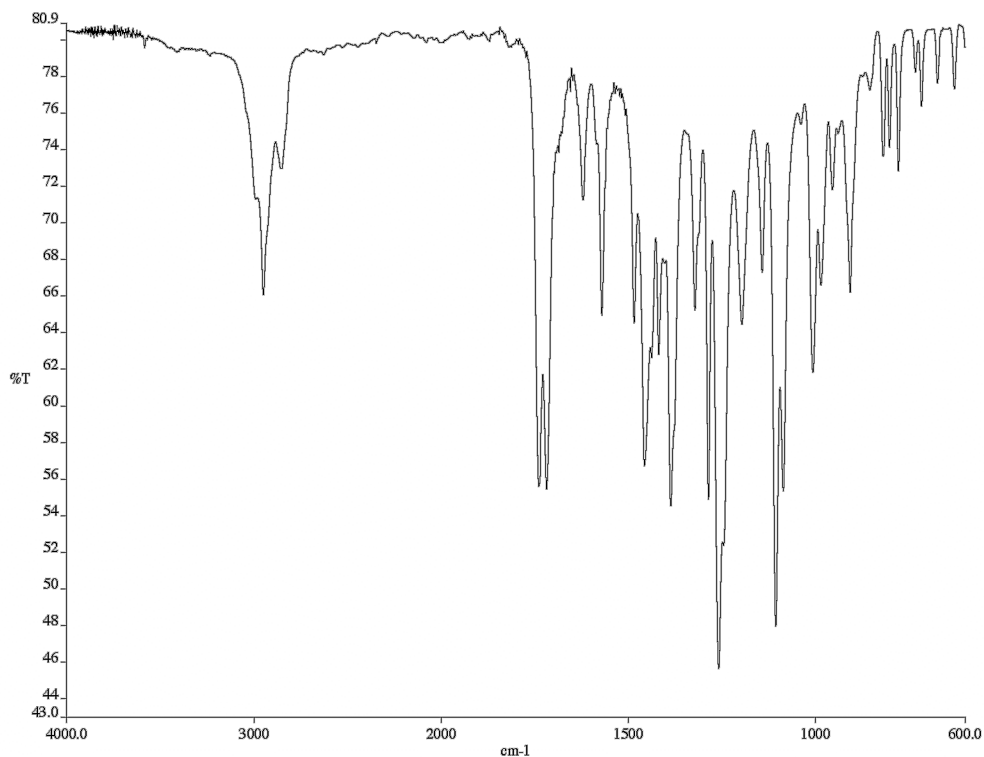
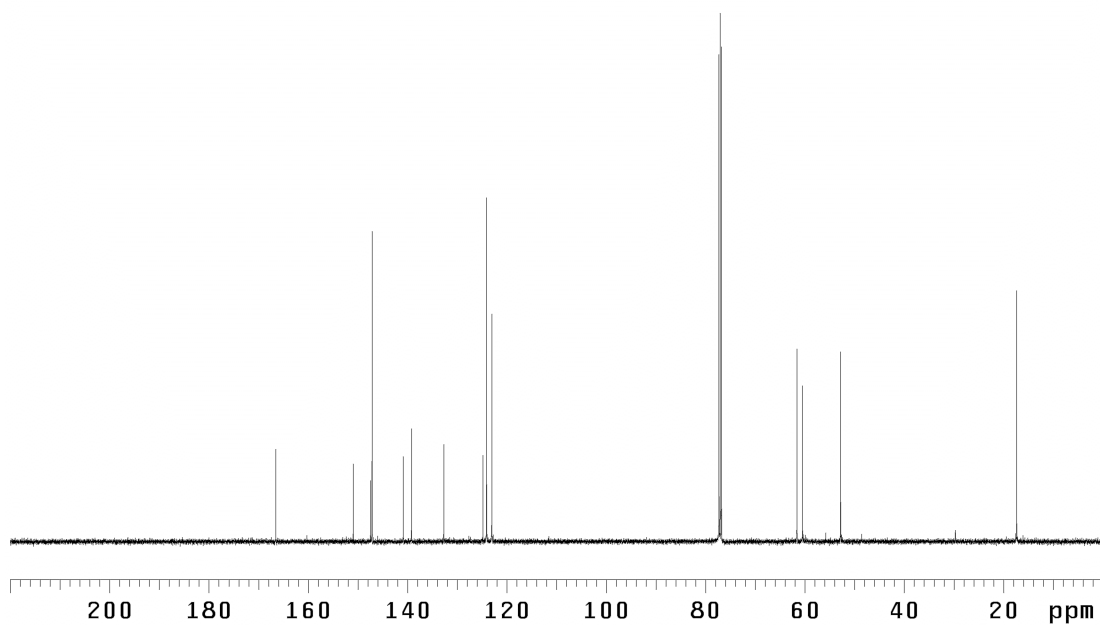
9. a) Mikami, Y.; Takahashi, K.; Yazawa, K.; Arai, T.; Namikoshi, M.; Iwasaki, S.; Okuda, S. *J. Biol. Chem.* **1985**, *260*, 344–348. b) Arai, T.; Yazawa, K.; Takahashi, K.; Maeda, A.; Mikami, Y. *Antimicrob. Agents Chemother.* **1985**, *28*, 5–11. c) Pospiech, A.; Cluzel, B.; Bietenhader, J.; Schupp, T. *Microbiology* **1995**, *141*, 1793–1803. d) Pospiech, A.; Bietenhader, J.; Schupp, T. *Microbiology* **1996**, *142*, 741–746. e) Koketsu, K.; Watanabe, K.; Suda, H.; Oguri, H.; Oikawa, H. *Nature Chem. Biol.* **2010**, *6*, 408–410.
10. a) Tambar, U. K.; Stoltz, B. M. *J. Am. Chem. Soc.* **2005**, *127*, 5340–5341. b) Gilmore, C. D.; Allan, K. M.; Stoltz, B. M. *J. Am. Chem. Soc.* **2008**, *130*, 1558–1559. c) Allan, K. M.; Stoltz, B. M. *A J. Am. Chem. Soc.* **2008**, *130*, 17270–17271. d) Allan, K. M.; Hong, B. D.; Stoltz, B. M. *Org. Biomol. Chem.* **2009**, *7*, 4960–4964. e) Tadross, P. M.; Gilmore, C. D.; Bugga, P.; Virgil, S. C.; Stoltz B. M. *Org. Lett.* **2010**, *12*, 1224–1227.
11. Campeau, L.-C.; Rousseaux, S.; Fagnou, K. *J. Am. Chem. Soc.* **2005**, *127*, 18020–18020.
12. For reviews on asymmetric hydrogenations of aromatic heterocycles, see: a) Glorius, F. *Org. Biomol. Chem.* **2005**, *3*, 4171–4175. b) Zhou, Y.-G. *Acc. Chem. Res.* **2007**, *40*, 1357–1366.
13. a) Liu, W.; Liao, W.; Dong, W.; Yan, Z.; Wang, Z.; Liu, Z. *Tetrahedron* **2012**, *68*, 2759–2764. b) Liu, W.; Dong, W.; Liao, X.; Yan, Z.; Guan, B.; Wang, N.; Liu, Z. *Bioorg. Med. Chem.* **2011**, *21*, 1419–1421.
14. Rao, D. V.; Stuber, F. A. *Synthesis* **1983**, 308.

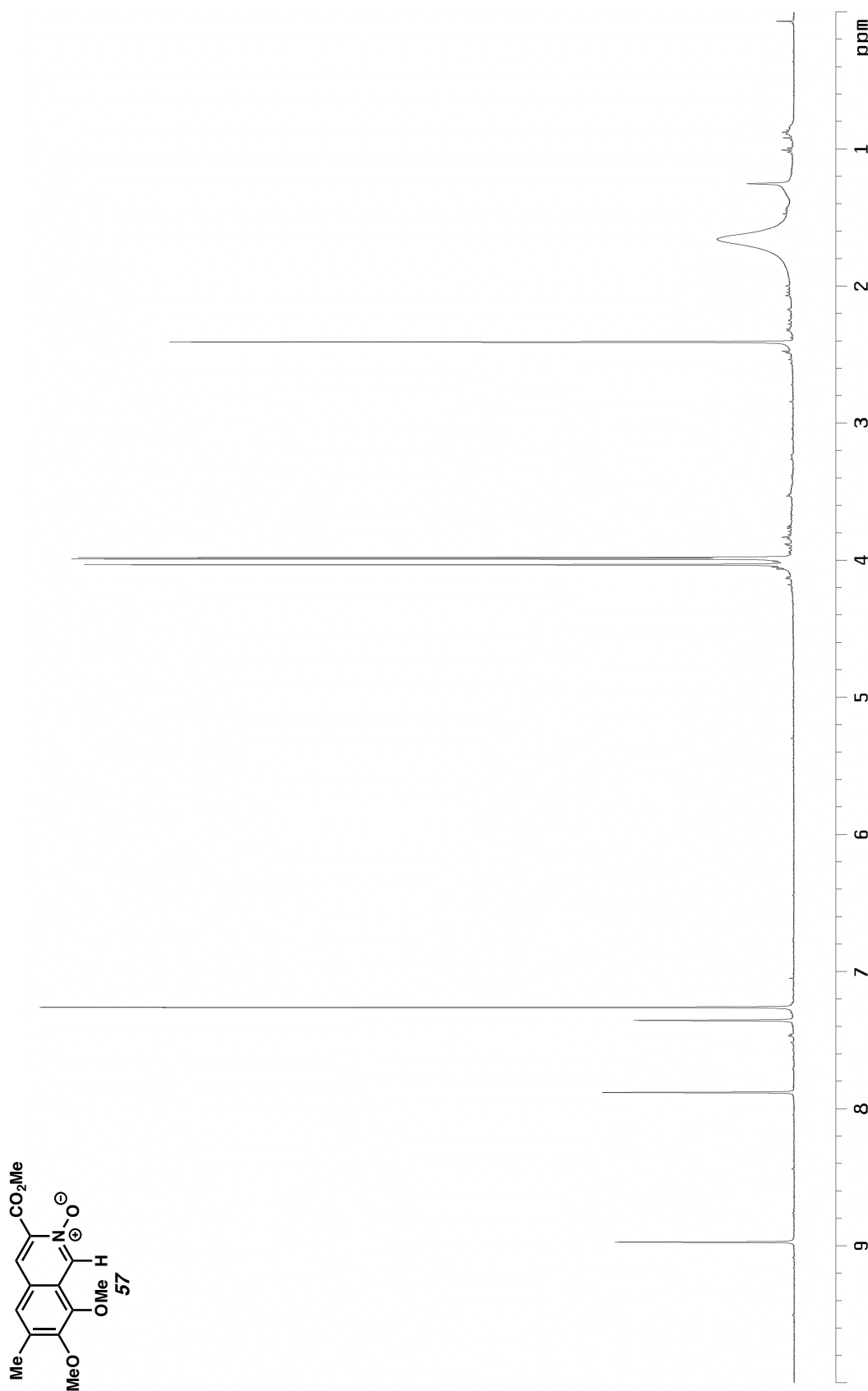
15. Cessation of the reaction occurs when exposed to air, and large amounts of Pd(0) black deposits result in a grey solution and reduced yields.
16. Bronner, S. M.; Garg, N. K. *J. Org. Chem.* **2009**, *74*, 8842–8843.
17. Panella, L.; Aleixandre, A. M.; Kruidhof, G. J.; Robertus, J.; Feringa, B. L.; de Vries, J. G.; Minnaard, A. J. *J. Org. Chem.* **2006**, *71*, 2026–2036.
18. Blackburn, T.; Ramtohul, Y. *Synlett* **2008**, 1159–1164.

Appendix 2

Spectra Relevant to Chapter 2

Figure A2.1.1 ^1H NMR (500 MHz, CDCl_3) of compound 61

Figure A2.1.2 Infrared spectrum (thin film/NaCl) of compound **61**Figure A2.1.3 ¹³C NMR (125 MHz, CDCl₃) of compound **61**

Figure A2.2.1 ^1H NMR (500 MHz, CDCl_3) of compound 75

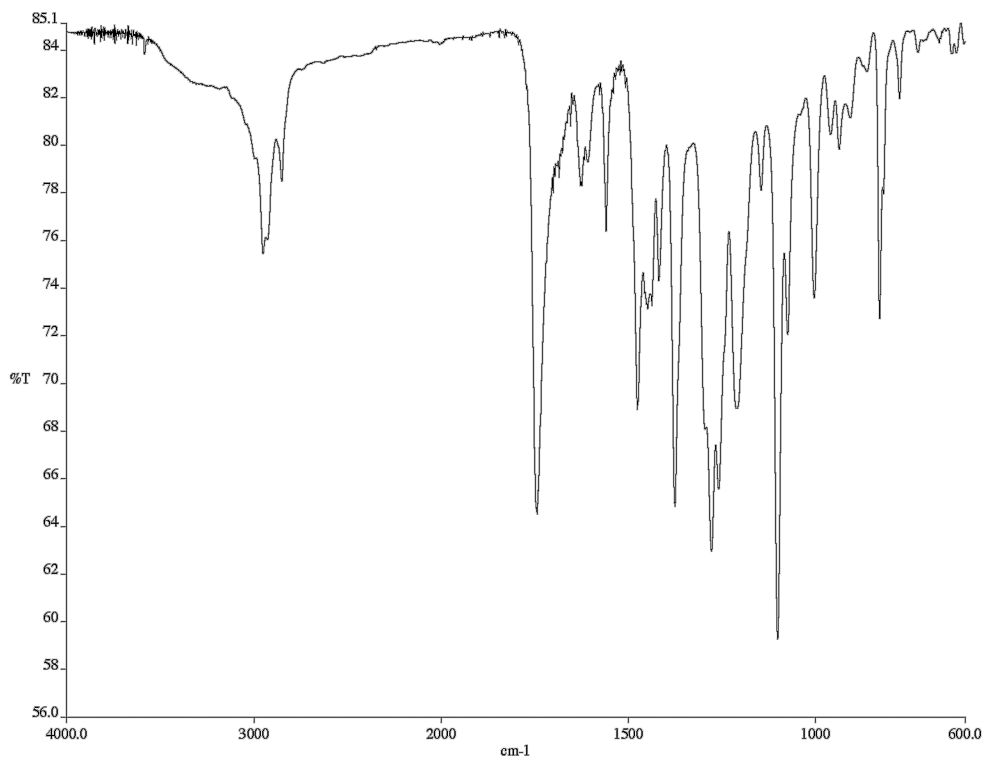


Figure A2.2.2 Infrared spectrum (thin film/NaCl) of compound **75**

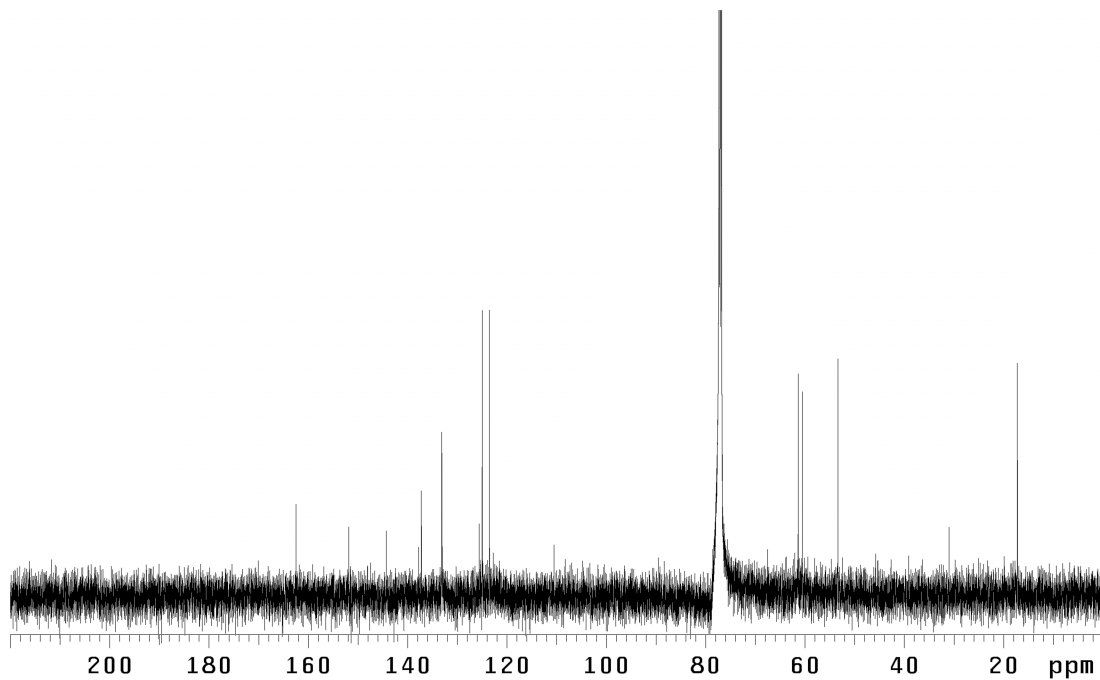


Figure A2.2.3 ^{13}C NMR (125 MHz, CDCl_3) of compound **75**

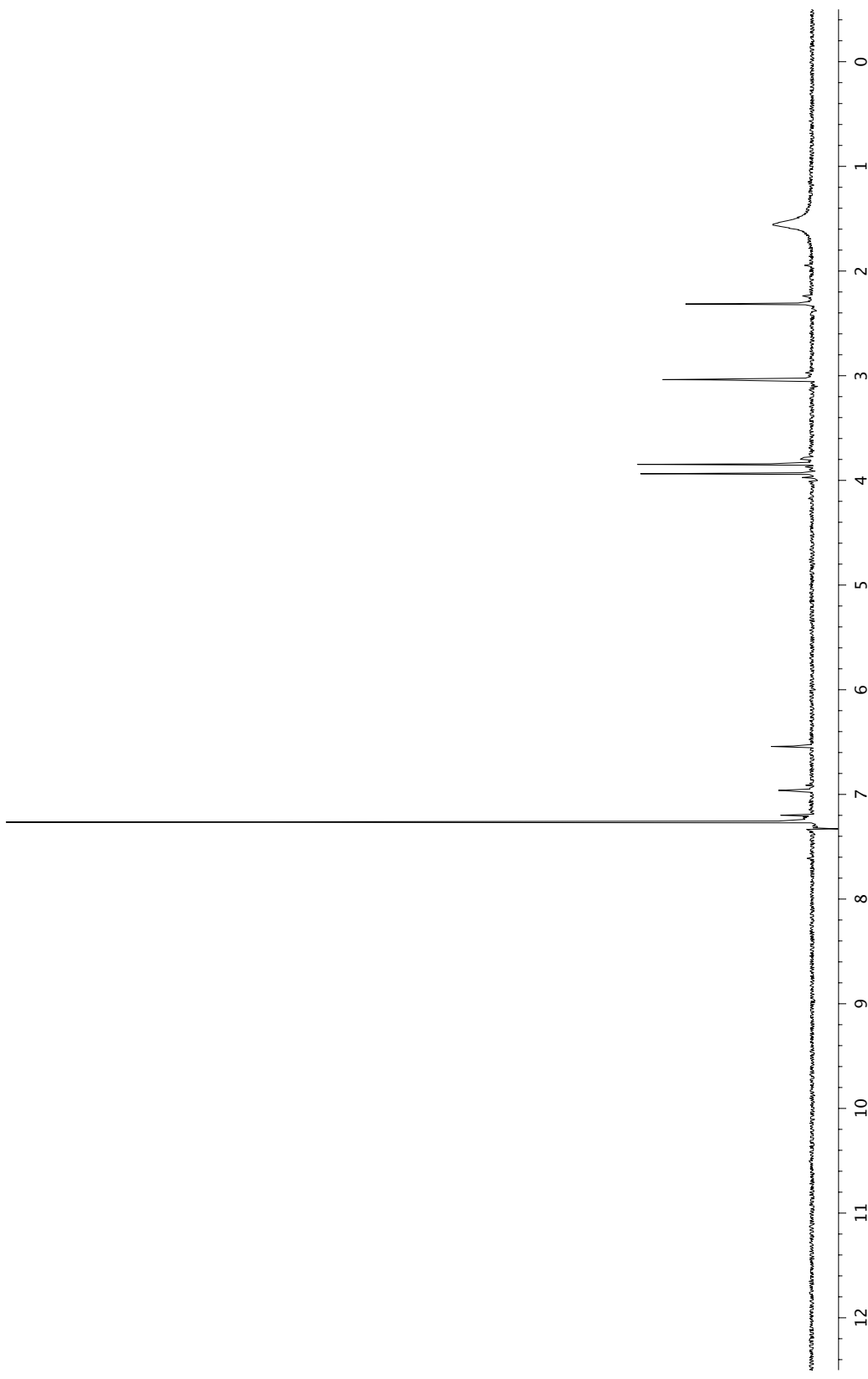


Figure A2.3.1 ^1H NMR (500 MHz, CDCl_3) of compound 63.

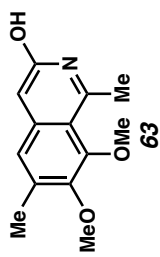


Figure A2.3.2 Infrared spectrum (Thin Film, NaCl) of compound **63**.

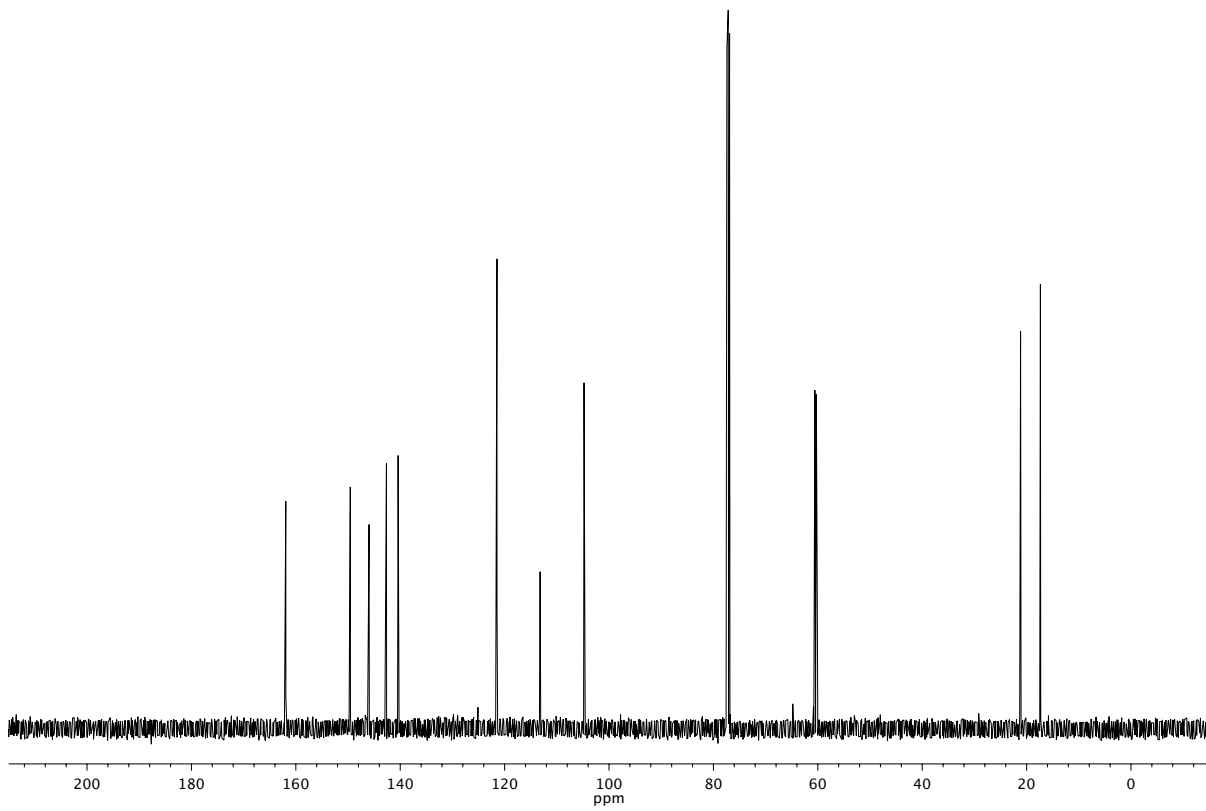


Figure A2.3.2 ^{13}C NMR (126 MHz, CDCl_3) of compound **63**.

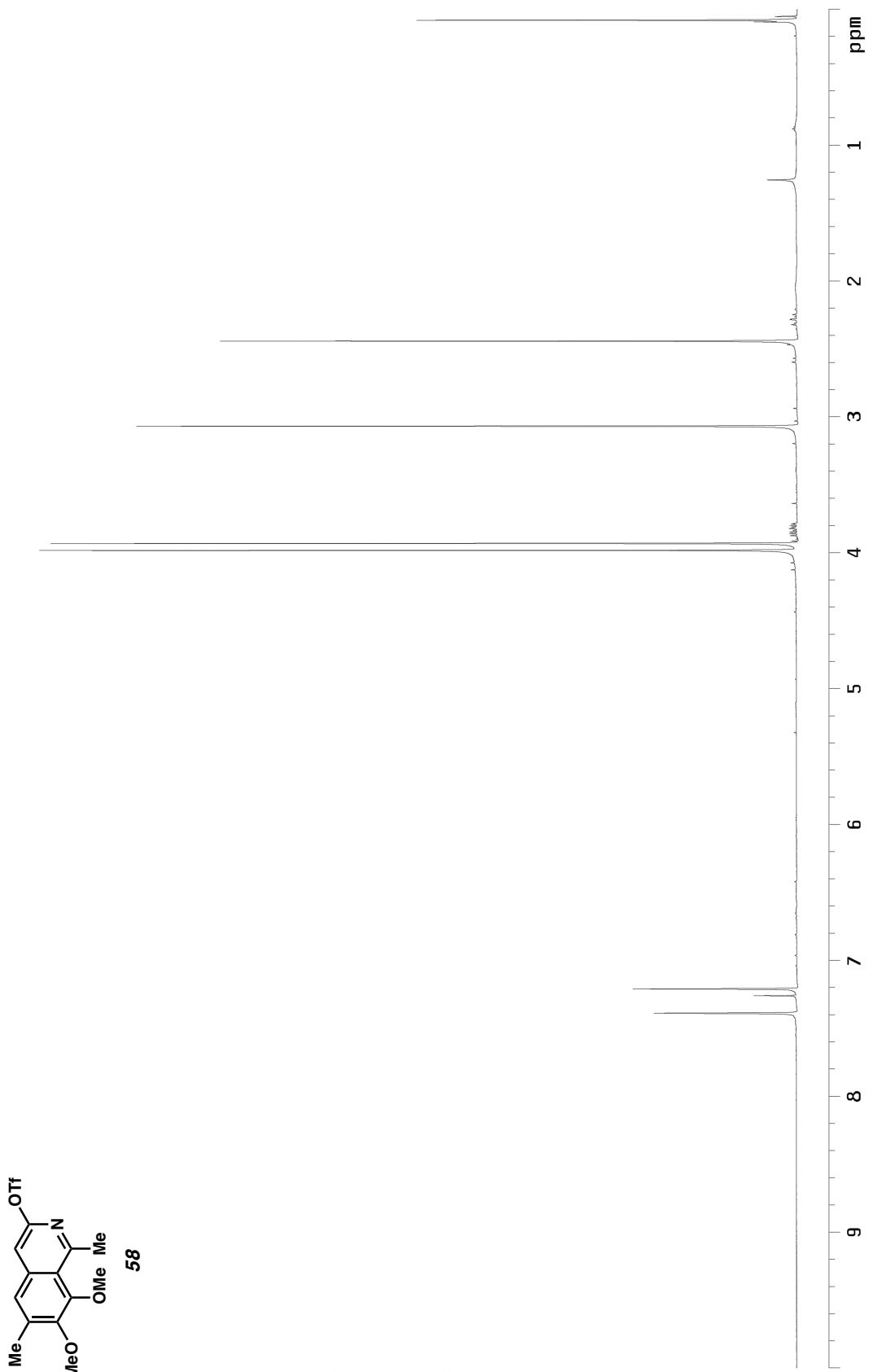
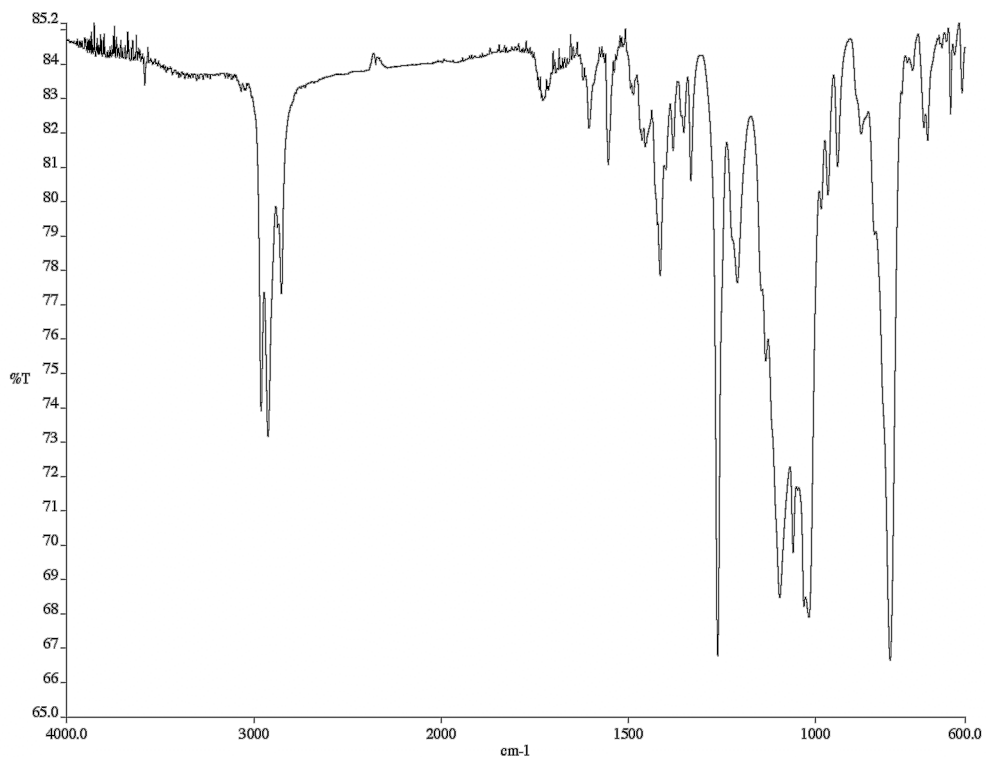
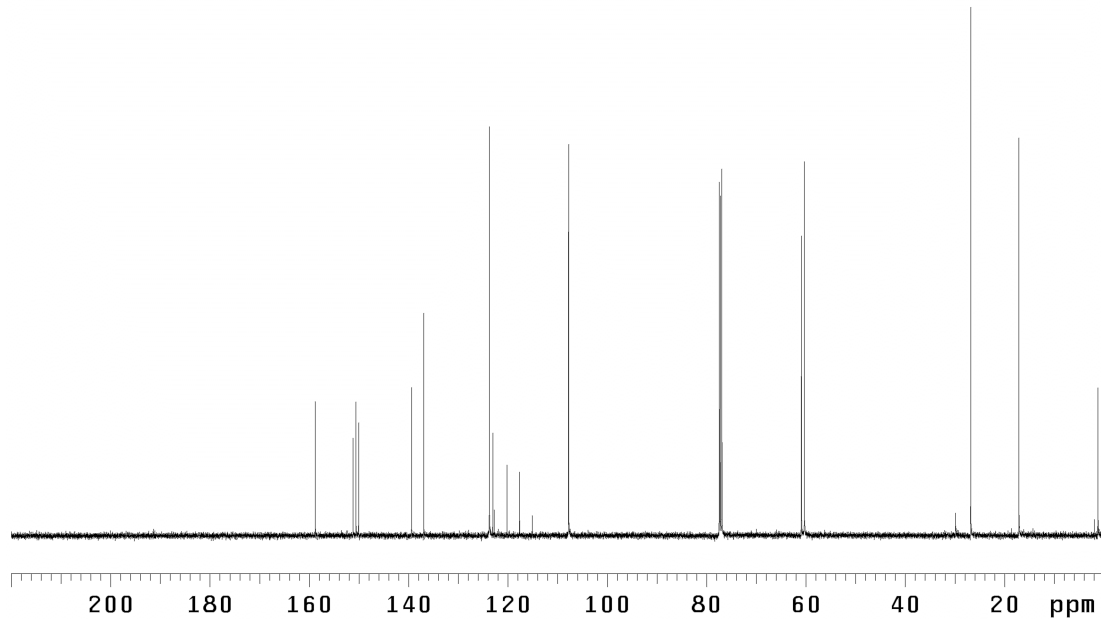


Figure A2.4.1. ^1H NMR (500 MHz, CDCl_3) of compound **58**.

Figure A2.4.2. Infrared spectrum (thin film/NaCl) of compound **58**.Figure A2.4.3. ^{13}C NMR (125 MHz, CDCl_3) of compound **58**.

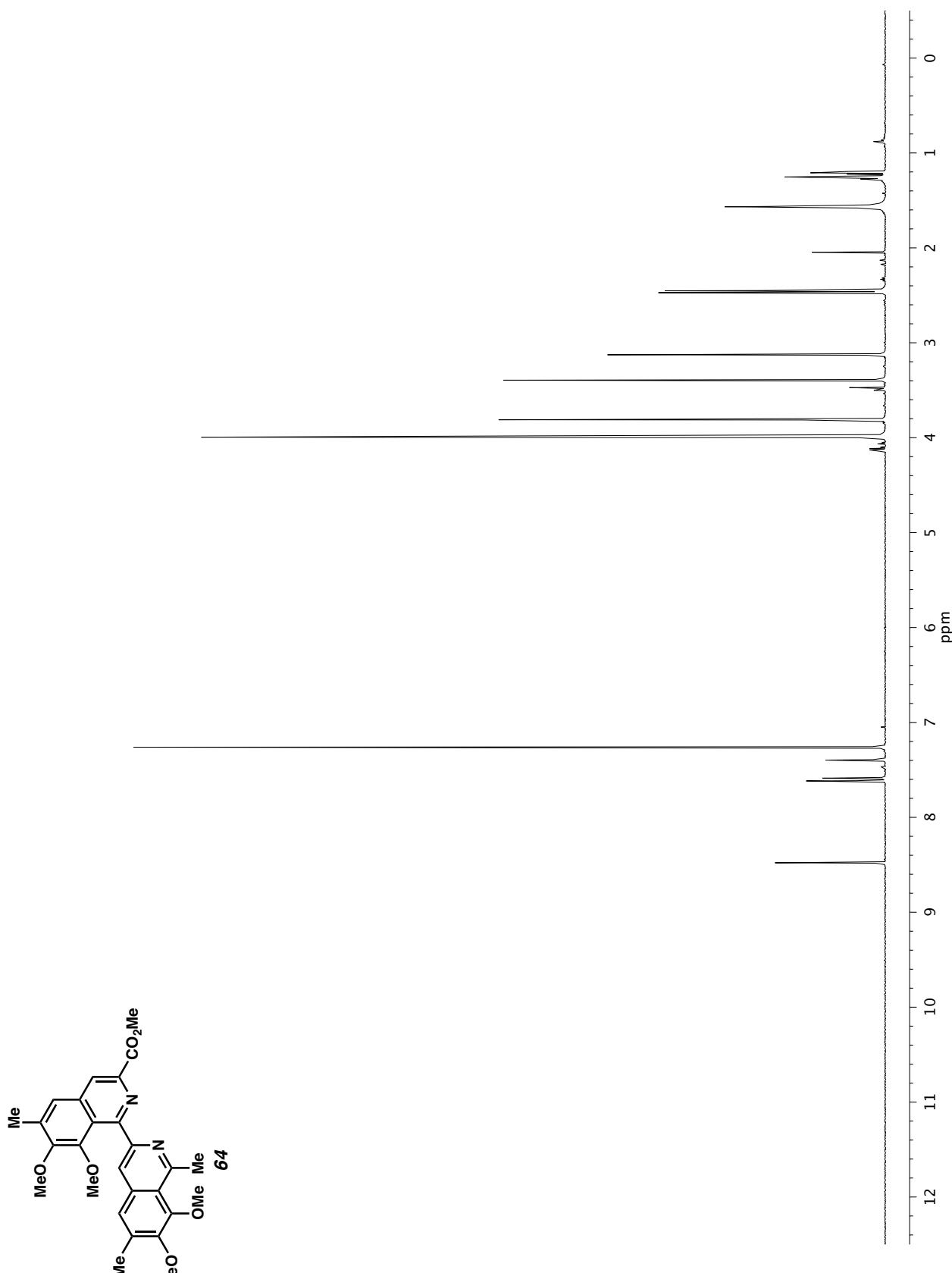
Figure A2.5.1. ^1H NMR (500 MHz, CDCl_3) of compound 64.

Figure A2.5.2. Infrared spectrum (Thin Film, NaCl) of compound **64**.

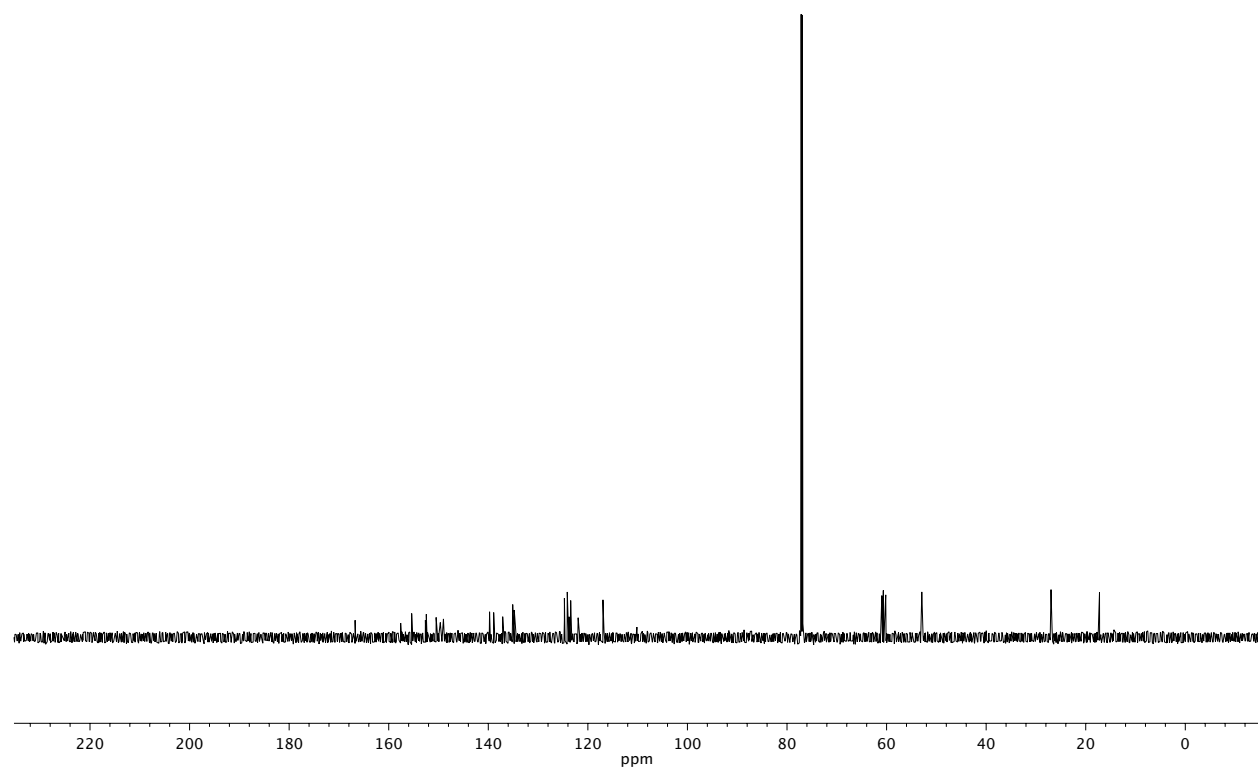


Figure A2.5.3. ^{13}C NMR (126 MHz, CDCl_3) of compound **64**.

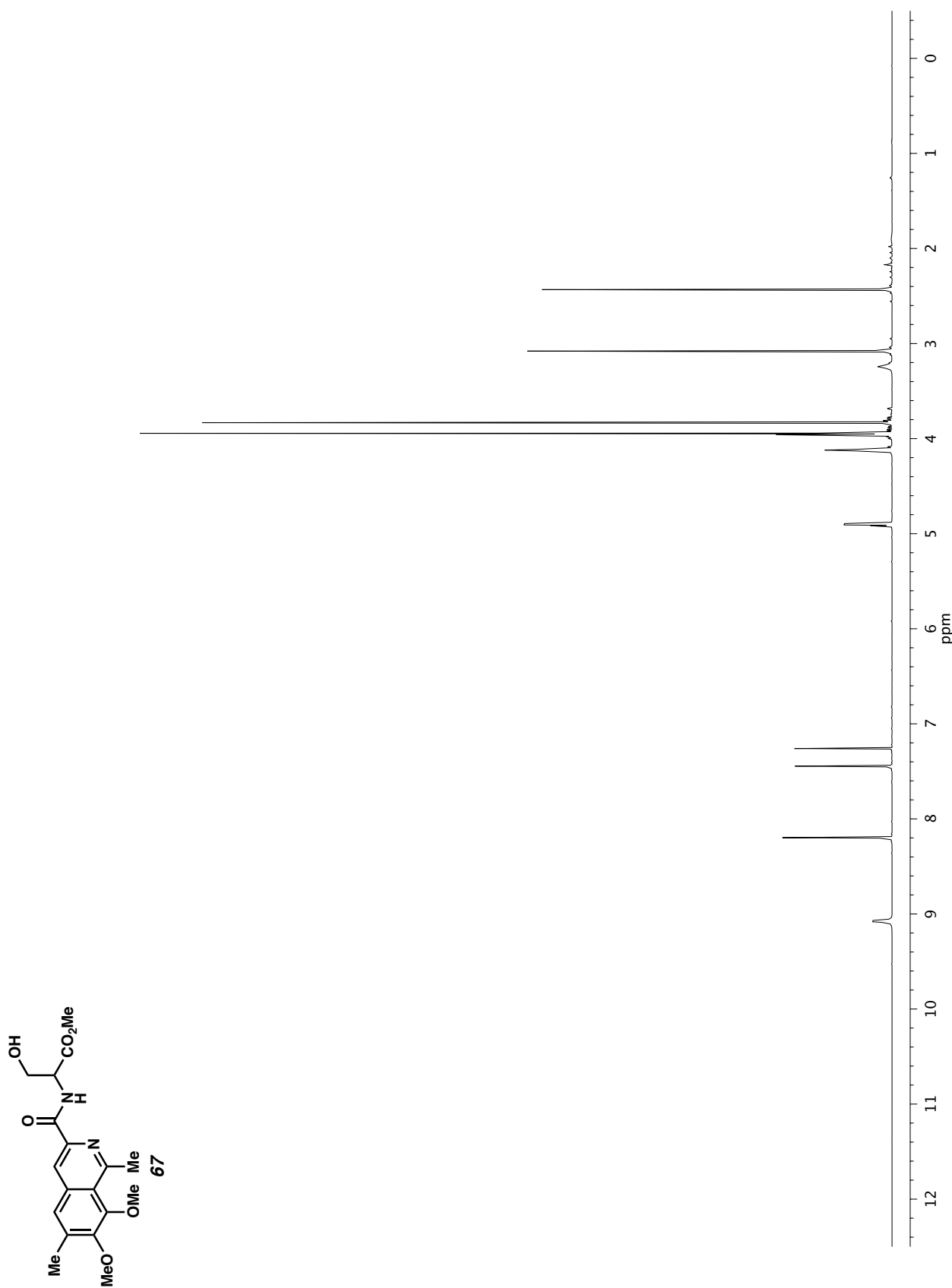
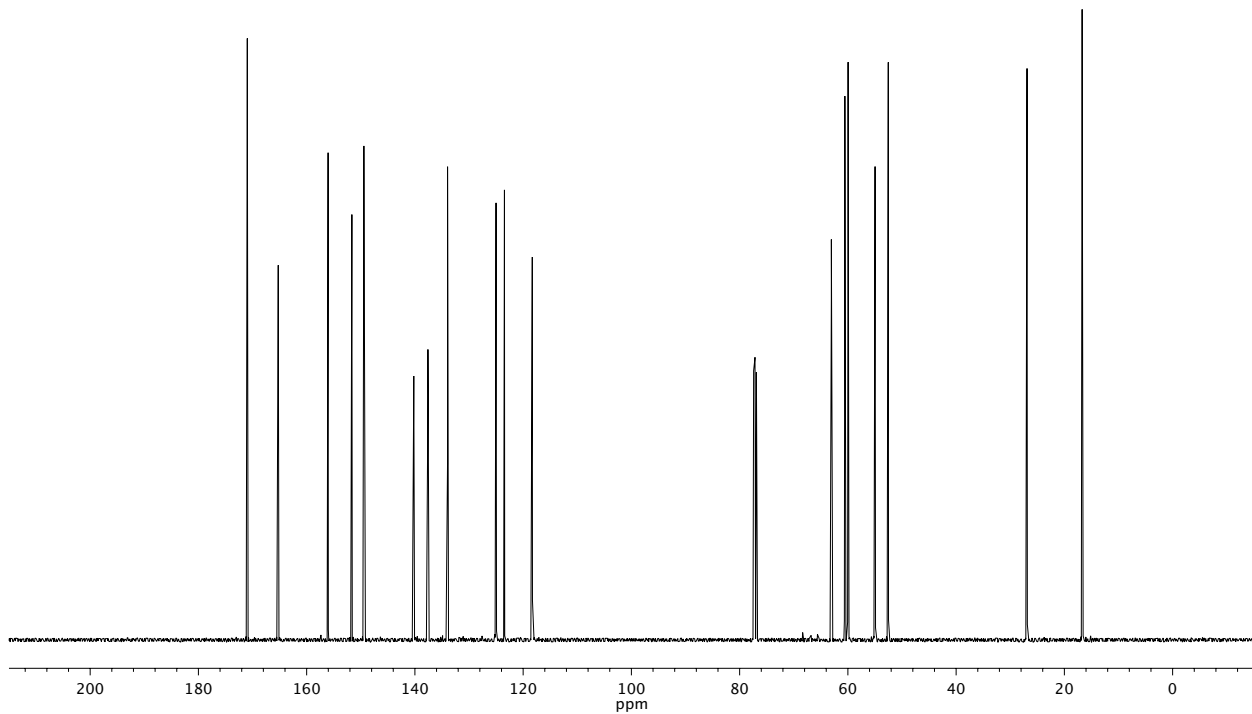
Figure 2.6.1. ^1H NMR (500 MHz, CDCl_3) of compound 67.

Figure 2.6.2. Infrared spectrum (Thin Film, NaCl) of compound **67**.Figure 2.6.3. ^{13}C NMR (126 MHz, CDCl_3) of compound **67**.

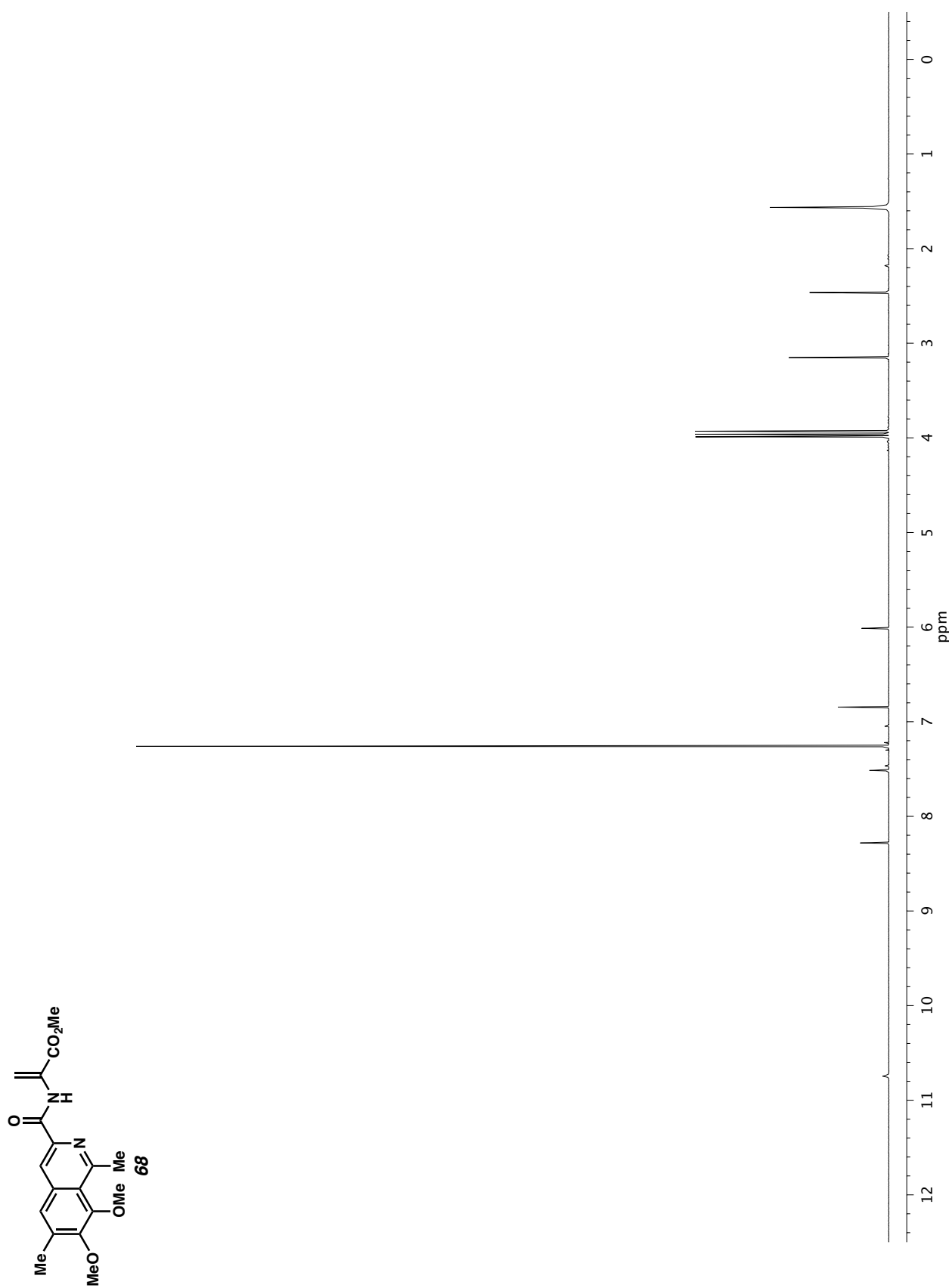
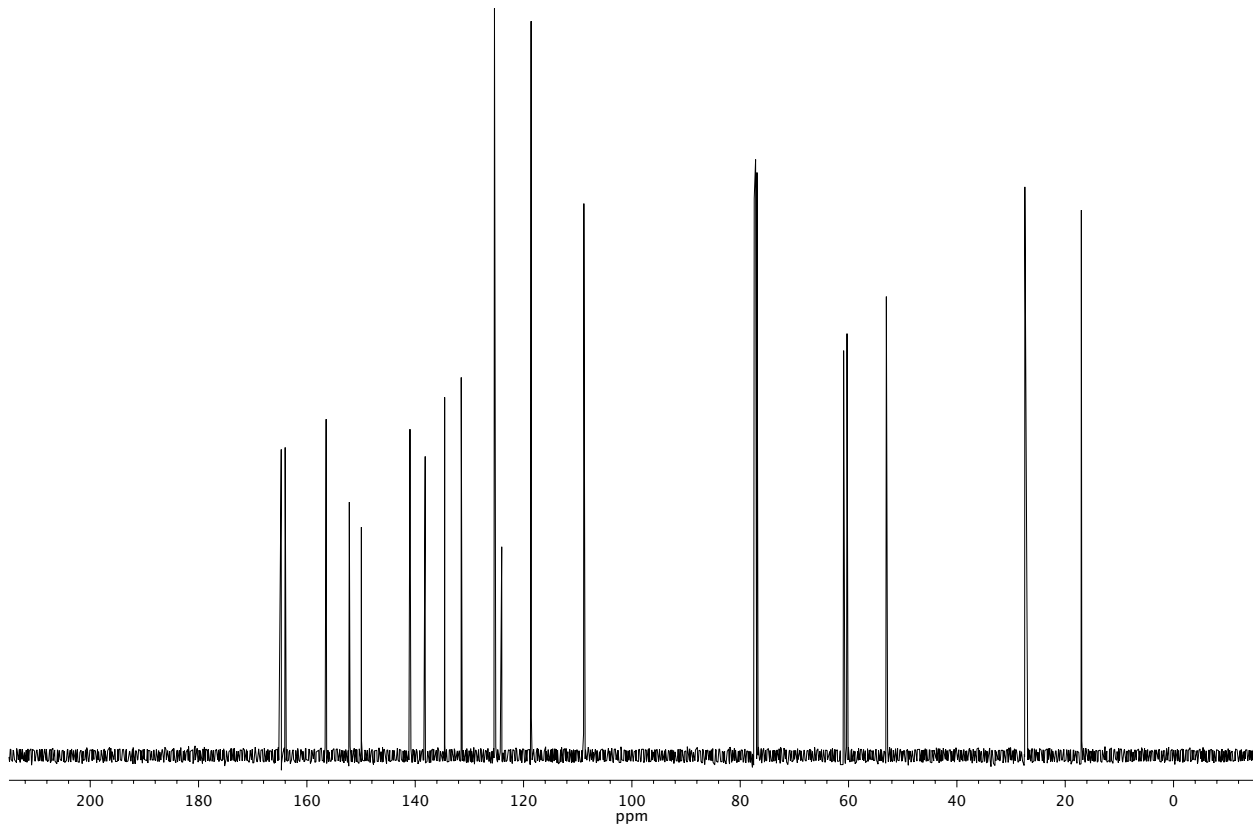
Figure A2.7.1. ^1H NMR (500 MHz, CDCl_3) of compound **68**.

Figure A2.7.2. Infrared spectrum (Thin Film, NaCl) of compound **68**.Figure A2.7.3. ^{13}C NMR (126 MHz, CDCl_3) of compound **68**.

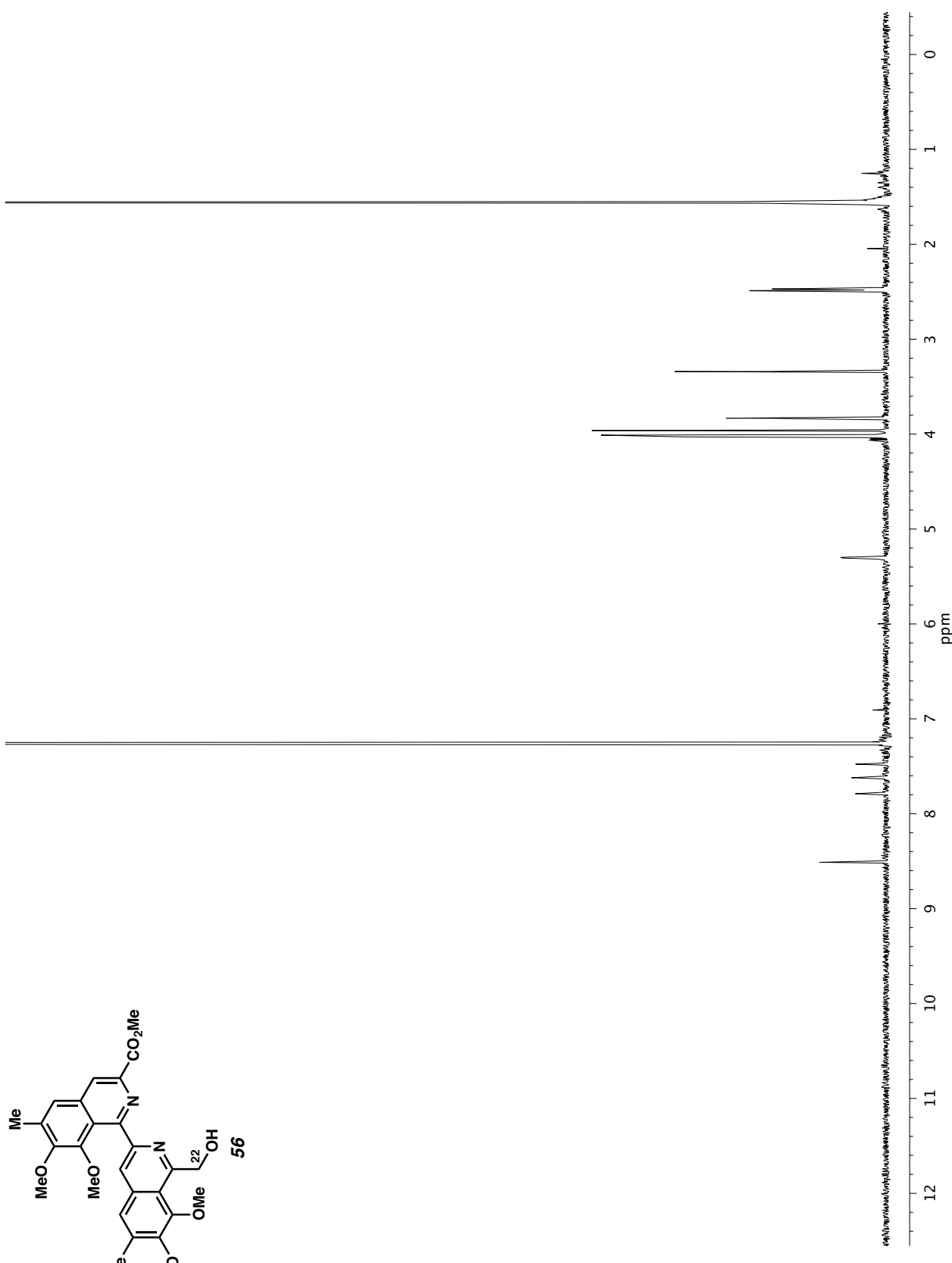
Figure A2.8.1. ^1H NMR (500 MHz, CDCl_3) of compound 56.

Figure A2.8.2. Infrared spectrum (Thin Film, NaCl) of compound **56**.

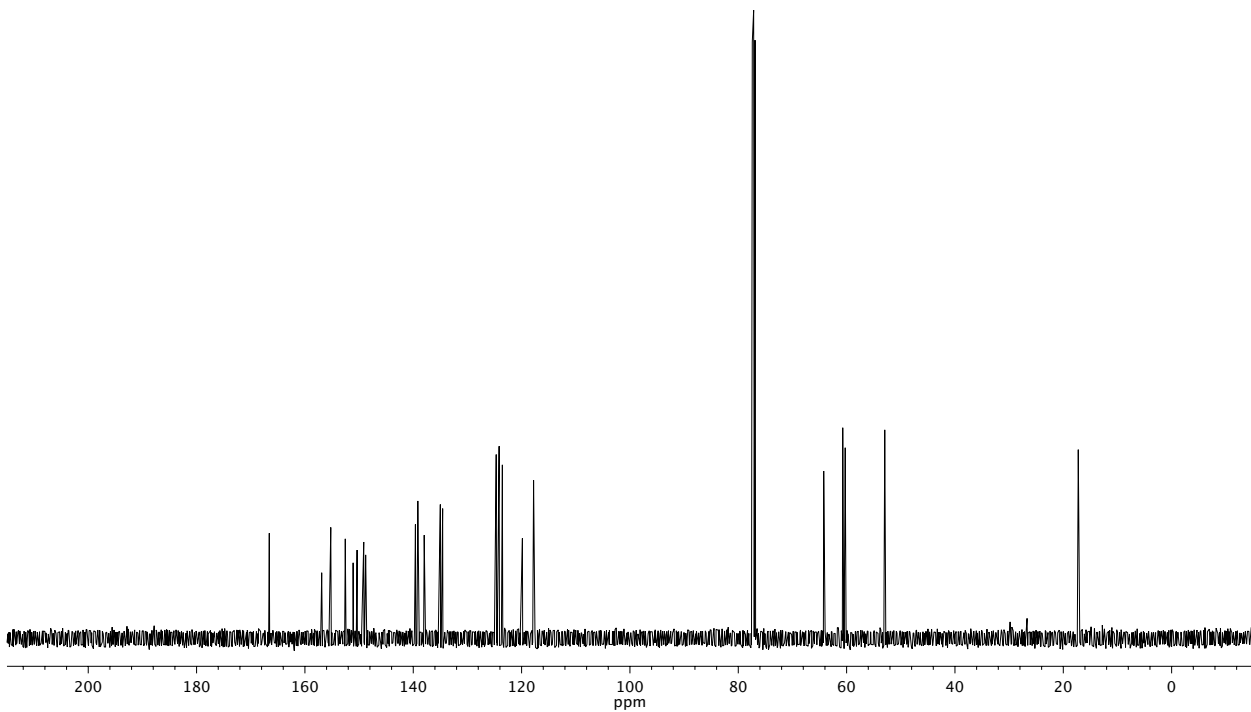


Figure A2.8.3. ^{13}C NMR (126 MHz, CDCl_3) of compound **56**.

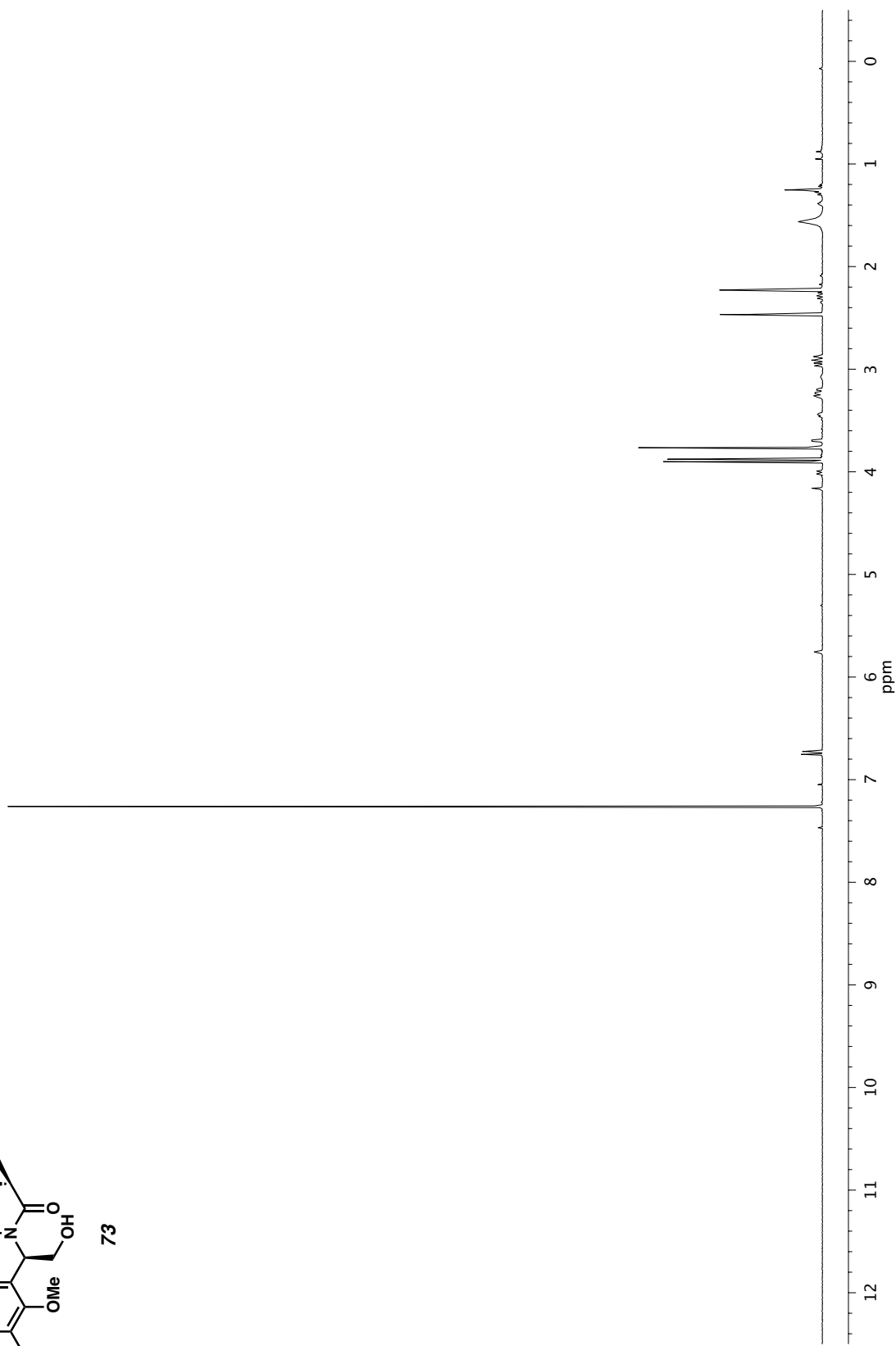
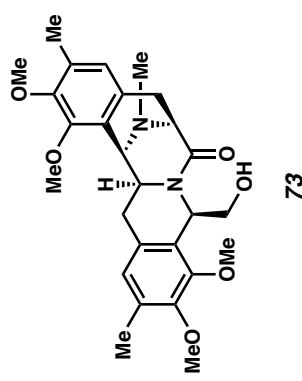


Figure A2.9.1. ^1H NMR (500 MHz, CDCl_3) of compound 73.

Figure A2.9.2. Infrared spectrum (Thin Film, NaCl) of compound **73**.

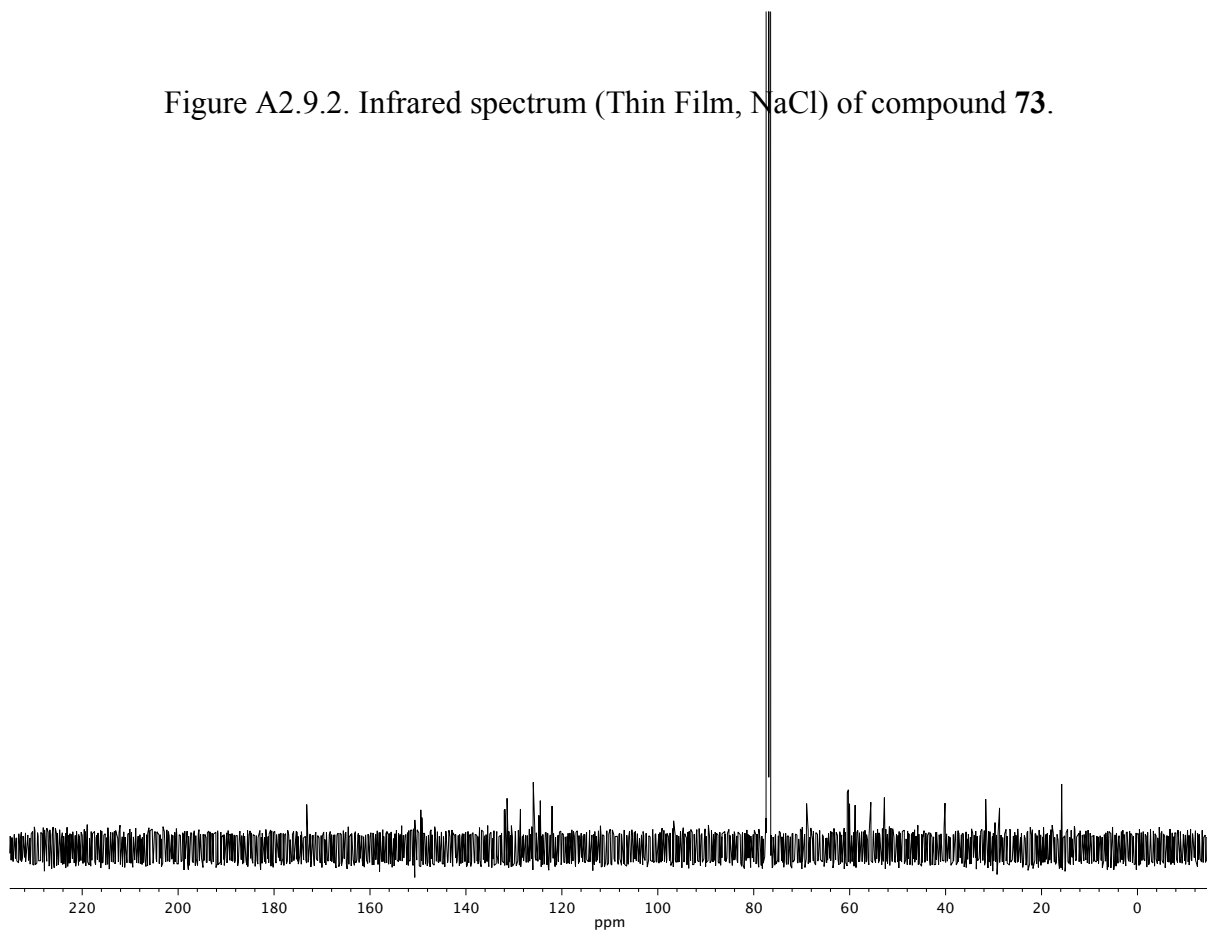


Figure A2.9.3. ^{13}C NMR (126 MHz, CDCl_3) of compound **73**.

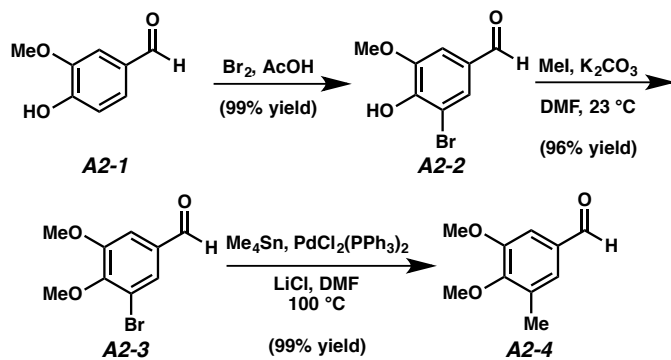
Appendix 3

A Tin-Free Route to a Complex Aryne Precursor

A3.1 Introduction and Synthesis

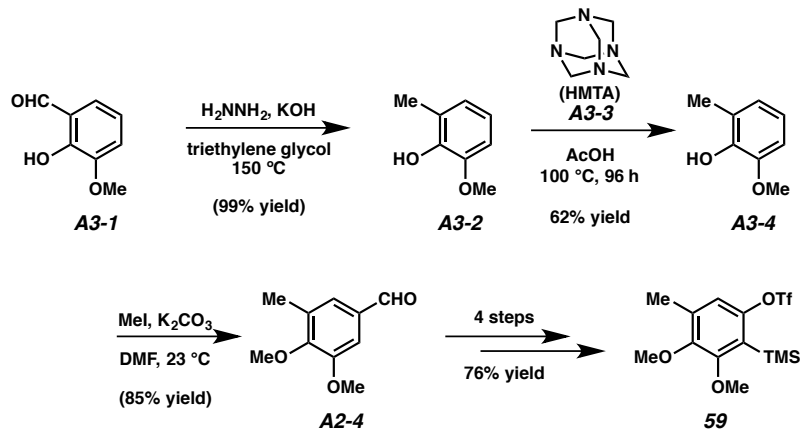
The synthetic sequence originally devised for the preparation of aryne precursor **59** proved to be reliable and high yielding.¹ However the third step of the route relied on the cross-coupling of 3-bromovanillin (**A2-1**) with tetramethyl tin (Scheme A3-1). While this reaction proceeded in quantitative yield, its sensitivity to oxygen and its use of a highly toxic stannane (i.e. tetramethyl tin) limited its scalability. To overcome this challenge, we developed a tin-free route to benzaldehyde **A2-4**.

Scheme A3-1. First generation synthesis of benzaldehyde **A2-4**.



We began with the Wolff–Kishner reduction of *ortho*-vanillin (**A3-1**), which upon treatment with hydrazine monohydrate and potassium hydroxide afforded 6-methyl guaiacol (**A3-2**) in quantitative yield (Scheme A3-2). This synthetic step could be performed on 100 g (657.2 mol) scale. With 6-methyl guaiacol (**A3-2**) in hand, we sought to prepare aldehyde **A3-4** using a Duff reaction. Exposure of 6-methyl guaiacol (**A3-2**) to hexamethylenetetramine (HMTA) (**3-3**) in acetic acid furnished benzaldehyde **A3-4** in 62% yield in a regioselective manner. The Duff reaction to prepare this aldehyde could be carried out on as large as 180 g scale with without loss of yield. Methylation of phenol **A3-4** using MeI could be accomplished in 85% yield give aldehyde **A2-4**. This synthetic sequence allows us to access the identical benzaldehyde intermediate (**A2-4**) used in our first generation synthesis, however in a more scalable fashion, providing 125 g of the desired arene (**A2-4**). This material was taken forward as previously disclosed to afford aryne precursor **59** in just 4 steps and 76% yield from aldehyde **A2-4**.

Scheme A3-2. Preparation of Benzaldehyde A2-4.

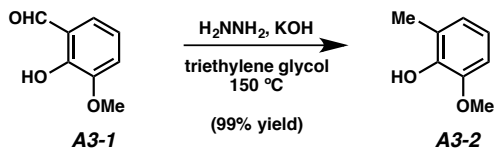


A3.2 Experimental Section

A3.2.1 Materials and Methods

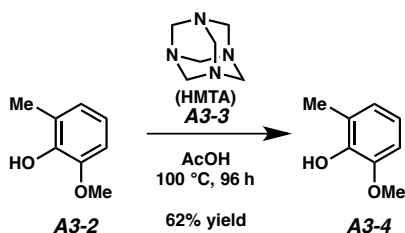
Unless stated otherwise, reactions were performed in flame-dried glassware under an argon or nitrogen atmosphere using dry, deoxygenated solvents (distilled or passed over a column of activated alumina). Commercially obtained reagents were used as received. Reaction temperatures were controlled by an IKA mag temperature modulator. Thin-layer chromatography (TLC) was performed using E. Merck silica gel 60 F254 precoated plates (0.25 mm) and visualized by UV fluorescence quenching, potassium permanganate, or CAM staining. SiliaFlash P60 Academic Silica gel (particle size 0.040-0.063 mm) was used for flash chromatography. ^1H and ^{13}C NMR spectra were recorded on a Varian 500 (at 500 MHz and 125 MHz, respectively) and are reported relative to CHCl_3 (δ 7.24). Data for ^1H NMR spectra are reported as follows: chemical shift (δ ppm) (multiplicity, coupling constant (Hz), integration). Data for ^{13}C spectra are reported in terms of chemical shift relative to CHCl_3 (δ 77.23). IR spectra were recorded on a Perkin Elmer Paragon 1000 Spectrometer and are reported in frequency of absorption (cm^{-1}). HRMS were acquired using an Agilent 6200 Series TOF with an Agilent G1978A Multimode source in electrospray ionization (ESI), atmospheric pressure chemical ionization (APCI) or mixed (MM) ionization mode.

A3.2.2 Experimental Procedures



6-methyl guaiacol (**A3-1**)

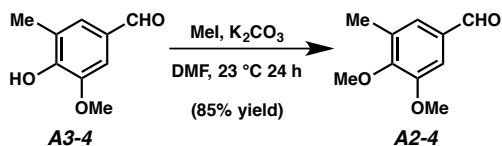
O-vanillin (**A3-1**) (100.0 g, 0.6572 mol) was dissolved in triethylene glycol (500.0 mL) in a 3-neck round-bottom flask equipped with a reflux condenser, overhead stirrer and an internal thermometer. Hydrazine monohydrate was added (63.5 ml, 1.31 mol) dropwise through the condenser. The reaction mixture was heated to 110 °C for 10 min. After which time, the reaction was cooled to ~90 °C and KOH (228.0 g, 4.063 mol) was added portion-wise. (WARNING: Addition of KOH was exothermic and gas evolved). The orange solution was heated to 150 °C for 12 h. The reaction was then cooled to room temperature and the base neutralized (pH = 7) using NH_4Cl (aq.). This was extracted 4 times with CHCl_3 . The organic layers were combined, washed with brine, dried over Na_2SO_4 , filtered and volatiles were removed in vacuo to afford 6-methyl guaiacol (**A3-2**, 90.81g, 0.6572 mol, 99% yield). Spectroscopic data were identical to literature reported values.²



Benzaldehyde A3-4³

6-methyl guaiacol (**A3-2**) (181.6 g, 1.314 mol) was placed in a 12 L 3-neck round-bottom flask equipped with an overhead stirrer, temperature probe and reflux condenser to this flask was added acetic acid (6.0 L). Hexamethylenetetramine (460.5 g, 3.285 mol) was added portion-wise. A small increase in temperature was observed during addition (~8 °C). The reaction mixture was stirred and heated to an internal temperature of 100 °C using a heating mantle. It was kept at 100 °C for 96 h. The yellow/orange solution darkened to brown over the course of the reaction. At this time the heating mantle was removed and volatiles were removed in vacuo. The brown residue was split into two parts for ease of handling. Water was added to each part and extracted with CH₂Cl₂ (4 x 200 mL). The organic layers were combined and washed with brine. The organic layers were then dried over Na₂SO₄, filtered and the volatiles were removed in vacuo. The residue was filtered through a silica pad using 50% EtOAc in Hexanes. The solvent was removed in vacuo. The desired aldehyde (**A3-4**) could be recrystallized from CH₂Cl₂ (136.0 g, 0.8180 mol, 61% yield) as a tan solid. R_f = 0.36 (20% EtOAc in Hexanes); ¹H NMR; (500 MHz, CDCl₃) δ 9.80 (s, 1H), 7.31 (m, 1H), 7.29 (m, 1H), 6.28 (s, 1H), 3.96 (s, 3H), 2.32 (s, 3H). ¹³C NMR (126 MHz, CDCl₃) δ 191.17, 149.74, 146.70, 128.88, 128.80, 124.03, 106.68, 77.27, 77.02, 76.76, 56.21, 15.28; IR (NaCl/film) 3322, 3007, 2841, 1665, 1651, 1593, 1501, 1463, 1428, 1404, 1366, 1311, 1195, 1146, 1094, 1011, 985,

931, cm^{-1} ; HRMS (MM: ESI-APCI) m/z calc'd for $\text{C}_9\text{H}_{10}\text{O}_3$ [M+H]: 167.0703, found 167.0709.



Benzaldehyde A2-4

Phenol **A3-4** (1.00 g, 6.02 mmol) and K_2CO_3 (1.22 g, 9.02 mmol) were dissolved in dry DMF (9.0 mL)⁴ in a flame-dried round bottom flask equipped with a magnetic stir bar and a rubber septum under nitrogen atmosphere. Methyl iodide (0.450 mL, 7.22 mmol) was added drop-wise via syringe and the reaction was stirred at ambient temperature for 24 h. At which time, 20 mL of saturated aqueous NaHCO_3 was added. This was then extracted with Et_2O (3 x 25 mL). The organic layers were combined, washed with water (2 x 25 mL), dried over Na_2SO_4 , filtered and the volatiles were removed in vacuo to cleanly afford desired benzaldehyde **A2-4** (0.918 g, 5.09 mmol, 85% yield) without need for further purification. Spectroscopic data were identical to that reported in chapter 1 of this thesis.

A3.3 References

1. Tadross, P. M.; Gilmore, C. D.; Bugg, P.; Virgil, S. C. Stoltz, B. M. *Org. Lett.* **2010**, *12*, 1224–1227.
2. Stevens, R. V.; Angle, S. R.; Kloc, K.; Mak, K. F.; Liu, Y. X.; Trueblood, K. N. *J. Org. Chem.* **1986**, *51*, 4347–4353.
3. Razafindrabe, C. R.; Aubry, S.; Bourdon, B.; Andriantsiferana, M.; Pellet-Rostaing, S.; Lemaire, M. *Tetrahedron*, **2010**, *66*, 9061–9066.
4. On large scale (>100 g), dry MeCN was used and heated to 50 °C for 24 h. Aqueous work up was not performed. Volatiles were removed in vacuo and the desired aldehyde could be recrystallized from CH₂Cl₂/hexanes.

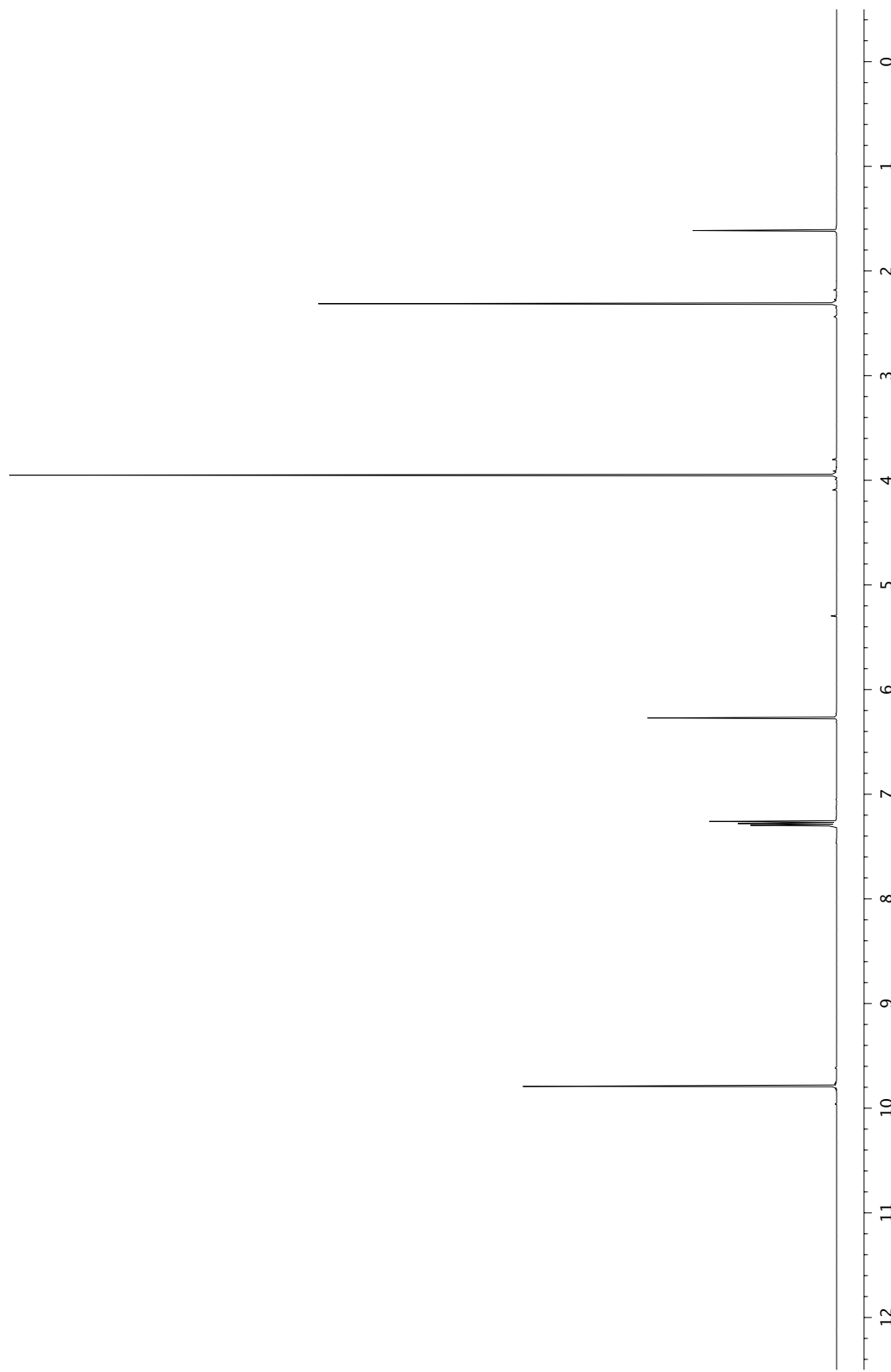
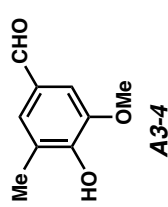


Figure A3.1.1 ^1H NMR (500 MHz, CDCl_3) of compound A3-4.

Figure A3.1.2 Infrared spectrum (Thin Film, NaCl) of compound **A3-4**.

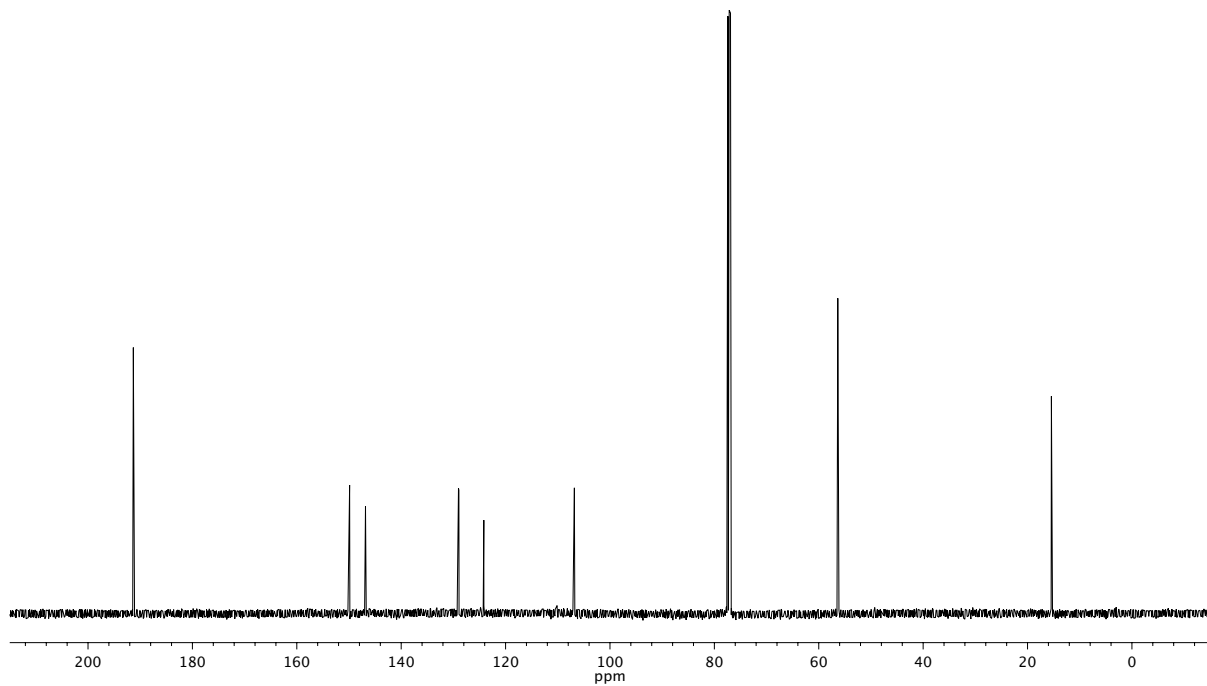
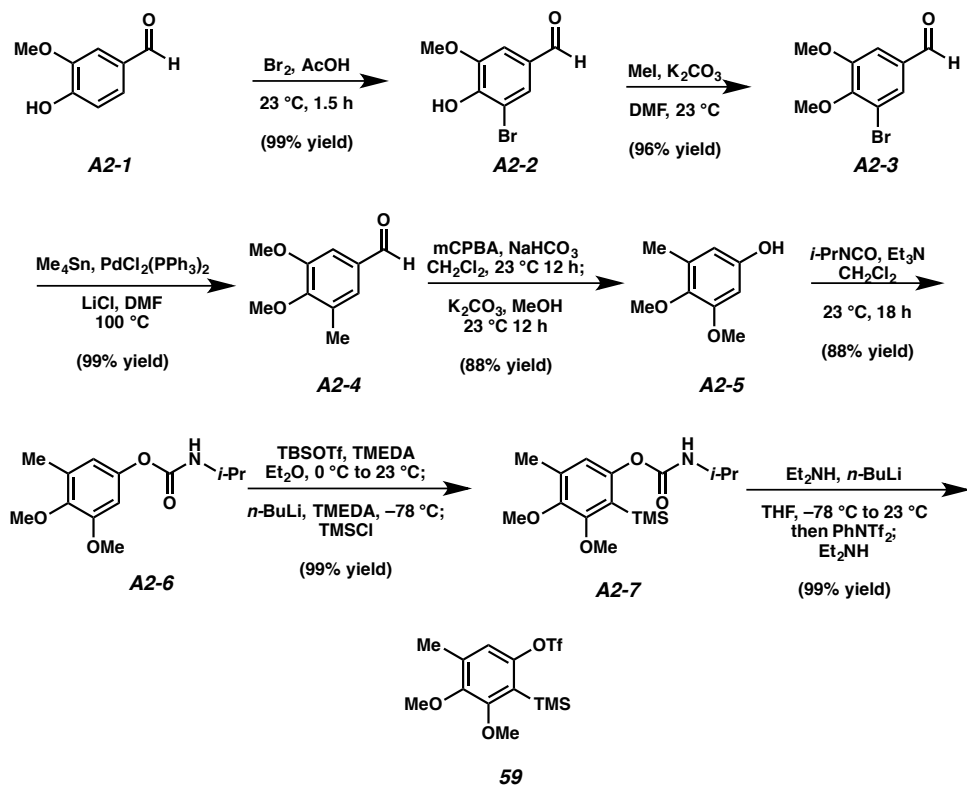
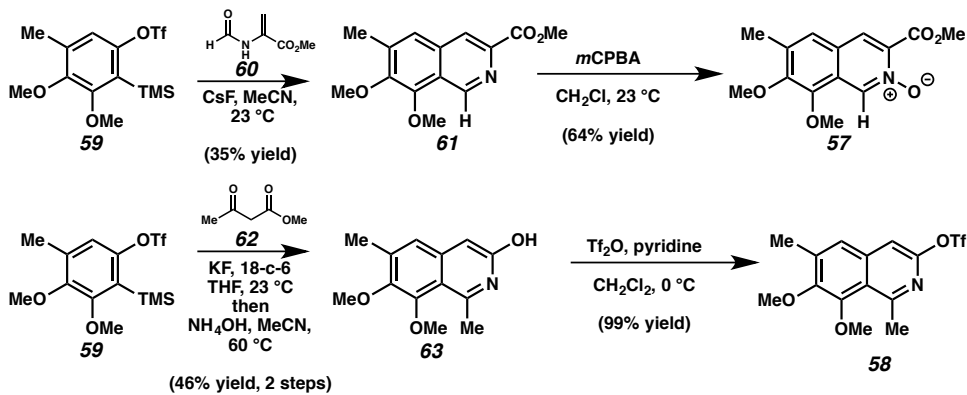
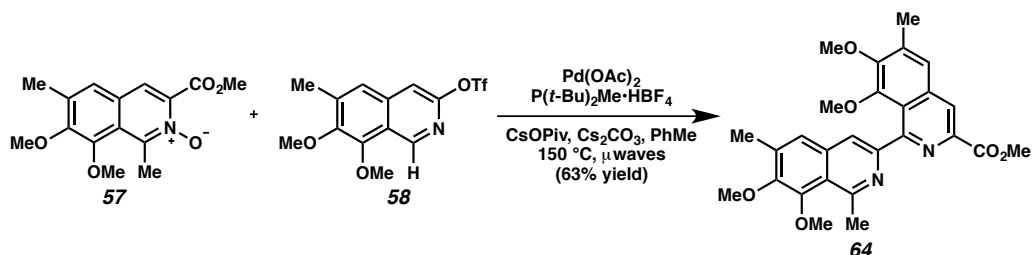
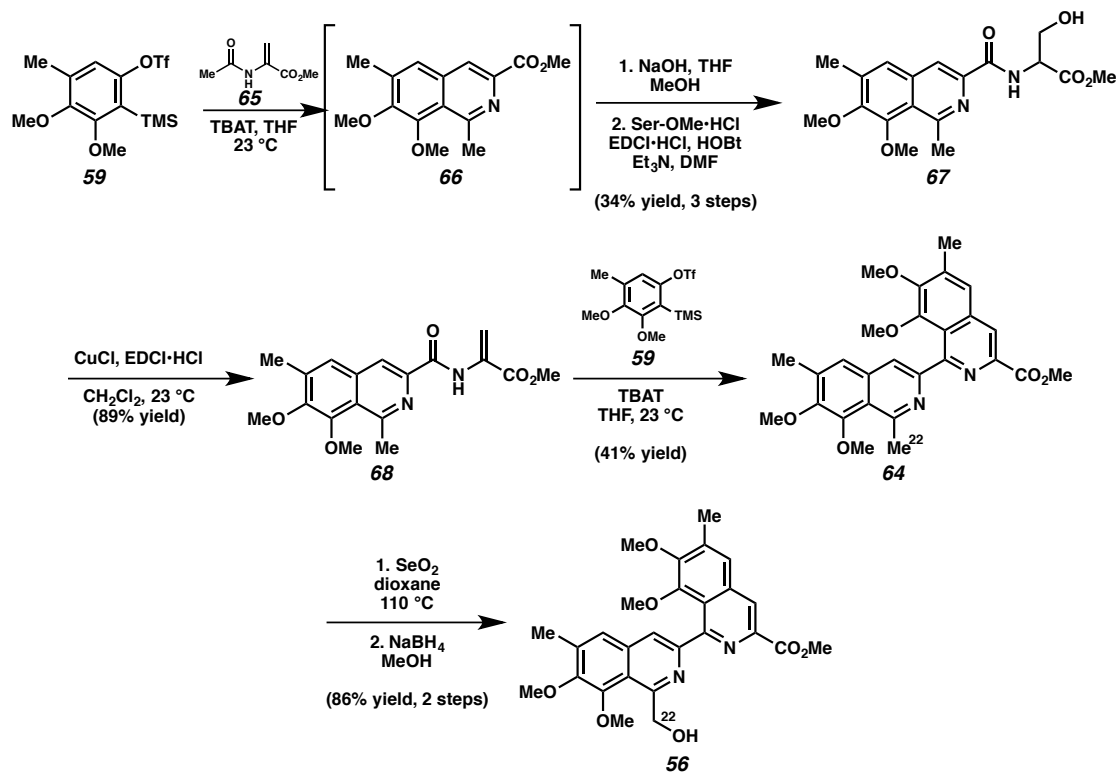


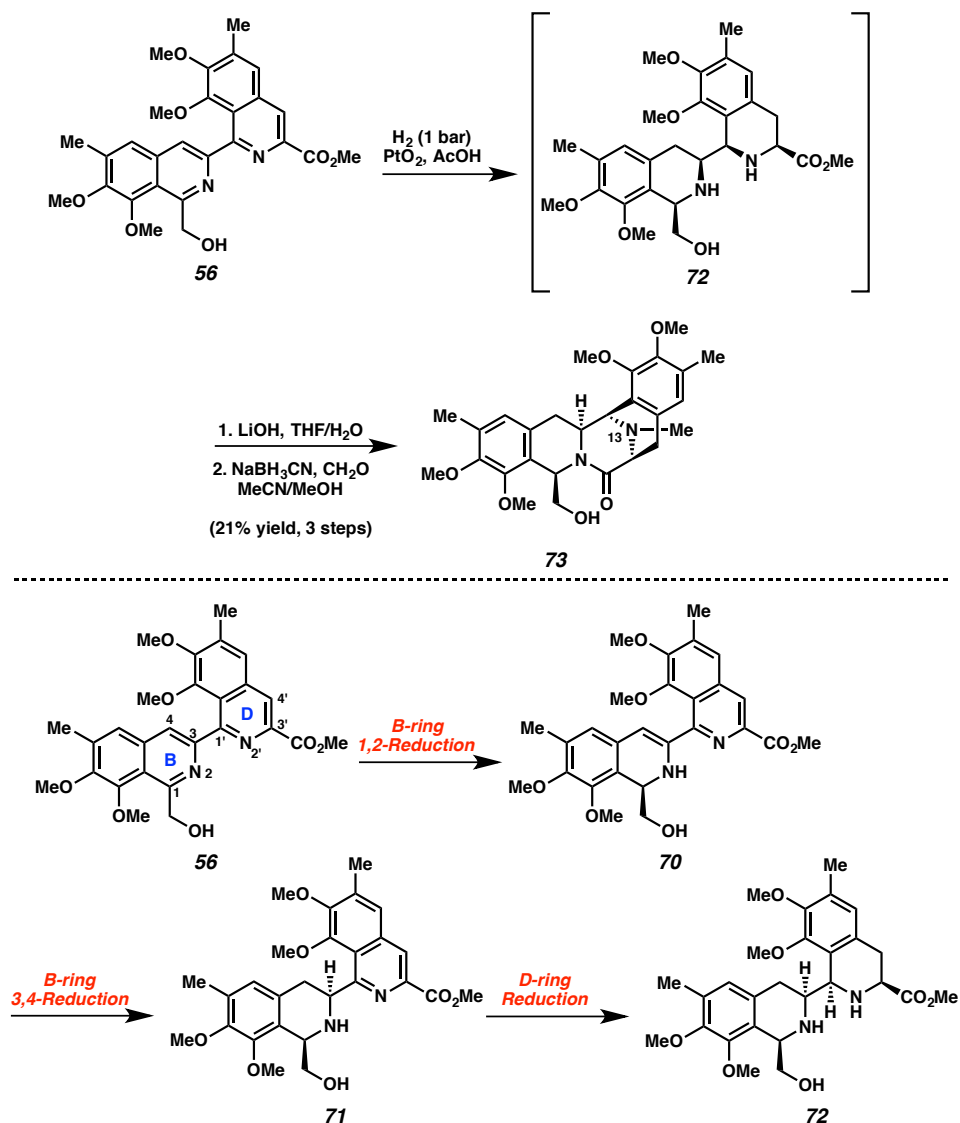
Figure A3.1.3 ^{13}C NMR (126 MHz, CDCl_3) of compound **A3-4**.

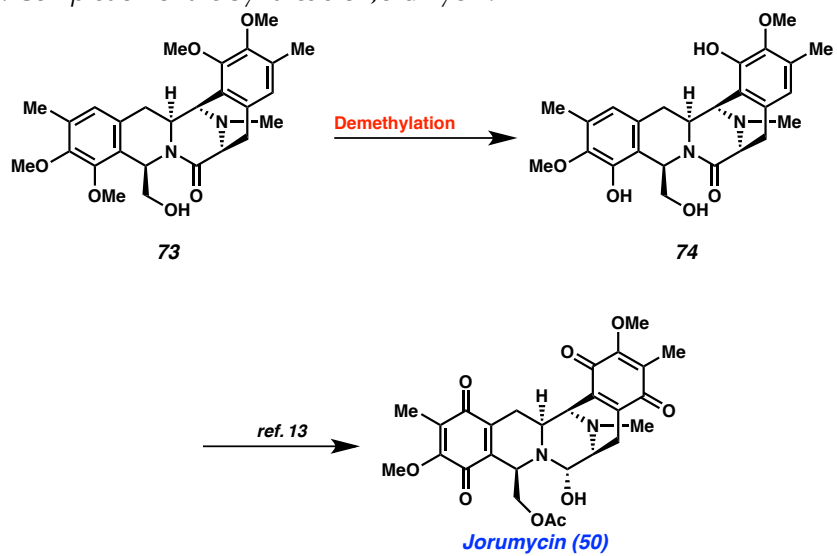
Appendix 4

Synthetic Summary of The Total Synthesis of Jorumycin

Scheme A4-1. Preparation of aryne precursor **59**.**Scheme A4-2.** Aryne annihilations

Scheme A4-3. Cross-coupling of isoquinolines **57** and **58**.**Scheme A4-4.** Alternative approach to bis-isoquinoline **XX**.

Scheme A4-5. Origins of Diastereoselectivity for the Reduction of Bis-Isoquinoline XX.

Scheme A4-6. Completion of the Synthesis of Joramycin.

CHAPTER 3

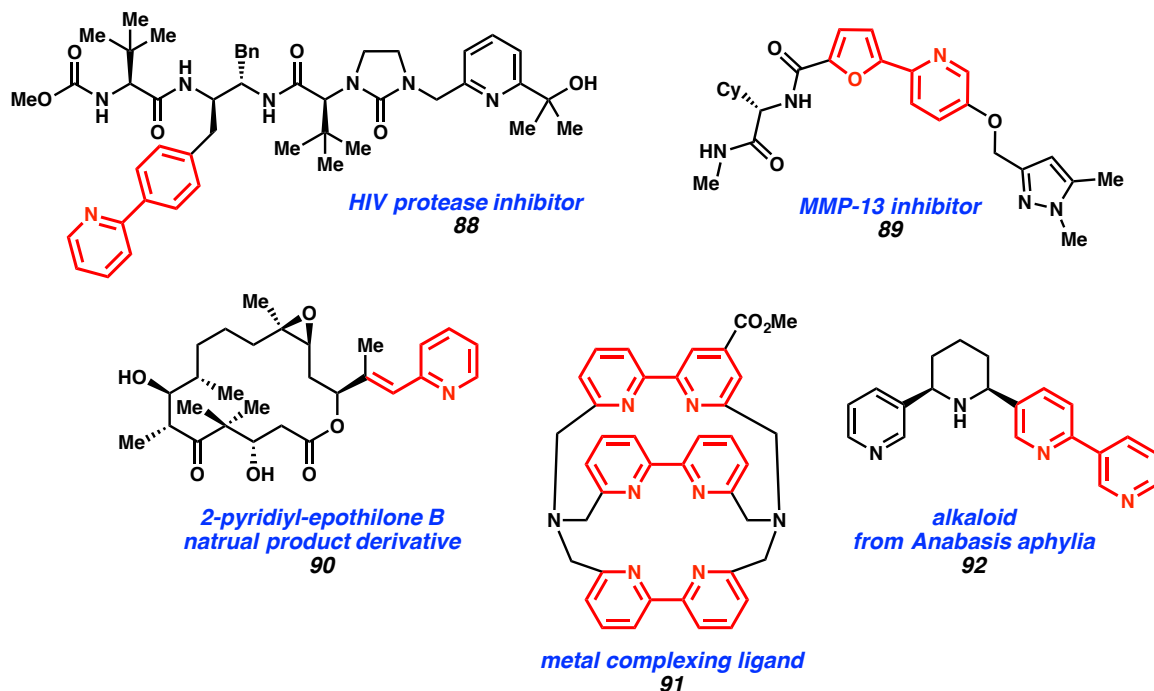
Decarboxylative Cross-Coupling of (2-azaaryl)carboxylates with Aryl Halides

3.1 Introduction

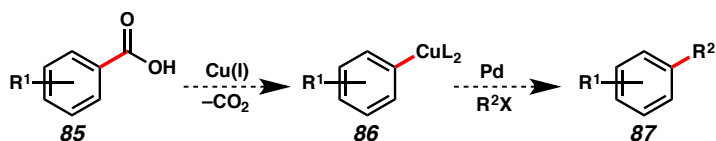
The 2-substituted pyridine motif (Figure 3.1), is present in a number of important small molecules,¹ however 2-azaaryl nucleophiles typically used in cross-coupling reactions, such as organozincs, Grignards, organolithiums, organostannanes, and boronic acids, are notoriously unstable and difficult to prepare.² While some modifications have been made to improve their synthetic viability, especially within the realm of boronic acid derivatives, these approaches are often inconvenient or produce toxic waste.³ The development of a decarboxylative method of generating these organometallic species (e.g., **86**) *in situ* from (2-azaaryl)carboxylates (**85**) represents a desirable alternative to traditional aryl nucleophiles for the synthesis of 2-aryl pyridine structures (**87**) (Scheme

3.1). 2-(azaaryl)carboxylates are generally inexpensive, are stable to both air and water, and represent a more ecologically friendly alternative to their organometallic counterparts.

Figure 1.1. The importance of 2-substituted pyridine.



Scheme 3.1. Decarboxylative cross-coupling of aryl carboxylic acids with aryl halides.



Myers and co-workers reported the first practical decarboxylative cross-coupling in 2002,⁴ a palladium-catalyzed decarboxylative Heck-type olefination (Scheme 3.2). This work demonstrated that olefinated arenes are accessible from benzoic acids and

olefins in the presence of catalytic palladium(II) triflate and silver carbonate. This represented an important advance as it provided an alternative to aryl halides and aryl pseudo-halides usually used in Heck reactions. A critical development within the field of decarboxylative cross-coupling was reported in 2006; Goossen and co-workers disclosed a catalytic decarboxylative cross-coupling reaction, utilizing a dual-catalyst system of copper and palladium. Mechanistically, this dual catalyst approach likely proceeds through a decarboxylative cupration of the arylcarboxylate partner. The resulting aryl copper species subsequently undergoes transmetalation onto the palladium, which furnishes the coupled product through reductive elimination (Figure 3.2).⁵ Unlike typical cross-couplings, which require stoichiometric aryl organometallic nucleophiles, decarboxylative couplings proceed through an *in situ* generation of the nucleophilic coupling partner.

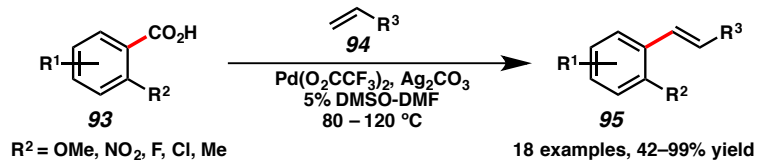
A variety of non-aryl carboxylates have proven to act as efficient coupling partners in decarboxylative cross-coupling reactions,⁶ including alkynes,⁷ α -keto acids,⁸ and 2-(2-azaaryl)acetates.⁹ While these represent great advances within the field, the robust coupling of a key class of molecules, namely 2-(azaaryl)carboxylates, has been elusive. Recently, during the course of our own work on this topic, Wu and co-workers reported on the palladium-catalyzed decarboxylative cross-coupling reactions of 2-picolinic acid.¹⁰ In light this work, we sought to supplement their studies with our own findings.

Our laboratory became interested in the cross-coupling to (2-azaaryl)nucleophiles within the context of jorumycin. We sought to prepare the bisisoquinoline **100** via a

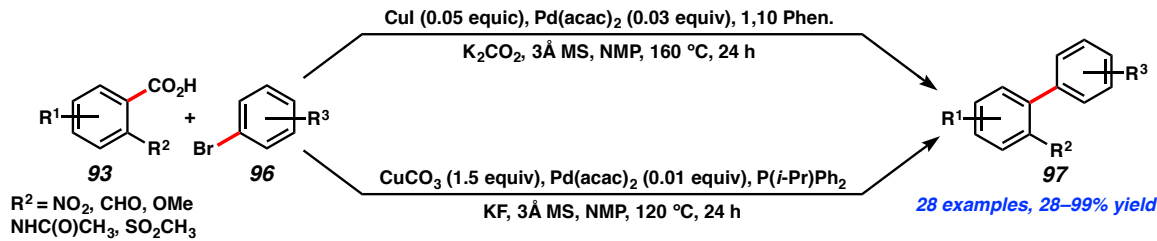
convergent cross-coupling between two aryl fragments. Because both of our coupling partners were isoquinolines, we initiated exploration of the decarboxylative cross-coupling between 3-triflyl isoquinoline **98** and 1-carboxy isoquinoline **99** (Scheme 3.3). Owing to the importance of these motifs, we also looked to develop a general method of performing the decarboxylative cross-coupling of (2-azaaryl)carboxylates with aryl electrophiles.

Scheme 3.2. Myers's decarboxylative olefination and Goossen's decarboxylative coupling of benzoic acids and aryl bromides.

Myer's Decarboxylative Olefination

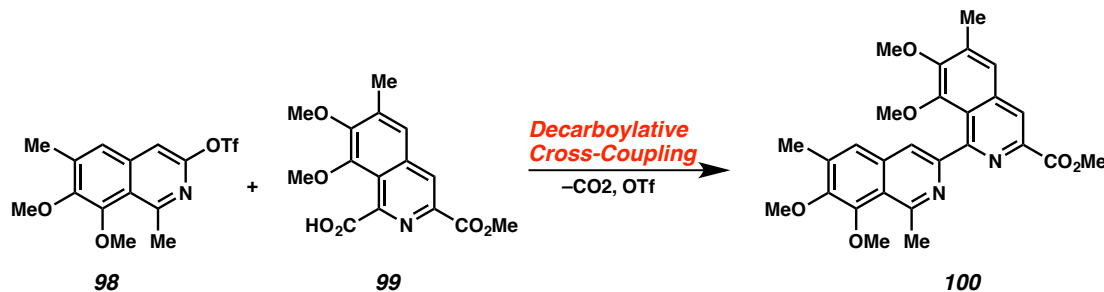


Goossen's Decarboxylative Cross-Coupling



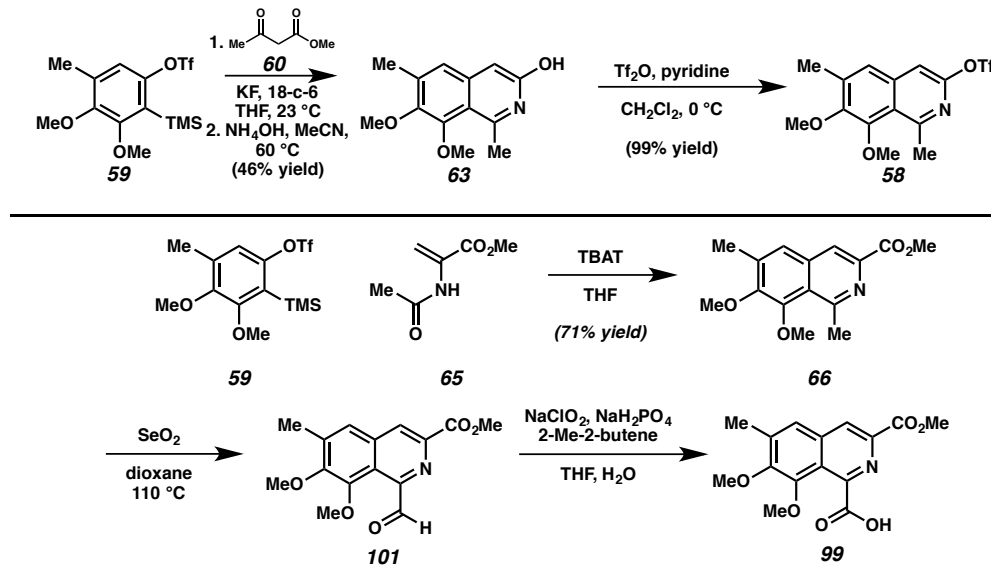
Both of the isoquinoline fragments necessary for the decarboxylative cross-coupling could be prepared utilizing methodologies developed within our laboratory which exploit the unique reactivity of arynes. Isoquinoline triflate **99** could be accessed through the acyl-alkylation of aryne-precursor **59** followed by condensation with ammonium hydroxide to afford 3-hydroxy isoquinoline **63**, which could be quantitatively triflated using triflic anhydride to furnish our electrophilic coupling partner (**98**).

Scheme 3.3. The decarboxylative cross-coupling of two isoquinolines for the total synthesis of *jorumycin*.



1-carboxy isoquinoline **99** was prepared using our aryne annulation methodology, in which aryne precursor **59** is treated with a fluoride source and methyl acetamido acrylate **65**. The methyl group could be selectively oxidized in a two-step protocol to the carboxylic acid (**99**). Because each of these coupling partners requires many steps to prepare, we focused our efforts on developing a more general approach to this problem.

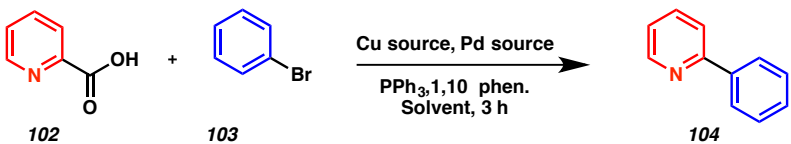
Scheme 3.4. Preparation of isoquinoline triflate **98** and carboxylic acid **99**.



3.2 Optimization of a Decarboxylative Cross-coupling of Picolinic Acid with Bromobenzene

To develop a general cross-coupling methodology, we selected simple substrates for optimization studies, namely picolinic acid (**102**) and bromobenzene (**103**, Table 3.1). We began our investigations by applying conditions similar to those reported by Goossen with disappointing results. (Table 3.1, entry 1). Using the same catalyst system we examined microwave irradiation and observed an increase in yield over heating in an oil bath (Table 3.1, entry 2). Similar results were disclosed by Goossen and Crabtree who independently reported enhanced yields using microwave irradiation.¹¹

With these initial results in hand we set about screening palladium and copper sources. Both palladium(II) and palladium(0) sources were examined, with palladium(II) iodide providing 2-phenyl pyridine (**104**) in 36% yield (Table 3.1, entry 2). Ultimately, cuprous oxide (Cu_2O), the copper source reported by Goossen and co-workers, gave consistently higher yields than copper (I) halides (Table 3.1, entries 12–16). Importantly, for both copper and palladium sources, weakly coordinating counterions were favored. While these results were encouraging, we sought to further improve the system. Concurrent with these studies, we examined several other solvents, however were limited to high boiling solvents as a consequence of the temperatures required for the copper-catalyzed decarboxylation of picolinic acid (Table 3.1, entries 17–20).

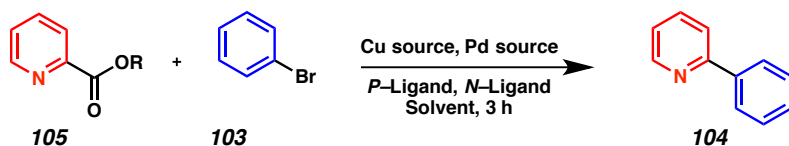
Table 3.1. Decarboxylative cross-coupling of picolinic acid with aryl halides.


Entry	Cu Source	Pd Source	Solvent	Temperature (°C)	Heat Source	% Yield*
1	Cu ₂ O	PdI ₂	NMP	170	Oil bath	6
2	Cu ₂ O	PdI ₂	NMP	170	μwave	36
3	Cu ₂ O	PdI ₂	NMP	120	μwave	-
4	Cu ₂ O	PdCl ₂	NMP	170	μwave	9
5	Cu ₂ O	PdBr ₂	NMP	170	μwave	12
6	Cu ₂ O	PdI ₂	NMP	170	μwave	36
7	Cu ₂ O	Pd(OAc) ₂	NMP	170	μwave	6
8	Cu ₂ O	Pd(acac) ₂	NMP	170	μwave	8
9	Cu ₂ O	Pd(TFA) ₂	NMP	170	μwave	14
10	Cu ₂ O	Pd(F ₆ -acac) ₂	NMP	170	μwave	6
11	Cu ₂ O	Pd(PPh ₃) ₄	NMP	170	μwave	13
12	Cu ₂ O	Pd ₂ (dba) ₂	NMP	170	μwave	14
13	CuCl	PdI ₂	NMP	170	μwave	7
14	CuBr	PdI ₂	NMP	170	μwave	16
15	CuI	PdI ₂	NMP	170	μwave	31
16	CuOTf	PdI ₂	NMP	170	μwave	20
17	Cu ₂ O(1.0eq)	PdI ₂	NMP	170	μwave	7
18	Cu ₂ O	PdI ₂	DMSO	170	μwave	12
19	Cu ₂ O	PdI ₂	DMF	170	μwave	4
20	Cu ₂ O	PdI ₂	NMP:Quin(1:1)	170	μwave	18
21	Cu ₂ O	PdI ₂	Toluene	170	μwave	2

Conditions: 0.4645 mmol **102**, 1.3935 mmol **103**, 10% mol Cu, 5% mol Pd, 15% mol PPh₃, 30% mol 1,10 phen., 0.5 mL Solvent *Yields determined by LCMS analysis with 4,4' di-*tert*-butyl biphenyl as internal standard

With these copper and palladium sources, we next examined several phosphine ligands. None showed improvement over the triphenylphosphine used in our initial studies. During the course of our studies we discovered that preheating the mixture at 50 °C for 10 minutes prior to heating to 190 °C was advantageous. Gratifyingly, we discovered that changing from the bidentate ligand 1,10 phenanthroline to the monodentate ligand pyridine caused a substantial increase in yield (Table 3.2, entry 6).

Table 3.2. Investigation of *P*- and *N*- ligands for the decarboxylative cross-coupling of picolinic acid with aryl halides.

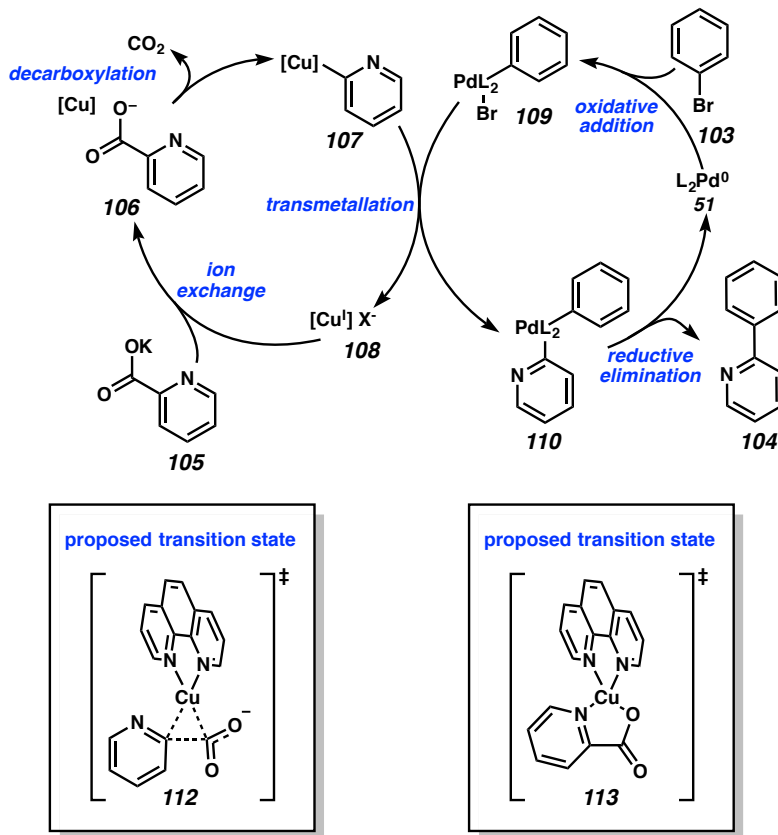


Entry	R	Cu Source	Pd Source	Solvent	Phosphine Ligand	Nitrogen Ligand	Temperature (°C)	Heat Source	Base	% Yield*
1	H	Cu ₂ O	PdI ₂	NMP	dppm	1,10 Phen	170	μwave	K ₂ CO ₃	7
2	H	Cu ₂ O	PdI ₂	NMP	dppb	1,10 Phen	170	μwave	K ₂ CO ₃	16
3	H	Cu ₂ O	PdI ₂	NMP	dppe	1,10 Phen	170	μwave	K ₂ CO ₃	31
4	H	Cu ₂ O	PdI ₂	NMP	BINAP	1,10 Phen	170	μwave	K ₂ CO ₃	6
5	H	Cu ₂ O	PdI ₂	NMP	PPh ₃ /KF	1,10 Phen	170	μwave	K ₂ CO ₃	2
6	H	Cu ₂ O	PdI ₂	NMP	PPh ₃	Pyridine	50→190	μwave	K ₂ CO ₃	52
7	K	Cu ₂ O	PdI ₂	NMP	PPh ₃	Pyridine	50→190	μwave	-	62
8	K	Cu ₂ O	PdI ₂	NMP	PPh ₃	2,6 Lutidene	50→190	μwave	-	46
9	K	Cu ₂ O	PdI ₂	NMP	PPh ₃	Ethyl Isonicotinate	50→190	μwave	-	49
10	K	Cu ₂ O	PdI ₂	NMP	PPh ₃	DMAP	50→190	μwave	-	56
11	K	Cu ₂ O	PdI ₂	NMP	PPh ₃	4-MeO Pyridine	50→190	μwave	-	43
12	K	Cu ₂ O	PdI ₂	NMP	PPh ₃	DABCO	50→190	μwave	-	43
13	K	Cu ₂ O	PdI ₂	NMP	PPh ₃	Et ₃ N	50→190	μwave	-	38
14	K	Cu ₂ O	PdI ₂	NMP	PPh ₃	Hunig's Base	50→190	μwave	-	60
15	K	Cu ₂ O	PdI ₂	NMP	PPh ₃	TMEDA	50→190	μwave	-	27
16	K	Cu ₂ O	PdI ₂	NMP	PPh ₃	(iPr) ₂ NH	50→190	μwave	-	51
17	K	Cu ₂ O	PdI ₂	NMP	PPh ₃	Quinuclidine	50→190	μwave	-	62

Conditions: 0.4645 mmol **105**, 1.3935 mmol **103**, 10% mol Cu, 5% mol Pd, 15% mol *P*-ligand, 30% mol *N*-ligand, 0.5 mL Solvent *Yields determined by LCMS analysis with 4,4'-di-*tert*-butyl biphenyl as internal standard

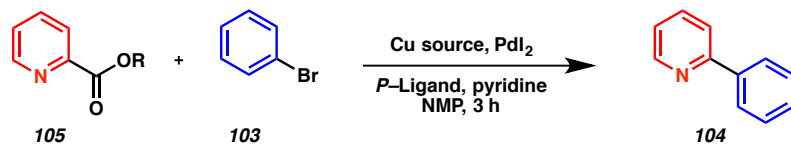
The implementation of a pre-formed potassium picolinate salt lead to a 10% increase in yield over its *in situ* generated counterpart (Table 3.2, entry 7). In examining the stereoelectronics of the *N*-ligand we discovered sterically encumbered nitrogen-contain ligands proved detrimental to the yield (Table 3.2, entries 8 and 13), while both electron-rich and deficient ligands also did not improve yields. Interestingly, as observed with 1,10 phenanthroline, other bidentate ligands such as TMEDA lead to lower yields (Table 3.2, entry 15). We hypothesize the formation of a stable 18 electron copper complex (**12**) is detrimental to decarboxylation (Figure 3.3).

Scheme 3.5. Proposed mechanism of the decarboxylative cross-coupling of picolinic acid with aryl halides.



With a suitable *N*-ligand in hand we hoped to gain better insight into the influence of the *P*-ligands on our catalytic system; like their nitrogen counter parts, bidentate phosphorous ligands performed poorly under the reaction conditions (Table 3.3, entries 8 and 13). We also reexamined copper sources, this time including copper(II) salts (Table 3.3, entries 16–20). All of these were inferior to copper(I) oxide. We investigated other counter ions of the picolinate salts such as cesium and sodium (Table 3.3, entries 14 and 15). None of these fared as well as potassium; confirming a trend was also observed in Goossen's studies.

Table 3.3. Investigation of *P*-ligands and copper sources for the decarboxylative cross-coupling of picolinic acid with aryl halides.

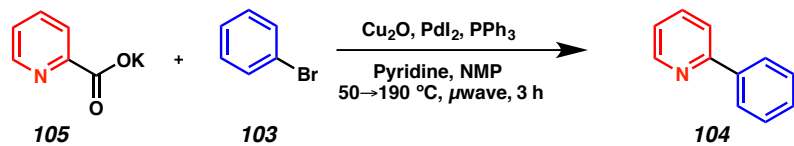


Entry	R	Cu Source	<i>P</i> -Ligand	% Yield*
1	K	Cu ₂ O	P(o-Tolyl) ₃	26
2	K	Cu ₂ O	P(Cy) ₃	42
3	K	Cu ₂ O	P(<i>t</i> -Bu) ₃	21
4	K	Cu ₂ O	P(2-Furyl) ₃	42
5	K	Cu ₂ O	P((CF ₃) ₂ Ph) ₃	36
6	K	Cu ₂ O	P(4-MeO-Ph) ₃	45
7	K	Cu ₂ O	P(EtO) ₃	31
8	K	Cu ₂ O	dppe	46
9	K	Cu ₂ O	Ph ₂ PO	49
10	K	Cu ₂ O	(PhO) ₂ POH	20
11	K	Cu ₂ O	JohnPhos	44
12	K	Cu ₂ O	AsPh ₃	48
13	K	Cu ₂ O	BINAP	38
14	Na	Cu ₂ O	PPh ₃	4
15	Cs	Cu ₂ O	PPh ₃	1
16	K	Cu(OAc)	PPh ₃	34
17	K	Cu ₂ (CO ₃)(OH) ₂	PPh ₃	29
18	K	Cu(SO ₄)	PPh ₃	47
19	K	CuO	PPh ₃	27
20	K	Cu(OTf) ₂	PPh ₃	31

Conditions: 0.4645 mmol **105**, 1.3935 mmol **103**, 10% mol Cu, 5% mol Pd, 15% mol *P*-ligand, 30% mol *N*-ligand, 0.5 mL NMP. *Yields determined by LCMS analysis with 4,4'-di-*tert*-butyl biphenyl as internal standard.

One of the unproductive side-reactions of our decarboxylative cross-coupling is the formation of biphenyl through an Ullmann-type dimerization of bromobenzene. By modulating the stoichiometry of bromobenzene (**103**) we attempted to suppress the unproductive dimerization and increase cross-coupling (Table 3.4). Ultimately, reducing the equivalents of bromobenzene from 3.0 to 2.0 was slightly beneficial to our yield (Table 3.4, entry 5).

Table 3.4. Examination of the equivalents of bromobenzene in the decarboxylative cross-coupling of picolinic acid with aryl halides.

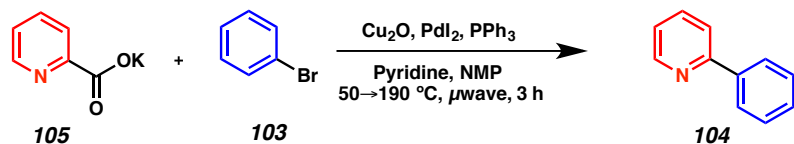


Entry	Bromobenzene (equiv)	% Yield*
1	3.0	62
2	2.0	65
3	1.0	55
4	0.75	57

Conditions: 0.4645 mmol **105**, X mmol **103**, 10% mol Cu_2O , 5% mol PdI_2 , 15% mol PPh_3 , 30% mol pyridine, 0.5 mL NMP
 **Yields determined by LCMS analysis with 4,4'-di-*tert*-butyl biphenyl as internal standard

Concurrent to these studies, we examined the impact of reaction times on the yield of our cross-coupling. Though a reaction time of 8 hours provided the highest yield of 2-phenylpyridine at 72%, it represented only a marginal improvement over shorter times (Table 3.5).

Table 3.5. Examination of reaction time in the decarboxylative cross-coupling of picolinic acid with aryl halides.



Entry	Time (h)	% Yield*
1	0.5	15
2	1.0	38
3	2.5	64
4	4	62
5	5	69
6	8	72

Conditions: 0.4645 mmol **105**, 0.929 mmol **103**, 10% mol Cu_2O , 5% mol PdI_2 , 15% mol PPh_3 , 30% mol pyridine, 0.5 mL NMP
 **Yields determined by LCMS analysis with 4,4'-di-*tert*-butyl biphenyl as internal standard

In order to better understand the reaction mechanism, we performed a series of control experiments in which we omitted each of the reagents. We discovered pyridine was not able to facilitate the necessary deprotonation of picolinic acid *in situ* (Table 3.6, entry 1). Omission of triphenylphosphine substantially decreased the yield of 2-phenyl pyridine (**10**) (Table 3.6, entry 2). Both copper and palladium proved crucial for our reaction; removal of either metal lead to little or no reactivity (Table 3.6, entries 3 and 4). Ultimately, pyridine was not necessary to facilitate the reaction (Table 3.6, entry 5). However this is most likely due to an unproductive protodecarboxylative side reaction that produces pyridine from picolinic acid. 2-Phenylpyridine is a common substrate for functional group directed C–H activation and can serve as a ligand for copper or palladium.¹² Consequently, we explored the possibility of product inhibition. However, yields were not effected by addition of 2-phenylpyridine to the reaction (Table 3.6, entry 6), ruling out this inhibitory interaction.

Table 3.6. Control experiments for the decarboxylative cross-coupling of picolinic acid with aryl halides.

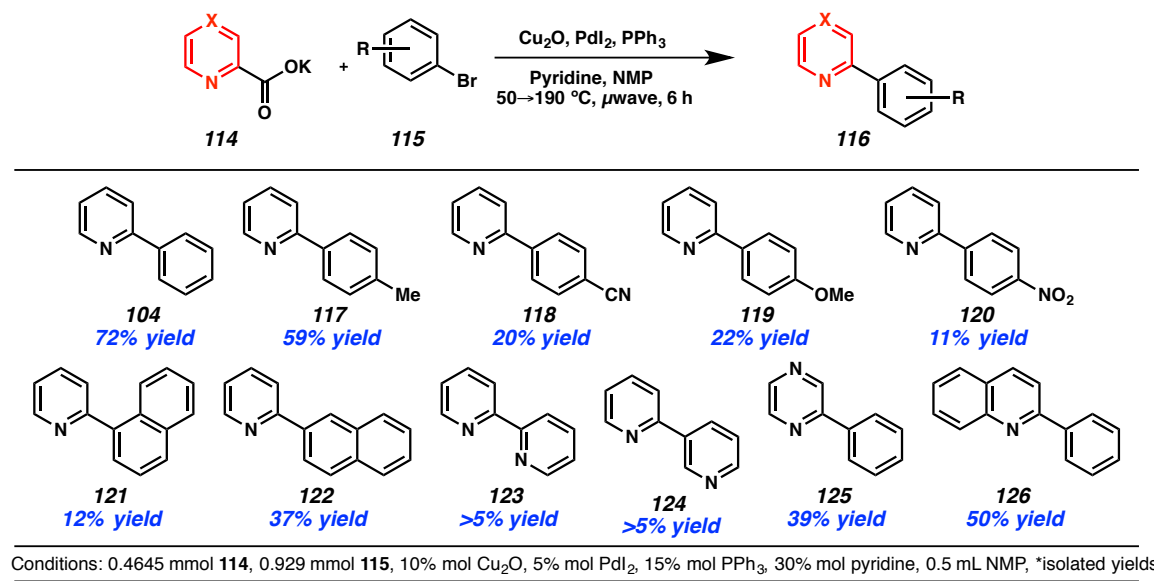
Entry	R	Cu Source	Pd Source	Solvent	Phosphine Ligand	Nitrogen Ligand	Temperature (°C)	Heat Source	Additive	% Yield*	
										P-Ligand, N-Ligand	Solvent, 3 h
1	H	Cu ₂ O	PdI ₂	NMP	PPh ₃	pyridine	50→190	μwave	Pyridine	5	
2	K	Cu ₂ O	PdI ₂	NMP	-	pyridine	50→190	μwave	-	22	
3	K	-	PdI ₂	NMP	PPh ₃	pyridine	50→190	μwave	-	9	
4	K	Cu ₂ O	-	NMP	PPh ₃	pyridine	50→190	μwave	-	0	
5	K	Cu ₂ O	PdI ₂	NMP	PPh ₃	-	50→190	μwave	-	62	
6	K	Cu ₂ O	PdI ₂	NMP	PPh ₃	pyridine	50→190	μwave	2-phenyl pyridine	65	

Conditions: 0.4645 mmol **105**, 0.929 mmol **103**, 10% mol Cu₂O, 5% mol PdI₂, 15% mol PPh₃, 30% mol pyridine, 0.5 mL NMP **Yields determined by LCMS analysis with 4,4'-di-*tert*-butyl biphenyl as internal standard

3.3 The cross-coupling of (2-azaaryl)carboxylates with aryl halides

With our best conditions to date identified, we turned our attention to examination of the substrate scope of the decarboxylative cross-coupling (Figure 4). Electronically neutral aryl halides (**104** and **117**) performed well under the reaction conditions. Both electron rich and electron deficient aryl halides fared modestly (**118** and **119**). One of the major byproducts of reactions using electron deficient aryl bromides was an Ullmann-type coupled product. Heteroaromatic halides produced coupled products in disappointingly low yields (**123** and **124**). Most interestingly, other (2-azaaryl)carboxylates performed well under the reaction conditions (**125** and **126**).

Table 3.7. The decarboxylative cross-coupling of picolinic acid with aryl halides.



Lastly, attempts to perform the decarboxylative cross-coupling within the context of our synthesis of jorumycin proved unfruitful, resulting mainly in the proto-decarboxylation of carboxy isoquinoline **99**.

3.4 Conclusion

Decarboxylative coupling is an attractive alternative to traditional cross-coupling reactions. The starting materials are stable and inexpensive, and the byproducts of these reactions are less toxic and easier to dispose of than traditional organometallic reagents and boronic acids. 2-metallated heteroarenes are particularly unstable, difficult to prepare and expensive. Herein we have reported an approach to circumvent the need to use these undesirable reagents. We have shown that 2-(azaaryl)carboxylates can be effectively used in decarboxylative cross-coupling reactions with aryl halides to furnish 2-(azaaryl)arenes, a motif present in a wide variety of important small molecules.

3.5 EXPERIMENTAL SECTION

Spectral data for compounds **104**, **117**, **118**, **119**, **120**, **121**, **122**, **123**, **124**, **125** and **126** were consistent with previously reported data.^{10,13,14}

A representative procedure for the decarboxylative cross-coupling of (2-azaaryl)carboxylates with aryl halides:

2-phenylpyridine (104) The potassium salt of picolinic acid (**105**) (74.9 mg, 0.464 mmol), PPh₃ 18.3 mg (0.0697 mmol) PPh₃, 8.4 mg (0.046 mmol) PdI₂, and 6.6 mg (0.046 mmol) Cu₂O were added to a flame-dried 2.0 mL microwave vial equipped with a spin vane. The vial was sealed, evacuated and back-filled with argon (3 times). 0.50 mL NMP (degassed with Ar, >10 min.) and 97.6 μ L (0.929 mmol) bromobenzene (**103**) were added sequentially via syringe. The mixture was stirred at room temperature for 10 min. The mixture was then irradiated in the microwave, with a 90 s prestirring period followed by 10 min at 50 °C and increase in temperature to 190 °C. The reaction was heated at this temperature for 6 h. The crude mixture was purified on a silica column.

3.6 References

1. a) Henry, G. D. *Tetrahedron*, **2004**, *60*, 6043–6061.; b) Michael, J. P. *Nat. Prod. Rep.* **2005**, *22*, 627–646.; c) Schlosser, M.; Mongin, F. *Chem. Soc. Rev.* **2007**, *36*, 1161–1172.
2. a) Ishiyama, T.; Ishida, K.; Miyaura, N. *Tetrahedron* **2001**, *57*, 9813–9816.; b) Fuller, A. A.; Hester, H. R.; Salo, E. V.; Stevens, E. P. *Tetrahedron Lett.* **2003**, *44*, 2935–2938.; c) Lützen, A.; Hapke, M. *Eur. J. Org. Chem.* **2002**, 2292–2297.; d) Lee, S. H.; Jang, B.-B.; Kafafi, Z. H. *J. Am. Chem. Soc.* **2005**, *127*, 9071–9078.; e) Fray, M. J.; Mathias, J. P.; Nichols, C. L.; Po-Ba, Y. M.; Snow, H. *Tetrahedron Lett.* **2006**, *47*, 6365–6368.; f) Campeau, L.-C.; Fagnou, K. *Chem. Soc. Rev.* **2007**, *36*, 1058–1068.; g) Blakemore, D. C.; Marples, L. A. *Tetrahedron Lett.* **2011**, *52*, 4192–4195.
3. a) O'Neill, B. T.; Yohannes, D.; Bundesmann, M. W.; Arnold, E. P. *Org. Lett.* **2000**, *2*, 4201–4204.; b) Littke, A. F.; Schwarz, L.; Fu, G. C. *J. Am. Chem. Soc.* **2002**, *124*, 6343–6348.; c) Hodgson, P. B.; Salingue, F. H. *Tetrahedron Lett.* **2004**, *45*, 685–687.; d) Campeau, L.-C.; Rousseaux, S.; Fagnou, K. *J. Am. Chem. Soc.* **2005**, *127*, 18020–18021.; e) Billingsley, K. L.; Buchwald, S. L. *Angew. Chem., Int. Ed.* **2008**, *47*, 4695–4698. f) Campeau, L.-C.; Stuart, D. R.; Leclerc, J.-P.; Bertrand-Laperle, M.; Villemure, E.; Sun, H.-Y.; Lasserre, S.; Guimond, N.; Lecavallier, M.; Fagnou, K.; *J. Am. Chem. Soc.* **2009**, *131*, 3291–3306.; g) Schipper, D. J.; Campeau, L.-C.; Fagnou, K. *Tetrahedron* **2009**, *65*, 3155–3164.; h) Deng, J. Z.; Paone, D. V.; Ginnetti, A. T.; Kurihara, H.; Dreher, S. D.; Weissman, S. A.; Stauffer, S. R.; Burgey, C. S. *Org. Lett.*

2009, *11*, 345–347.; i) Yang, D. X.; Colletti, S. L.; Wu, K.; Song, M.; Li, G. Y.; Shen, H. C. *Org. Lett.* **2009**, *11*, 381–384.; j) Luzung, M. R.; Patel, J. S.; Yin, J. *J. Org. Chem.* **2010**, *75*, 8330–8332.; k) Crowley, B. M.; Potteiger, C. M.; Deng, J. Z.; Prier, C. K.; Paone, D. V.; Burgey, C. S. *Tetrahedron Lett.* **2011**, *52*, 5055–5059.; l) Tan, Y.; Barrios-Landeros, F.; Hartwig, J. F. *J. Am. Chem. Soc.* **2012**, *134*, 3683–3686.; m) Dick, G. R.; Woerly, E. M.; Burke, M. D. *Angew. Chem., Int. Ed.* **2012**, *51*, 2667–2672.; (n) Ren, W.; Li, J.; Zou, D.; Wu, Y.; Wu, Y. *Tetrahedron* **2012**, *68*, 1351–1358.

4. Myers, A. G.; Tanaka, D.; Mannion, M. R. *J. Am. Chem. Soc.*, **2002**, *124*, 11250–11251.
5. a) Goossen, L. J.; Deng, G.; Levy, L. M. *Science* **2006**, *313*, 662–664.; b) Goossen, L. J.; Rodríguez, N.; Melzer, B.; Linder, C.; Deng, G.; Levy, L. M. *J. Am. Chem. Soc.* **2007**, 4824–4833.
6. Rodríguez, N.; Goossen, L. J. *Chem. Soc. Rev.* **2011**, *40*, 5030–5048.
7. Jia, W.; Jiao, N. *Org. Lett.* **2010**, *12*, 2000–2003.
8. Goossen, L. J.; Rudolphi, F.; Oppel, C.; Rodríguez, N. *Angew. Chem., Int. Ed.* **2008**, *47*, 3043–3045.
9. Shang, R.; Yang, Z.-W.; Wang, Y.; Zhang, S.-L.; Liu, L. *J. Am. Chem. Soc.* **2010**, *132*, 14391–14393.
10. Li, X.; Zou, D.; Leng, F.; Sun, C.; Li, J.; Wu, Y.; Wu, Y. *Chem. Commun.* **2013**, *49*, 312–314.

11. a) Voutchkova, A.; Coplin, A.; Leadbeater, N. E.; Crabtree, R. H. *Chem. Commun.* **2008**, 6312–6314.; b) Goossen, L. J.; Manjolinho, F.; Khan, B. A.; Rodríguez, N. J. *Org. Chem.* **2009**, 74, 2620–2623.
12. Lyons, T. W.; Sanford, M. S. *Chem. Rev.* **2010**, 110, 1147–1169.
13. Wen, J.; Zhang, R.-Y.; Chen, S.-Y.; Zhang, J.; Yu, X.-Q. *J. Org. Chem.* **2012**, 77, 766–771.
14. Martinez, R.; Ramón, D. J.; Yus, M. J. *Org. Chem.* **2008**, 73, 9778–9780.

Appendix 5

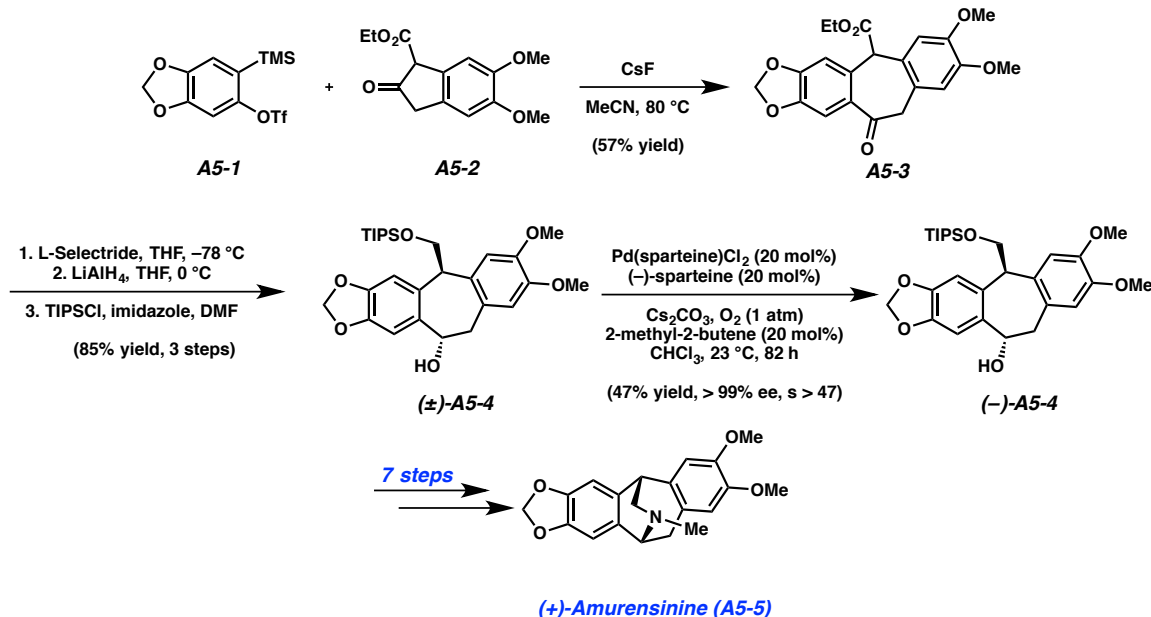
The Ring-Expansive Acyl-Alkylation of Arynes

A5.1 Introduction

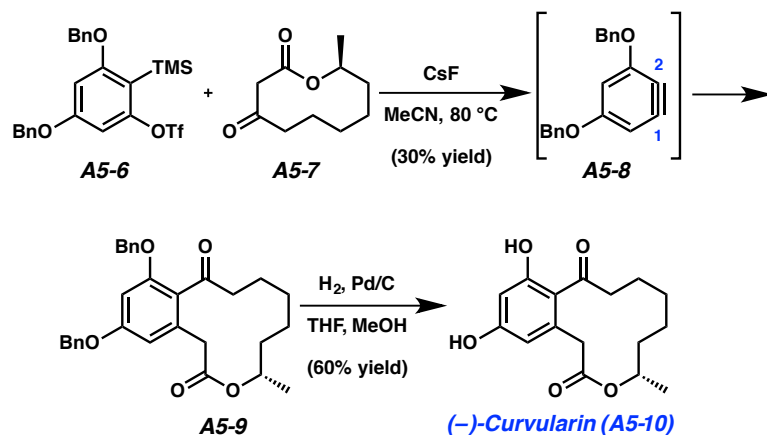
The ring-expansive direct acyl alkylation of arynes has been successfully showcased in the total synthesis of a number of natural products to date by the Stoltz group, including (+)-amurensinine (**A5-5**) and (–)-curularin (**A5-10**).^{1,2} The 2006 synthesis of (+)-amurensinine began with the acyl-alkylation of an alkyne generated in situ from sesamol-derived silyl aryl triflate **A5-1**, with benzannulated β -ketoester **A5-2**, resulting in direct access of the tetracyclic core **A5-3** (Scheme A5.1). The synthesis was completed in 11 additional steps. Subsequent to this work, the benzannulated macrolactone (–)-curularin was completed in 6 steps from known compounds (Scheme A5.2). Lactone **A5-9** was prepared via ring-expansive acyl-alkylation from unsymmetrical alkyne precursor **A5-5** and chiral 10-membered lactone **A5-7**. Debenzylation revealed the resorcinol core, completing the total synthesis. These two

syntheses highlight the utility of acyl-alkylation and its ability to rapidly prepare complex benzannulated motifs within the context of natural product total synthesis.

Scheme A5.1. Total synthesis of (+)-amurensinine (A5-5).



Scheme 2. Total synthesis of (−)-curvularin (A5-10).

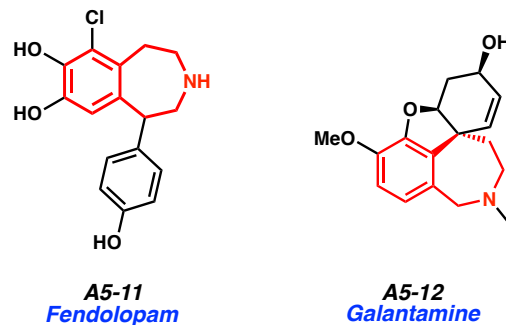


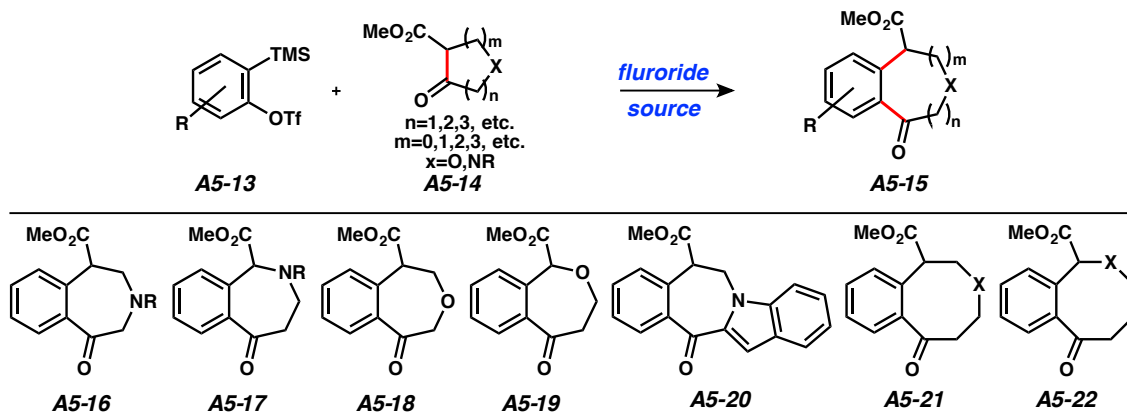
A5.2 The Development of the Ring Expansive Acyl-Alkylation of Arynes with Heterocyclic β -ketoesters

Thus far only fused carbocycles and lactones have been reported as products of this ring expansive acyl-alkylation methodology. An investigation utilizing this methodology to form benzannulated heterocyclic frameworks had not been pursued.

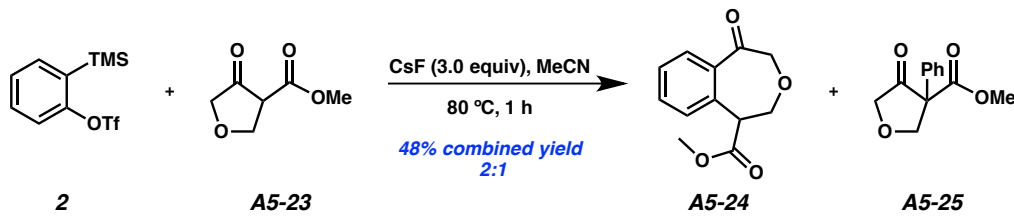
We hoped to expand the methodology to heterocyclic β -ketoesters to prepare benzannulated heterocycles, providing a convergent, single-step strategy to synthesize a variety of important structural motifs including benzazepine derivatives (**A5-16**, **A5-17** and **A5-20**), benzoxyppines derivatives (**A5-18** and **A5-19**), as well as more challenging larger rings (**A5-21** and **A5-22**) (Scheme A5.3). These heterocycles are found in the cores of many biologically active natural products. In particular, benzazepine derivatives are a scaffold within many important pharmaceuticals such as galantamine (**A5-11**), a treatment for Alzheimer's disease, and fenoldopam (**A5-12**), an antihypertensive agent (Figure A5.1).^{3,4} By developing reaction conditions to prepare the cores of these important molecules, we would be able to rapidly access complex intermediates, providing a more convergent approach to these compounds.

Figure A5.1. Benzannulated heterocycles in biologically active compounds.



Scheme A5.3. Proposed products of ring expansive acyl-alkylation of arynes.

We choose β -ketoester **A5-23** on which to optimize our ring-expansive acyl-alkylation. While less prevalent in natural products and pharmaceuticals it does not require a protecting group, thereby simplifying optimization. We began our development by replicating the previously reported conditions of Tambar and co-workers (Scheme A5.4). This lead to a 2 to 1 mixture of acyl alkylated product **A5-24** and α -arylated product **A5-25** in 48% combined yield.

Scheme A5.4. The acyl-alkylation of benzyne with β -ketoester **A5-23**.

We next examined the effect of varying the fluoride source on the reaction (Table A5.1, entries 1–3). Both TBAT and KF/18-Crown-6 gave higher yields of our desired acyl-alkylated product. Interestingly, we saw no undesired α -arylated β -ketoester. Increasing the temperature to 40 °C had a positive effect on the yield (Table A5.1, entry

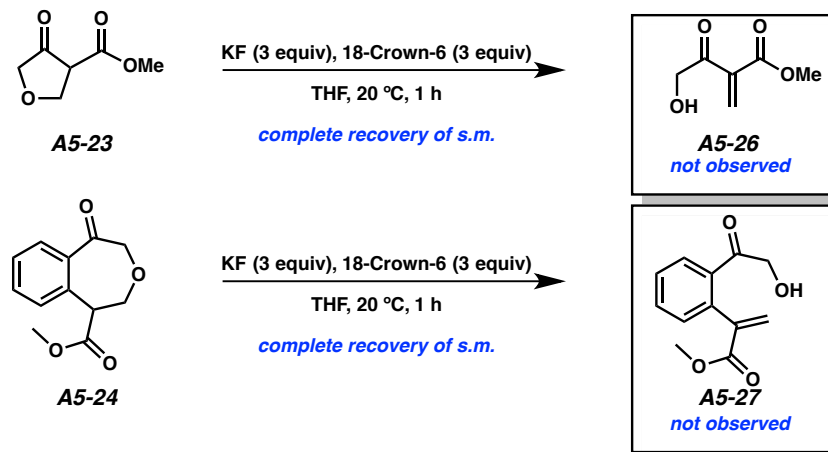
4–5). However at higher temperature, we observed a decrease in yield. Extended reaction times also led to lower yields (Table A5.1, entries 6–7). This is most likely due to over arylation at either of the two α -carbons of our acyl-alkylated product. However, decreasing equivalents of fluoride source or aryne precursor had a deleterious effect on the yield.

Table A5.1. Optimization of the ring-expansive acyl-alkylation of arynes.

2	A5-23	fluoride source	A5-24	A5-25		
Entry	Fluoride Source	Solvent	Time (h)	Temperature (°C)	% yield*	26 : 32
1	KF/18-crown-6	THF	1.0	20	46	1 : 0
2	CsF	MeCN	0.5	80	48	2 : 1
3	TBAT	THF	3.0	20	46	1 : 0
4	KF/18-crown-6	THF	0.5	40	54	2 : 1
5	TBAT	THF	3.0	40	46	3 : 1
6	TBAT	THF	16	20	63	5 : 1
7	KF/18-crown-6	THF	3.0	20	22	1 : 0
8	KF/18-Crown-6 (1.5 equiv)	THF	2.0	20	28	1 : 0

*isolated yield. Conditions: 0.33 mmol **2**, 0.26 mmol **A5-23**, 0.67 mmol fluoride source, 2.5 mL solvent

During our investigation of any potential side reactions, we hoped to rule out any elimination pathways. To probe this possibility, we separately subjected β -ketoester **A5-23** and benzoxapene **A5-24** to the reaction conditions. Gratifyingly, both compounds were stable to these conditions and were recovered in near quantitative yields (Scheme A5.5).

Scheme A5.5. Potential unproductive side reactions of ring-expansive acyl alkylation

Similarly, changes in solvent did not improve yields (Table A5.2). We were limited to ethereal solvents due to the solubility restrictions of our fluoride source, KF/18-Crown-6. In reactions that used any non-ethereal solvents, we were only able to isolate starting material. The use of a pregenerated enolate of our β -ketoester using sodium hydride or potassium *tert*-butoxide resulted in recovery of starting material.

Table A5.2. Solvent effects on ring-expansive acyl-alkylation.

2 **A5-23** **A5-24** **A5-26**

KF, 18-Crown-6
22 °C, solvent 1 h

Entry	Solvent	Time (h)	% Yield*
1	dioxane	1	16
2	diethyl Ether	24	25
3	dimethyloxyethane	0.33	30
4	TBME	24	9
5	2-methyl THF	2	46

Conditions: 2 (1.25 equiv), A5-23 (1.00 equiv), KF/18-Crown-6 (3.0 equiv)
*isolated yield

A5.3 Future Directions

We will expand this methodology to other heterocyclic β -keto esters, includes 6-, 7- and 8-membered rings. Nitrogen-bearing heterocycles provide the opportunity to attenuate the nucleophilicity of the heteroatom through the introduction of a protection groups. We hope this will bring about synthetically useful yields which could eventually be applied to one of a number of natural products contain these benzanulated heterocycles.

A5.4 References

1. Tambar, U. K.; Ebner, D. C.; Stoltz, B. M. *J. Am. Chem. Soc.* **2006**, *128*, 11752–11753.
2. Tadross, P. M.; Virgil, S. C.; Stoltz, B. M. *J. Am. Chem. Soc.* **2010**, *132*, 1612–1614.
3. Troste, B. M.; Tang, W.; Toste, D. F. *J. Am. Chem. Soc.* **2005**, *127*, 14785–14803.
4. Wünsch, B.; et al. *J. Org. Chem.* **2009**, *74*, 2788–2793.

Appendix 6

Preparation of Benzotriazoles via an Aryne-Based Three-Component

Cross-Coupling

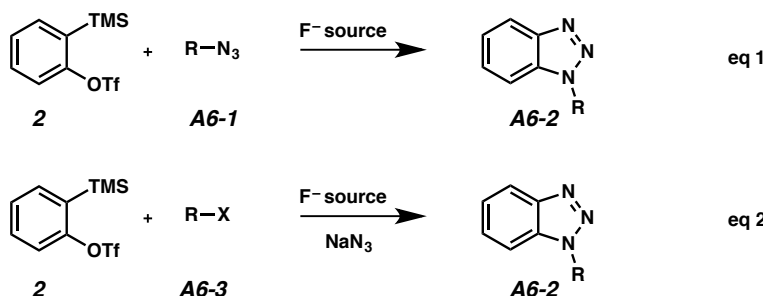
1H-benzo[d][1,2,3]triazoles (hereafter referred to as benzotriazoles) have been used in a variety of applications within the context of organic synthesis.¹ The implementation of arynes has allowed for facile preparation of this important class of molecules. Huisgen 1,3 dipolar cycloadditions, commonly referred to as “click” reactions, have found broad application in the synthesis of 1,2,3 triazoles.² Specifically, organoazides have been shown to readily undergo [3+2] cycloaddition with the characteristic strained triple bond of alkyne without the need of transition metal catalysts.

While this reactivity has been known since the early 1960s, in 2008 Larock and co-workers reported a simple procedure using alkyl azides and arynes generated *in situ* from the fluoride-induced *ortho*-elimination of *o*-(trimethylsilyl)aryl triflates (Scheme A6.1, eq 1). The use of microwave irradiation development has lead to decreased

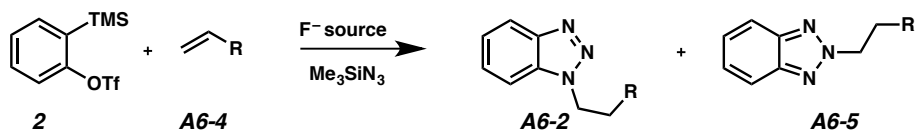
reaction times and improved yields. The need to pre-generate the organoazides was alleviated by a method developed by Beihl and Ankati. This methodology utilized alkyl halides in the presence of sodium azide to follow by [3+2] cycloaddition (Scheme A6.1, eq. 2).

Scheme A6-1. Previous preparations of benzotriazoles from benzyne.

Previous Research:



This Research:

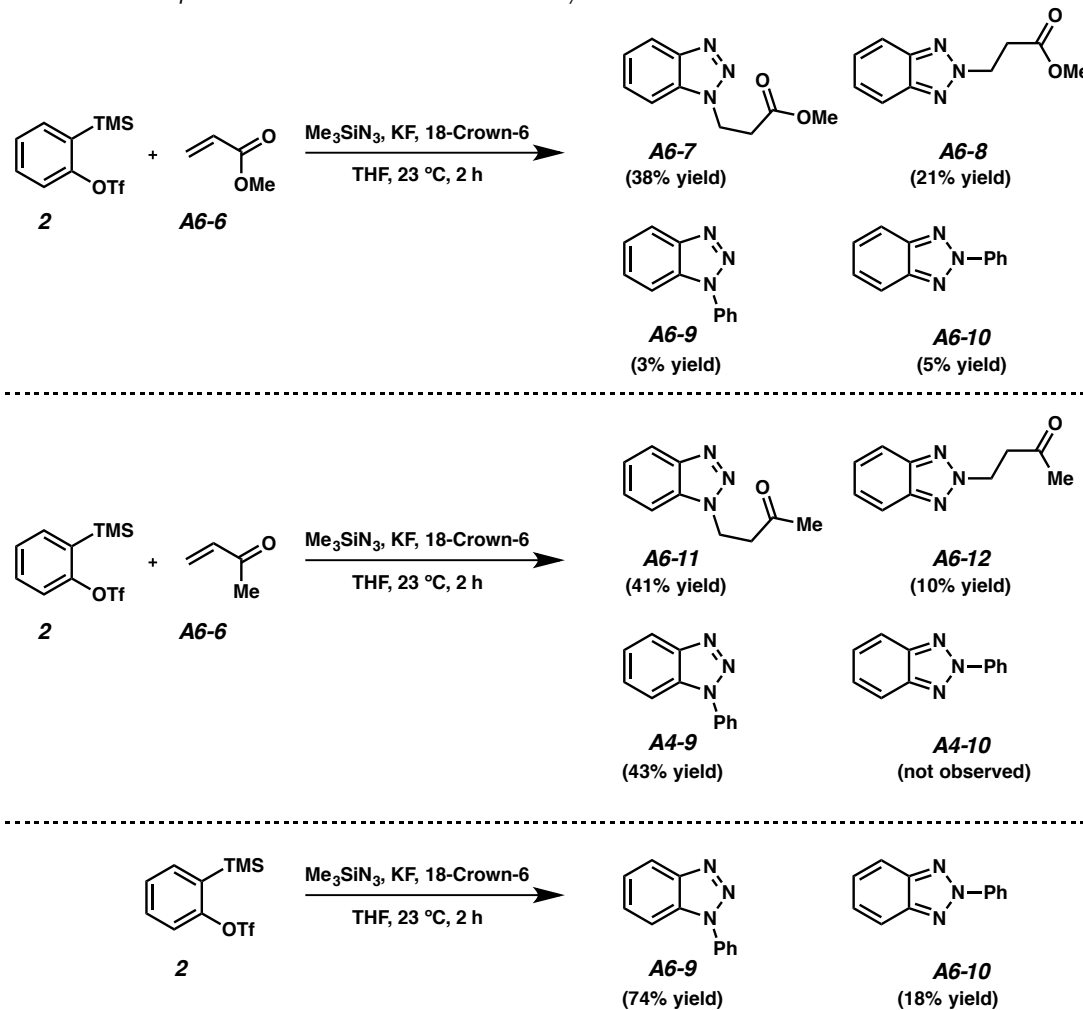


Continuing our sustained interest in 3-component couplings, we sought to examine the use of electrophiles in the preparation of benzotriazoles. We initiated our studies by attempting to react sodium azide with methyl acrylate and an in situ generated aryne. However, this lead to no detectable 3-component coupling products. Switching our azide source to trimethylsilyl azide lead to a mixture of three benzotriazole products. Both 1-phenyl benzotriazole (**A6-9**) and 3-benzotriazole-1-yl propionic acid methyl ester (**A6-9**) were prepared in 43% and 41% yield, respectively (Scheme A6.2). Interestingly, 3-benzotriazole-2-yl propionic acid methyl ester (**A6-8**) was also isolated in 10% yield,

suggesting initial formation of a benzotriazole anion, followed by subsequent nucleophilic attack. However no 2-phenyl benzotriazole (**A6-10**) was observed.

A similar mixture of products was observed when the reaction is performed with methyl vinyl ketone. Intriguingly, both 1- and 2-phenyl benzotriazole (**A6-9**, **A6-10**) were formed (Scheme A6.2). Finally, when the aryne was used as the electrophile, a mixture of 1-phenyl benzoltrizale (**A6-9**) and 2-phenyl benzotriazole (**A6-10**) are produced in 74% and 18% yield, respectively.

Scheme A6.2. Preparation of benzotriazoles from aryne.



Herein we have report a novel 3-component coupling for the synthesis of *N*-substituted benzotriazoles, exploiting the reactivity of benzyne and its propensity to undergo dipolar cycloadditions.

Representative Procedure

Representative procedure: A flame-dried 2 dram vial equipped with a stir bar was sequentially charged with 18-crown-6 (194.8 mg, 0.75 mmol, 2.2 equiv.) and potassium fluoride (42.8 mg, 0.75 mmol, 2.2 equiv.). The vial was sealed with a septum and parafilm. The vial was evacuated and back-filled with N₂ 3 times. THF (3.3 mL), aryne precursor (**2**) (0.081 mL, 0.34 mmol, 1.0 equiv.), trimethylsilyl azide (0.044 mL, 0.34 mmol, 1.0 equiv), and methyl vinyl ketone (0.054 mL, 0.68 mmol, 2.0 equiv) were sequentially added via syringe. This was stirred at room temperature (23 °C) for 2 hours, at which time aryne precursor had been fully consumed, as indicated by TLC (silica, 10% hexanes in EtOAc). After 2 hours, the reaction mixture was diluted with 10 mL Et₂O. This was washed 3 times with 10 mL brine. The aqueous layers were combined and extracted with 20 mL Et₂O. The organic layers were combined and dried over sodium sulfate. This was filtered and the solvent was removed in vacuo to afford a yellow-brown oil. The resultant oil was purified on a silica column (1 cm x 20 cm) using a gradient of 15% to 60% EtOAc in hexanes as an eluent.

References

1. For reviews, see: a) Katritzky, A. R.; Lan, X.; Yang, J. Z.; Denisko, O. V. *Chem. Rev.* **1998**, *98*, 409–548. b) Katritzky, A. R.; Rogovoy, B. V. *Chem.—Eur. J.* **2003**, *9*, 4586–4593. c) Katritzky, A. R., Rachwal, S. *Chem. Rev.* **2011**, *111*, 7063–7120.
2. For reviews, see a) Dedola, S.; Nepogodiev, S. A.; Field, R. A. *Org. Biomol. Chem.* **2007**, *5*, 1006–1017. b) Binder, W. H.; Sachsenhofer, R. *Macromol. Rapid Commun.* **2007**, *28*, 15–54. c) Meldal, M.; Tornøe, C. W. *Chem. Rev.* **2008**, *108*, 2952–3015. d) Amblard, F.; Cho, J. H.; Schinazi, R. F. *Chem. Rev.* **2009**, *109*, 4207–4220. e) Sletten, E. M.; Bertozzi, C. R. *Angew. Chem. Int. Ed.* **2009**, *48*, 6974–6998. f) Lallana, E.; Fernandez-Trillo, F.; Sousa-Herves, Ana; Riquera, R.; Fernandez-Megia, E. *Pharm. Res.* **2012**, *29*, 902–921.

Comprehensive Bibliography

Allan, K. M.; Gilmore, C. D.; Stoltz, B. M. *Angew. Chem., Int. Ed.* **2011**, *50*, 4488–4491.

Allan, K. M.; Hong, B. D.; Stoltz, B. M. *Org. Biomol. Chem.* **2009**, *7*, 4960–4964.

Allan, K. M.; Stoltz, B. M. *A J. Am. Chem. Soc.* **2008**, *130*, 17270–17271.

Amblard, F.; Cho, J. H.; Schinazi, R. F. *Chem. Rev.* **2009**, *109*, 4207–4220.

Arai, T.; Yazawa, K.; Takahashi, K.; Maeda, A.; Mikami, Y. *Antimicrob. Agents Chemother.* **1985**, *28*, 5–11.

Asaoka, T.; Yazawa, K.; Mikami, Y.; Arai, T. *J. Antibiot.* **1982**, *35*, 1708–1710.

Baker, W. *J. Chem. Soc.*, **1933**, 1381–1389.

Billingsley, K. L.; Buchwald, S. L. *Angew. Chem., Int. Ed.* **2008**, *47*, 4695–4698.

Binder, W. H.; Sachsenhofer, R. *Macromol. Rapid Commun.* **2007**, *28*, 15–54.

Blackburn, T.; Ramtohul, Y. *Synlett* **2008**, 1159–1164.

Blakemore, D. C.; Marples, L. A. *Tetrahedron Lett.* **2011**, *52*, 4192–4195.

Bhunia, A.; Yetra, S. R.; Biju, A. T. *Chem. Soc. Rev.* **2012**, *41*, 3140–3152.

Bronner, S. M.; Garg, N. K. *J. Org. Chem.* **2009**, *74*, 8842–8843.

Carter, N.; Keam, S. J. Trabectedin. *Drugs*, **2010**, *70*, 355–376.

Campbell, C. D.; Rees, C. W. *J. Chem. Soc. (C)* **1969**, 742–747.

Campeau, L.-C.; Fagnou, K. *Chem. Soc. Rev.* **2007**, *36*, 1058–1068.

Campeau, L.-C.; Rousseaux, S.; Fagnou, K. *J. Am. Chem. Soc.* **2005**, *127*, 18020–18020.

Campeau, L.-C.; Stuart, D. R.; Leclerc, J.-P.; Bertrand-Laperle, M.; Villemure, E.; Sun, H.-Y.; Lasserre, S.; Guimond, N.; Lecavallier, M.; Fagnou, K.; *J. Am. Chem. Soc.* **2009**, *131*, 3291–3306.

Canonne, P.; Boulanger, R.; Chantegrel, B. *Tetrahedron* **1987**, *43*, 663–668.

Charupant, K.; Daikuhara, N.; Saito, E.; Amnuopol, S.; Suwanborirux, K.; Owa, T.; Saito, N. *Bioorg. Med. Chem.* **2009**, *17*, 4548–4558.

Cross, R. M.; Manetsch, R. *J. Org. Chem.* **2010**, *24*, 8654–8657.

Crowley, B. M.; Potteiger, C. M.; Deng, J. Z.; Prier, C. K.; Paone, D. V.; Burgey, C. S. *Tetrahedron Lett.* **2011**, *52*, 5055–5059.

Dedola, S.; Nepogodiev, S. A.; Field, R. A. *Org. Biomol. Chem.* **2007**, *5*, 1006–1017.

Deng, J. Z.; Paone, D. V.; Ginnetti, A. T.; Kurihara, H.; Dreher, S. D.; Weissman, S. A.; Stauffer, S. R.; Burgey, C. S. *Org. Lett.* **2009**, *11*, 345–347.

Dick, G. R.; Woerly, E. M.; Burke, M. D. *Angew. Chem., Int. Ed.* **2012**, *51*, 2667–2672.

Fontana, A.; Cavalieri, P.; Wahidulla, S.; Naik, C. G.; Cimino, G. *Tetrahedron* **2000**, *56*, 7305–7308.

Fray, M. J.; Mathias, J. P.; Nichols, C. L.; Po-Ba, Y. M.; Snow, H. *Tetrahedron Lett.* **2006**, *47*, 6365–6368.

Friedman, L.; Logullo, F. M. *J. Am. Chem. Soc.* **1963**, *85*, 1792–1797.

Frincke, J. M.; Faulkner, D. J. *J. Am. Chem. Soc.* **1982**, *104*, 265–269.

Fuller, A. A.; Hester, H. R.; Salo, E. V.; Stevens, E. P. *Tetrahedron Lett.* **2003**, *44*, 2935–2938.

Garg, N. K.; Goetz, A. E. *J. Org. Chem.* **2014**, *79*, 846–851.

Gilmore, C. D.; Allan, K. M.; Stoltz, B. M. *J. Am. Chem. Soc.* **2008**, *130*, 1558–1559.

Glorius, F. *Org. Biomol. Chem.* **2005**, *3*, 4171–4175.

Goossen, L. J.; Deng, G.; Levy, L. M. *Science* **2006**, *313*, 662–664.

Goossen, L. J.; Manjolinho, F.; Khan, B. A.; Rodríguez, N. *J. Org. Chem.* **2009**, *74*, 2620–2623.

Goossen, L. J.; Rudolphi, F.; Oppel, C.; Rodríguez, N. *Angew. Chem., Int. Ed.* **2008**, *47*, 3043–3045.

Goossen, L. J.; Rodríguez, N.; Melzer, B.; Linder, C.; Deng, G.; Levy, L. M. *J. Am. Chem. Soc.* **2007**, *129*, 4824–4833.

Henry, G. D. *Tetrahedron*, **2004**, *60*, 6043–6061.

Pintori, D. G.; Greaney, M. F. *Org. Lett.* **2010**, *12*, 168–171.

Himeshima, Y.; Sonoda, T.; Kobayashi, H. *Chem. Lett.* **1983**, 1211–1214.

Hodgson, P. B.; Salingue, F. H. *Tetrahedron Lett.* **2004**, *45*, 685–687.

Hoffmann, R. W. *Dehydrobenzene and Cycloalkynes*; Academic Press: New York, 1967.

Ikeda, Y.; Shimada, Y.; Honjo, K.; Okumoto, T.; Munakata, T. *J. Antibiot.* **1983**, *36*, 1290–1294.

Ishiyama, T.; Ishida, K.; Miyaura, N. *Tetrahedron* **2001**, *57*, 9813–9816.

Jia, W.; Jiao, N. *Org. Lett.* **2010**, *12*, 2000–2003.

Jones, C. P.; Anderson, K. W.; Buchwald, S. L. *J. Org. Chem.* **2007**, *72*, 7968–7973.

Katritzky, A. R.; Lan, X.; Yang, J. Z.; Denisko, O. V. *Chem. Rev.* **1998**, *98*, 409–548.

Katritzky, A. R.; Rachwal, S. *Chem. Rev.* **2011**, *111*, 7063–7120.

Katritzky, A. R.; Rogovoy, B. V. *Chem.—Eur. J.* **2003**, *9*, 4586–4593.

Kitamura, T.; Yamane, M. *J. Chem. Soc. Chem. Commun.* **1995**, 983–984.

Koketsu, K.; Watanabe, K.; Suda, H.; Oguri, H.; Oikawa, H. *Nature Chem. Biol.* **2010**, *6*, 408–410.

Lallana, E.; Fernandez-Trillo, F.; Sousa-Herves, Ana; Riquera, R.; Fernandez-Megia, E. *Pharm. Res.* **2012**, *29*, 902–921.

Lane, J. W.; Chen, Y.; Williams, R. M. Asymmetric Total Syntheses of (–)-Jorumycin, (–)-Renieramycin G, 3-*epi*-Jorumycin, and 3-*epi*-Renieramycin G. *J. Am. Chem. Soc.* **2005**, *127*, 12684–12690.

Lee, J.; Hong, M.; Jung, Y.; Cho, E. J.; Rhee, H. *Tetrahedron* **2012**, *68*, 2045–2051.

Lee, S. H.; Jang, B.-B.; Kafafi, Z. H. *J. Am. Chem. Soc.* **2005**, *127*, 9071–9078.

Logullo, F. M.; Seitz, A. H.; Friedman, L. *Org. Synth.* **1968**, *48*, 12–17.

Li, X.; Zou, D.; Leng, F.; Sun, C.; Li, J.; Wu, Y.; Wu, Y. *Chem. Commun.* **2013**, *49*, 312–314.

Liu, G.-B.; Xu, J.-L.; He, C. C.; Chen, G.; Qiang Xu, Q.; Xu, H.-X.; Jian-Xin Li, J.-X. *Bioorg. Med. Chem.* **2009**, *17*, 5433–5441.

Liu, W.; Liao, W.; Dong, W.; Yan, Z.; Wang, Z.; Liu, Z. *Tetrahedron* **2012**, *68*, 2759–2764.

Liu, W.; Dong, W.; Liao, X.; Yan, Z.; Guan, B.; Wang, N.; Liu, Z. *Bioorg. Med. Chem.* **2011**, *21*, 1419–1421.

Liu, Y.-L.; Liang, Y.; Pi, S.-F.; Li, J.-H. *J. Org. Chem.* **2009**, *74*, 5691–5694.

Liu, Z.; Larock, R. C. *Org. Lett.* **2003**, *5*, 4673–4675.

Littke, A. F.; Schwarz, L.; Fu, G. C. *J. Am. Chem. Soc.* **2002**, *124*, 6343–6348.

Lützen, A.; Hapke, M. *Eur. J. Org. Chem.* **2002**, 2292–2297.

Luzung, M. R.; Patel, J. S.; Yin, J. *J. Org. Chem.* **2010**, *75*, 8330–8332.

Lyons, T. W.; Sanford, M. S. *Chem. Rev.* **2010**, *110*, 1147–1169.

Mahal, H. S.; Venkataraman, K. *J. Chem. Soc.*, **1934**, 1767–1769.

Matsumoto, T.; Hosoya, T.; Katsuki, M.; Suzuki, K. *Tetrahedron Lett.* **1991**, *32*, 6735–6736.

Martinez, R.; Ramón, D. J.; Yus, M. *J. Org. Chem.* **2008**, *73*, 9778–9780.

Meldal, M.; Tornøe, C. W. *Chem. Rev.* **2008**, *108*, 2952–3015.

Michael, J. P. *Nat. Prod. Rep.* **2005**, *22*, 627–646.

Mikami, Y.; Takahashi, K.; Yazawa, K.; Arai, T.; Namikoshi, M.; Iwasaki, S.; Okuda, S. *J. Biol. Chem.* **1985**, *260*, 344–348.

Myers, A. G.; Tanaka, D.; Mannion, M. R. *J. Am. Chem. Soc.*, **2002**, *124*, 11250–11251.

O'Neill, B. T.; Yohannes, D.; Bundesmann, M. W.; Arnold, E. P. *Org. Lett.* **2000**, *2*, 4201–4204

Panella, L.; Aleixandre, A. M.; Kruidhof, G. J.; Robertus, J.; Feringa, B. L.; de Vries, J. G.; Minnaard, A. J. *J. Org. Chem.* **2006**, *71*, 2026–2036.

Peña, D.; Escudero, S.; Pérez, D.; Gutián, E.; Castedo, L. *Angew. Chem., Int. Ed.* **1998**, *37*, 2659–2661.

Pialat, A.; Liégault, B.; Marc Taillefer, M. *Org. Lett.* **2013**, *15*, 1764–1767.

Pospiech, A.; Cluzel, B.; Bietenhader, J.; Schupp, T. *Microbiology* **1995**, *141*, 1793–1803.

Pospiech, A.; Bietenhader, J.; Schupp, T. *Microbiology* **1996**, *142*, 741–746.

Rao, D. V.; Stuber, F. A. *Synthesis* **1983**, 308.

Razafindrabe, C. R.; Aubry, S.; Bourdon, B.; Andriantsiferana, M.; Pellet-Rostaing, S.; Lemaire, M. *Tetrahedron*, **2010**, *66*, 9061–9066.

Ren, W.; Li, J.; Zou, D.; Wu, Y.; Wu, Y. *Tetrahedron* **2012**, *68*, 1351–1358.

Roberts, J. D.; Simmons, H. E., Jr.; Carlsmith, L. A.; Vaughan, C. W. *J. Am. Chem. Soc.* **1953**, *75*, 3290–3291.

Rodríguez, N.; Goossen, L. J. *Chem. Soc. Rev.* **2011**, *40*, 5030–5048.

Schipper, D. J.; Campeau, L.-C.; Fagnou, K. *Tetrahedron* **2009**, *65*, 3155–3164.

Schlosser, M.; Mongin, F. *Chem. Soc. Rev.* **2007**, *36*, 1161–1172.

Scott, J. D.; Williams, R. M. Chemistry and Biology of the Tetrahydroisoquinoline Antitumor Antibiotics. *Chem. Rev.* **2002**, *102*, 1669–1730.

Shang, R.; Yang, Z.-W.; Wang, Y.; Zhang, S.-L.; Liu, L. *J. Am. Chem. Soc.* **2010**, *132*, 14391–14393.

Sletten, E. M.; Bertozzi, C. R. *Angew. Chem. Int. Ed.* **2009**, *48*, 6974–6998.

Stevens, R. V.; Angle, S. R.; Kloc, K.; Mak, K. F.; Liu, Y. X.; Trueblood, K. N. *J. Org. Chem.* **1986**, *51*, 4347–4353.

Stevens, R. V.; Bisacchi, G. S. *J. Org. Chem.* **1982**, *47*, 2393–2396.

Tadross, P. M.; Gilmore, C. D.; Bugga, P.; Virgil, S. C.; Stoltz B. M. *Org. Lett.* **2010**, *12*, 1224–1227.

Tambar, U. K.; Stoltz, B. M. *J. Am. Chem. Soc.* **2005**, *127*, 5340–5341.

Tambar, U. K.; Ebner, D. C.; Stoltz, B. M. *J. Am. Chem. Soc.* **2006**, *128*, 11752–11753.

Tan, Y.; Barrios-Landeros, F.; Hartwig, J. F. *J. Am. Chem. Soc.* **2012**, *134*, 3683–3686.

Tomita, F.; Takahashi, K.; Shimizu, K.-I. *J. Antibiot.* **1983**, *36*, 463–467.

Trabectedin Improves Disease Control in Patients with Advanced Soft Tissue Sarcoma. <http://www.jnj.com/news/all/Trabectedin-Improves-Disease-Control-in-Patients-with-Advanced-Soft-Tissue-Sarcoma> (accessed July 13, 2015).

Trost, B. M.; Tang, W.; Toste, D. F. *J. Am. Chem. Soc.* **2005**, *127*, 14785–14803.

U.S. FDA Grants Priority Review for YONDELIS® (trabectedin) for the Treatment of Patients with Advanced Soft Tissue Sarcoma. <http://www.jnj.com/news/all/US-FDA-Grants-Priority-Review-for-YONDELIS-trabectedin-for-the-Treatment-of-Patients-with-Advanced-Soft-Tissue-Sarcoma> (accessed July 13, 2015).

Voutchkova, A.; Coplin, A.; Leadbeater, N. E.; Crabtree, R. H. *Chem. Commun.* **2008**, 6312–6314.

Wen, J.; Zhang, R.-Y.; Chen, S.-Y.; Zhang, J.; Yu, X.-Q. *J. Org. Chem.* **2012**, *77*, 766–771.

Wittig, G.; Hoffmann, R. W. *Org. Synth.* **1967**, *47*, 4–8.

Wittig, G.; Pohmer, L. *Chem. Ber.* **1956**, *89*, 1334–1351.

Wu, Y.-C.; Zhu, J. *Org. Lett.* **2009**, *11*, 5558–5561.

Wünsch, B.; et al. *J. Org. Chem.* **2009**, *74*, 2788–2793.

Yang, D. X.; Colletti, S. L.; Wu, K.; Song, M.; Li, G. Y.; Shen, H. C. *Org. Lett.* **2009**, *11*, 381–384.

Yoshida, H.; Ito, Y.; Yoshikawa, Y.; Ohshita, J.; Takaki, K. *Chem. Commun.*, **2011**, 8664–8666.

Yoshida, H.; Watanabe, M.; Ohshita, J.; Kunai, A. *Chem. Commun.* **2005**, 3292–3294.

Yoshida, H.; Watanabe, M.; Ohshita, J.; Kunai, A. *Tetrahedron Lett.* **2005**, 45, 6729–6731.

Zhou, Y.-G. *Acc. Chem. Res.* **2007**, 40, 1357–1366.

ABOUT THE AUTHOR

Christopher Haley was born on November 18, 1987 in Boston, MA to John and Amy Haley. He spent the first 18 years of his life living in the town of Wellesley, MA, a suburban town west of Boston. When Christopher was five, the Haleys welcomed the addition of Christopher's younger brother, James, to the family, and they've been brothers ever since. While this meant that Christopher was forced to share his toys, it also meant Christopher had a great companion for family trips, playing video games with and someone to blame whenever anything broke.

His time in Wellesley was spent pursuing a variety of interests. For a number of years he attempted to hone his skills at various sports: soccer, baseball, tennis and even figure skating. While attending Wellesley High School, he settled on track and field, running the 300m hurdles and the 4x400m relay. He also took classical piano lessons for 9 years and received his Eagle Scout award in 2004. It was through the Boy Scouts that Christopher developed a love of the outdoors, which has only grown deeper with time. His hiking, backpacking and camping trips are some of his most cherished memories.

Upon graduating from high school in 2006, Christopher left suburban life behind and began his undergraduate studies in the big city at New York University in New York City. While there, he was fortunate enough to learn organic chemistry from Prof. Maitland Jones, Jr., whom he subsequently worked for as a teaching assistant. While an undergraduate student, Christopher carried out research in the laboratory of Prof. David I. Schuster. Prof. Jones and Prof. Schuster, instilled in Christopher a love of organic chemistry. During his time at NYU, Christopher thoroughly explored the city. He particularly loved attending Broadway shows, operas and concerts.

After receiving his B.S. in chemistry, he set his sights on receiving a Ph.D. from the California Institute of Technology. While at Caltech, Christopher worked in the laboratory of Prof. Brian M. Stoltz, an advisor who further enriched his knowledge and interest in organic chemistry. He worked on a variety of projects within the field of synthetic organic chemistry.

Upon graduation, Christopher will be a staff scientist at the law firm of Choate, Hall & Stewart in Boston, MA.